The Journal of Antibiotics (2009) 62, 605–611

www.nature.com/ja

ORIGINAL ARTICLE

Design, synthesis and antibacterial activity of a novel alkylide: 3-*O*-(3-aryl-propenyl)clarithromycin derivatives

Jian-Hua Liang[1], Yue-Ying Wang[1], Dan-Yang Zhu[1], Li-Jing Dong[1], Mao-Mao An[2], Rui Wang[2] and Guo-Wei Yao[1]

A series of novel 3-*O*-(3-aryl-propenyl)clarithromycin derivatives were designed, synthesized and evaluated for their *in vitro* antibacterial activities. Regioselective allylation at 3-OH was efficiently achieved in the presence of 9-oxime ether, compared with 9-keto. Most of the side chains were identified as the 3-*O*-(3-aryl-*Z*-prop-1-enyl) group, not the expected 3-*O*-(3-aryl-*E*-prop-2-enyl) group. Some derivatives of this series showed improved activities against erythromycin-resistant *Staphylococcus aureus* and *Staphylococcus pneumoniae* compared with the reference compound, clarithromycin, but weaker activities against susceptible strains.
The Journal of Antibiotics (2009) **62,** 605–611; doi:10.1038/ja.2009.89; published online 28 August 2009

Keywords: allyl; erythromycin; heck; isomerization; regioselectivity

INTRODUCTION

Erythromycin, a 14-membered macrolide antibiotic, has been used safely and effectively against respiratory tract infections since 1952. However, owing to its acid-instability, clarithromycin (6-*O*-methylerythromycin) as the second-generation erythromycin was developed to address the problem of ketalization of the C-9 carbonyl group by the 6-OH group.[1] It is noted that regioselective methylation at 6-OH to yield clarithromycin was not achieved until the introduction of oxime ether in the 9-carbonyl group.[2] Similarly, new emerging cethromycin [3-oxo-6-*O*-(3-(3′-quinolyl)-2-propenyl)erythromycin derivative] as the third-generation erythromycin was synthesized by regioselective allylation at 6-OH[3–5] to overcome the relatively recent issues associated with the development of bacterial resistance.

Most of the third-generation erythromycin, cethromycin included, shares two distinguishing structural features: first, cladinose is not an essential moiety for the antibacterial activity, and removal of cladinose can prevent the induction of resistance (Figure 1). As a result, modification at 3-OH led to the emergence of ketolide,[3–6] acylide,[7] bicyclolide,[8] anhydrolide,[9] 2,3-enol-ether,[10] 3-deoxy,[11] 3-ether,[12] 3,6-ketal[13] and 3,6-ether.[14] Second, an aryl side chain tethered to the erythronolide core is believed to be very important for the improvement of activities against erythromycin-resistant bacteria, due to the interaction with a secondary ribosomal binding site.[15]

The results published were not ours. In the search for novel erythromycin derivatives against erythromycin-resistant bacteria, the allyl group was a very important one for various further modifications at 6-OH of erythromycin.[4,5] To the best of our knowledge, the introduction of the allyl group at 3-OH of 14-membered macrolides was not disclosed yet, in addition to the recent modification of 16-membered macrolides, leucomycin.[16]

RESULTS AND DISCUSSION

Initially, we attempted to attach an allyl group to 3-OH of the 2′-*O*-Ac-3-OH-6-*O*-methylerythromycin 11, 12-carbonate with the structure of 9-keto, but unfortunately it failed and the major product in the resulting mixture was identified as 10,11-anhydro-3-OH-6-*O*-methylerythromycin A after methanolysis. Later, we found that the introduction of 9-oxime ether could dramatically improve the selectivity of allylation at 3-OH. Thus, a facile synthesis of 3-*O*-allyl of clarithromycin was conducted as a lead compound. In this study, we report a novel series of macrolides: 3-*O*-(3-aryl-propenyl)clarithromycin derivatives, which we named alkylides.

The synthesis of the targeted alkylide **9** in five steps from the intermediate 3-OH-6-*O*-methylerythromycin 9-*O*-(2-chlorobenzyl) oxime **4** was outlined in Schemes 1 and 2. Compound **4** was obtained by the acidic hydrolysis of 2′,4″-*O*-bis(trimethylsilyl) 6-*O*-methylerythromycin 9-*O*-(2-chlorobenzyl)oxime **3**,[17] which was an important intermediate for the synthesis of clarithromycin. Next, acetylation at 2′-OH of **4** was followed by carbonation at 11, 12-OH generated **6**. Consequently, allylation at 3-OH was efficiently achieved in the presence of allyl bromide and KOtBu, and **7** was produced in high yield (95.2%). Thus, various hetero-aryl bromides were used to install

[1]School of Life Science, Beijing Institute of Technology, Beijing, China and [2]Department of Clinical Pharmacology, Chinese Peoples Liberation Army General Hospital, Beijing, China
Correspondence: Professor J-H Liang, School of Life Science, Beijing Institute of Technology, Zhongguancun South street 5, Beijing 100081, China.
E-mail: ljhbit@bit.edu.cn
Received 23 June 2009; revised 20 July 2009; accepted 4 August 2009; published online 28 August 2009

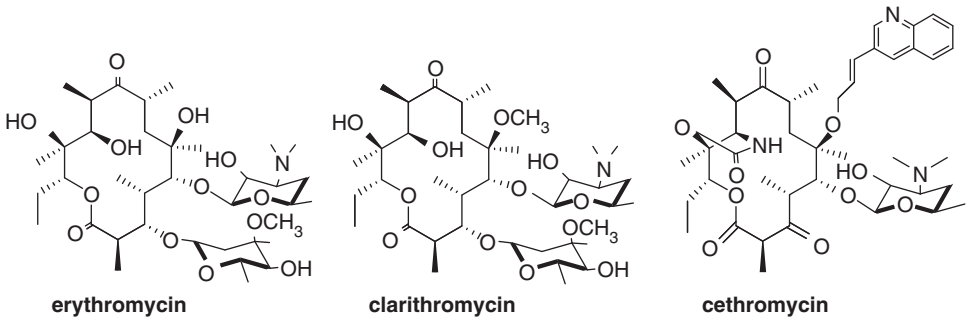

Figure 1 Structure of erythromycin, clarithromycin and cethromycin.

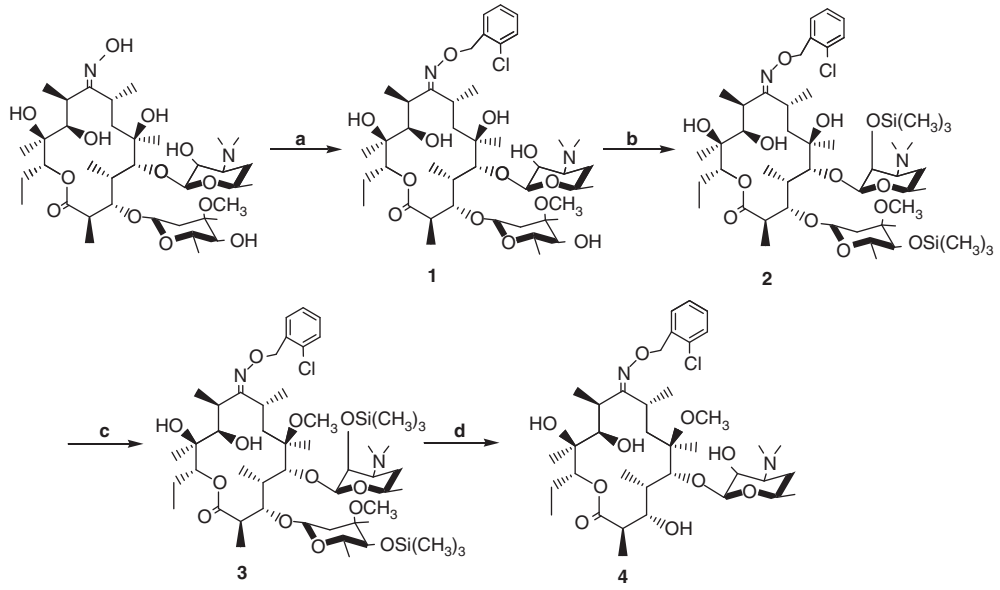

Scheme 1 Reagents and conditions: (**a**) 2-chlorobenzyl chloride, KOH, acetonitrile, 98.6%; (**b**) hexamethyldisilizane (HMDS), pyridine hydrochloride, acetonitrile, 85.8%; (**c**) CH_3I, KOH, THF/dimethyl sulfoxide (DMSO), 0 °C, 98.6%; (**d**) C_2H_5OH/H_2O, HCl, 73.8%.

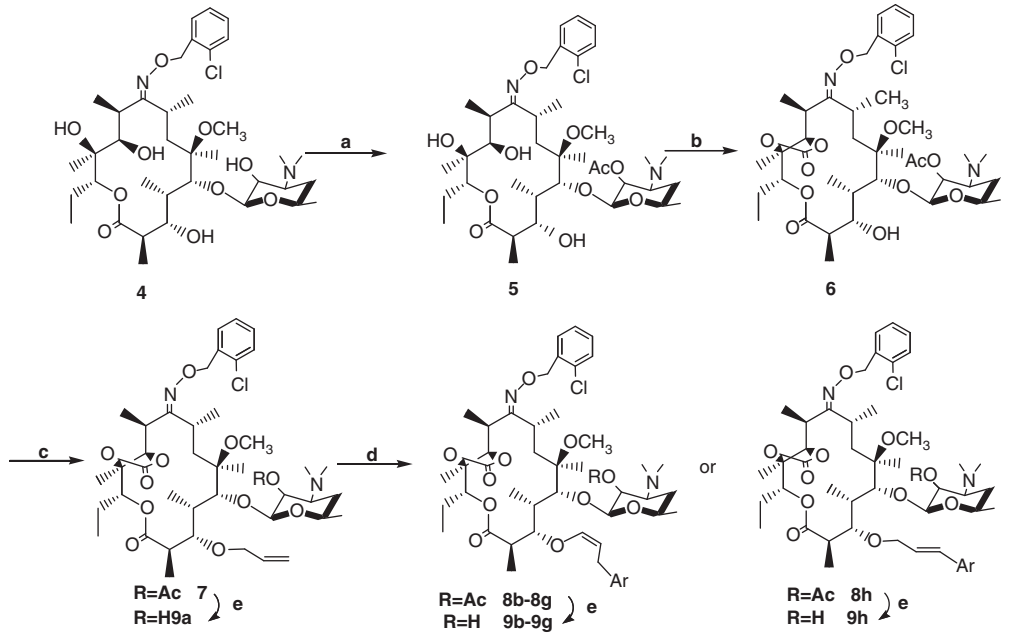

Scheme 2 Reagents and conditions: (**a**) Ac_2O, CH_2Cl_2, 94.5%; (**b**) bis(trichloromethyl)carbonate (BTC), pyridine, CH_2Cl_2, 0 °C, 98.7%; (**c**) allyl bromide, KOtBu, THF/DMSO, 0 °C, 95.2%; (**d**) $Pd(OAc)_2$, P(O-MePh)$_3$, Et_3N, acetonitrile, hetoro-aryl bromide, 60 °C 1 h then 90 °C 24 h; (**e**) MeOH, 60 °C.

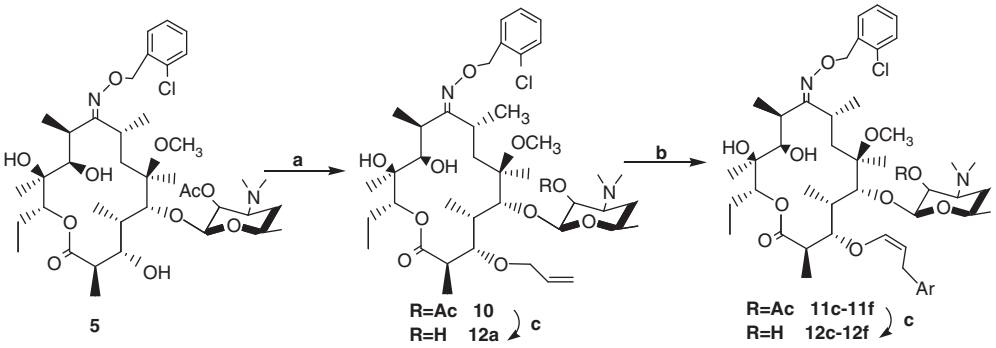

Scheme 3 Reagents and conditions: (**a**) allyl bromide, KOtBu, THF/DMSO, 0 °C, 85.7%; (**b**) $Pd(OAc)_2$, $P(O\text{-}MePh)_3$, Et_3N, acetonitrile, hetoro-aryl bromide, 60 °C 1 h then 90 °C 24 h; (**c**) MeOH, 60 °C.

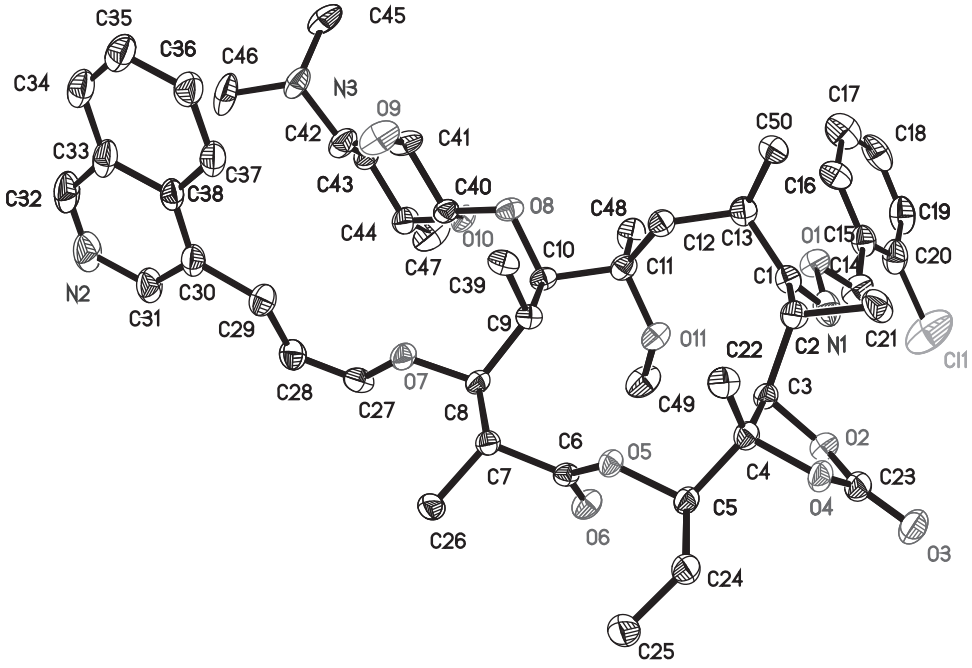

Figure 2 Crystal structure of 9f (4-isoquinolyl).

the aryl side chain by Heck reaction, catalyzed by $Pd(OAc)_2/P(o\text{-}MePh)_3$. The major products of Heck reaction and its methanolysis were purified to yield **8** and **9** by column chromatography using CH_2Cl_2/EtOH/$NH_3{\cdot}H_2O$ (15:0.4:0.1) and petroleum ether/acetone/triethylamine (5:5:0.2) as an eluent, respectively.

To confirm the regioselectivity of 3-OH, compound **12** was synthesized without the protection of 11, 12-OH (Scheme 3). The results proved that the regioselective allylation of **5** was also conducted in good yield (85.7%) and, as indicated, the regioselectivity at 3-OH was mainly influenced by 9-oxime ether.

A combination of ^1H NMR, COSY, ^{13}C NMR and HRMS was used to analyze the structure of this series. Surprisingly, the NMR spectrum showed that the aryl side chains of **9b–9g** and **12c–12f** were characterized by predominant *Z* configuration (J=6 Hz), such as the 1-phenyl (a mixture of *Z*/*E*: 10:4), 3-pyridyl, 5-pyrimidyl, 3-quinolyl, 4-isoquinolyl and 5-isoquinolyl groups, whereas the 5-indolyl **9h** side chain had *E* configuration (J=16 Hz). This was significantly different from the previous results of allylation at 6-OH.[4] Further study by X-ray crystallography of **9f** disclosed that the allylic double bond isomerized from 2-position to 1-position, and the Heck-isomerization to furnish enol concomitantly resulted in *Z* configuration, as shown in Figure 2. Therefore, with the exception of **9h**, the real structure of **9b-9g** and **12c-12f** should be the 3-*O*-(3-aryl-*Z*-prop-1-enyl)clarithromycin derivatives, not the expected 3-*O*-(3-aryl-*E*-prop-2-enyl)clarithromycin derivatives.

The *in vitro* antibacterial activity of alkylides **9** and **12** was assessed against erythromycin-susceptible and erythromycin-resistant bacteria, including *Staphylococcus aureus* and *Streptococcus pneumoniae*. Data are represented in Table 1 as the minimal inhibitory concentration, which is determined by the broth microdilution method as recommended by the NCCLS (National Committee of Clinical Laboratory Standard).[18]

Some of the alkylides such as **9**, **12** showed improved activities compared with the reference compound, clarithromycin, against resistant pathogens, particularly for *S. aureus*. Among them, **9d** and **12d** (3-pyrimidinyl) were promising candidates. The compounds with the mono-heteroaryl ring (**9c-9d, 12c-12d**) and the parent compounds **9a** and **12a** (H) possessed better activity against resistant pathogens than did those with fused aryl rings (**9e-9h**, **12e-12f**).

Table 1 Antibacterial effects of alkylides against selected respiratory tract pathogens

Compound			In vitro *MIC (μg/ml)*								
			Staphylococcus aureus				Staphylococcus pneumoniae				
	Aryl	*Config.*	*ATCC 29213*[a]	*D18*[b]	*D6*[b]	*D9*[b]	*ATCC 49619*[a]	*SPJ8*[b]	*SPJ15*[b]	*CP18*[b]	*SPM12*[b]
CAM	—	—	0.25	>64	>64	>64	<0.03	>16	>16	>16	>16
9a	H	—	8	16	16	16	4	>16	16	>16	>16
9b	1-phenyl	*Z*/*E*	64	64	>64	64	8	>16	16	>16	>16
9c	3-pyridyl	*Z*	8	32	32	16	1	>16	>16	>16	>16
9d	5-pyrimidyl	*Z*	4	32	32	4	2	>16	16	>16	>16
9e	3-quinolyl	*Z*	64	>64	>64	64	8	16	>16	>16	>16
9f	4-isoquinolyl	*Z*	>64	64	64	>64	4	>16	16	>16	>16
9g	5-isoquinolyl	*Z*	>64	>64	>64	>64	4	>16	8	>16	>16
9h	5-indolyl	*E*	>64	>64	>64	>64	8	>16	16	>16	>16
12a	H	—	32	16	64	16	16	>16	>16	>16	>16
12c	3-pyridyl	*Z*	32	16	32	16	4	>16	>16	>16	>16
12d	5-pyrimidyl	*Z*	8	16	32	16	1	>16	>16	>16	>16
12e	3-quinolyl	*Z*	32	64	>64	32	16	16	16	>16	>16
12f	4-isoquinolyl	*Z*	32	32	64	16	8	16	16	>16	>16

Abbreviations: Config., configuration; MIC, minimal inhibitory concentration.
[a]Erythromycin-susceptible.
[b]Erythromycin-resistant.

The crystal structure of **9f** (4-isoquinolyl) disclosed that the fused aryl rings, regardless of the location of the nitrogen (**e**-**g**), may sterically prevent the 3′-dimethylamino group from approaching the binding site, resulting in a decrease in activities. Compounds **9c**, **12c** (3-pyridyl) and **9d**, **12d** (3-pyrimidinyl) showed better activities than did the parent compounds **9a** and **12a** (H) against erythromycin-susceptible pathogens, but unfortunately no significant difference was found between them against erythromycin-resistant pathogens.

In conclusion, the 3-*O*-allyl clarithromycin derivative was synthesized in high regioselectivity to serve as a template. The introduction of the 3-*O*-aryl-propenyl group led to the acquisition of activities against erythromycin-resistant pathogens than reference compound, clarithromycin. The further chemical modification to improve activities is ongoing.

EXPERIMENTAL SECTION

All solvents and reagents were obtained from commercial sources and used without further purification unless otherwise noted. Column chromatography was performed on silica gel (200–300 mesh for **8** and 300–400 mesh for **9**). ^{1}H and ^{13}C NMR spectra were recorded in $CDCl_3$ on a Bruker ARX 400 and 600 MHz (Bruker BioSpin AG Ltd, Beijing, China) with tetramethylsilane (TMS) as an internal standard. The assignments of **4**, **7**, **9c** and **12a** were made on the basis of D_2O exchange and ^{1}H-^{1}H COSY. HRMS were obtained with Bruker Apex II ICRMS, or Bruker Apex IV FTMS.

Erythromycin A 9-*O*-(2-chlorobenzyl)oxime (1)

To a solution of Erythromycin A, 9-*O*-oxime (10 g, 13.3 mmol) in acetonitrile (120 ml) was added 2-chlorobenzyl chloride (2.1 ml, 16.5 mmol) and KOH (1.3 g, 21 mmol). The reaction mixture was stirred at room temperature for 2 h, and in ice bath for another 1 h. The resulting precipitate was filtrated and dried to yield **1** (11.5 g, 98.6%).

2, 4″-*O*-bis(trimethylsilyl)erythromycin A 9-*O*-(2-chlorobenzyl)oxime (2)

To a solution of **1** (23 g, 26.3 mmol) in acetonitrile (200 ml) was added pyridine hydrochloride (8.8 g, 76.1 mmol) and hexamethyldisilizane (HMDS) (20 ml, 94.2 mmol). The reaction mixture was stirred at room temperature for 1 h and extracted twice with petroleum ether. The organic phase was dried over $MgSO_4$ and evaporated to yield **2** (23.0 g, 85.8%).^{13}C NMR(100 MHz, $CDCl_3$) δ: 175.8, 172.0, 135.4, 133.0, 129.5, 129.2, 128.8, 126.8, 102.5, 96.5, 81.4, 80.8, 79.3, 76.9, 75.3, 74.2, 73.2, 73.1, 72.8, 70.4, 67.6, 65.1, 64.9, 49.6, 44.6, 40.9, 40.2, 38.4, 35.8, 33.2, 29.6, 26.8, 26.7, 22.1, 21.7, 21.2, 19.3, 18.5, 16.2, 15.6, 14.3, 10.7, 9.6, 0.9, 0.8.

2′, 4″-*O*-bis(trimethylsilyl)-6-*O*-methylerythromycin A 9-*O*-(2-chlorobenzyl)oxime (3)

To an ice-cold solution of **2** (23.0 g, 22.6 mmol) in 80 ml THF and 80 ml dimethyl sulfoxide (DMSO) was added CH_3I (2.4 ml, 47.3 mmol) and KOH (2.4 g, 42.8 mmol). The reaction mixture was stirred at 0° C for 1 h, and then was poured with water and extracted with petroleum ether. The organic layer was concentrated to yield **3** (23.0 g, 98.6%).

3-OH-6-*O*-methylerythromycin A 9-*O*-(2-chlorobenzyl)oxime (4)

To a solution of **3** (23.0 g, 22.3 mmol) in ethanol (80 ml) was slowly added a solution of diluted HCl (8 ml HCl in 80 ml water) over 10 min. The reaction mixture was stirred at room temperature for 1.5 h and neutralized with $NH_3{\cdot}H_2O$ (36%, 8 ml). The precipitate was collected by filtration and washed with water to yield **4** (12.0 g, 73.8%). MS(MALDI-TOF) ($M+Na^+$) *m/z* 751.5, calcd for $C_{37}H_{61}ClN_2O_{10}$ 728.4 (M). ^{1}H NMR(400 MHz, $CDCl_3$) δ: 7.41–7.22 (m, 4H, benzyl ring), 5.22–5.06 (m, 3H, H-13, –C**H**$_2$–PhCl), 4.36–4.35 (m, 2H, H-1′, 11-OH), 3.81 (s, 1H, H-11), 3.78–3.71 (m, 1H, H-8), 3.64 (m, 2H, H-5, 2′-OH), 3.54–3.51 (m, 2H, H-3, H-5′), 3.28 (s, 12-OH), 3.23 (dd, 1H, H-2′), 2.82 (s, 3H, 6-OCH_3), 2.66–2.62 (m, 1H, H-2), 2.57 (q, 1H, H-10), 2.49–2.43 (m, 1H, H-3′), 2.24 (s, 6H, –$N(CH_3)_2$), 2.09 (m, 1H, H-4), 1.97–19.2 (m, 1H, H-14eq), 1.67–1.50 (m, 3H, H-4′, H-7ax, H-14ax), 1.38 (s, 3H, 6-CH_3), 1.35–1.22 (m, 8H, H-7eq, H-4′eq, 5′-CH_3, 2-CH_3), 1.18 (s, 3H, 12-CH_3), 1.13 (d, 3H, 10-CH_3), 1.07 (d, 3H, 4-CH_3), 0.97 (d, 3H, 8-CH_3), 0.83 (t, 3H, 15-CH_3). ^{13}C NMR(100 MHz, $CDCl_3$) δ: 174.9, 170.5, 135.7, 133.4, 129.8, 129.2, 128.9, 126.5, 106.7, 87.9, 78.8, 78.3, 76.8, 73.9, 72.6, 70.6, 70.4, 70.1, 65.6, 49.3, 44.5, 40.2, 37.3, 35.9, 33.1, 28.0 26.4, 21.5, 21.2, 18.7, 18.3, 16.2, 15.3, 15.1, 10.4, 8.1.

2′-*O*-Ac-3-OH-6-*O*-methylerythromycin A 9-*O*-(2-chlorobenzyl)oxime (5)

A solution of **4** (5.0 g, 6.9 mmol) in CH_2Cl_2 (50 ml) was treated with acetic anhydride (1.7 ml, 17.9 mmol) at room temperature for 1 h. The reaction mixture was washed with saturated $NaHCO_3$ and brine. The organic layer was dried over $MgSO_4$ and evaporated to yield **5** (5.0 g, 94.5%).

2′-*O*-Ac-3-OH-6-*O*-methylerythromycin A 9-*O*-(2-chlorobenzyl)oxime 11,12-carbonate (6)

To an ice-cold solution of **5** (4.8 g, 6.3 mmol) in CH_2Cl_2 (120 ml) was added pyridine (5.0 ml, 61.9 mmol) and dropped by a solution of Bis(trichloromethyl)carbonate (3.73 g, 12.5 mmol)in CH_2Cl_2 (60 ml) over 1 h. The reaction mixture was stirred at room temperature for 18 h and then cooled to 0 °C. To the reaction mixture was added dropwise water (100 ml). The organic layer was washed with saturated $NaHCO_3$ and water, and then dried over $MgSO_4$ and evaporated to yield **6** (4.9 g, 98.7%).

2′-*O*-Ac-3-*O*-allyl-6-*O*-methylerythromycin A 9-*O*-(2-chlorobenzyl)oxime 11,12-carbonate (7)

To an ice-cold solution of **6** (2.0 g, 2.5 mmol) in 20 ml of DMSO and 20 ml THF was added allyl bromide (0.42 ml, 5.0 mmol) and KOtBu (0.56 g, 5.0 mmol). The reaction mixture was stirred for 30 min, and then poured with water and extracted with ethyl acetate. The organic phase was washed with water and brine. The organic layer was dried over $MgSO_4$ and concentrated to yield **7** (2.0 g, 95.2%). HRMS (ESI) ($M+H^+$) *m/z* 837.42967, calcd for $C_{43}H_{66}ClN_2O_{12}$ 837.42988. ^1H NMR (400 MHz, $CDCl_3$) δ: 0.82–0.91 (m, 9H, 15-CH_3, 8-CH_3, 4-CH_3), 1.18–1.30 (m, 13H, 10-CH_3, 5′-CH_3, 2-CH_3, 6-CH_3, H-7), 1.46 (s, 3H, 12-CH_3), 1.51–1.56 (m, 1H, H-14ax), 1.67 (dd, *J*=2.7 Hz, 1H, H-4′), 1.83–1.88 (m, 2H, H-4, H-14eq), 2.02 (s, 3H, 2′-$COCH_3$), 2.24 (s, 6H, –$N(CH_3)_2$), 2.44 (q, 1H, H-10), 2.62–2.64 (m, 1H, H-3′), 2.68 (s, 3H, 6-OCH_3), 2.78–2.82 (m, 1H, H-2), 3.19 (d, *J*=10.5 Hz, 1H, H-3), 3.39–3.45 (m, 1H, H-5′), 3.62 (d, *J*=3.2 Hz, 1H, H-5), 3.72 (m, 1H, H-8), 4.05 and 4.27 (dd, *J*=5.1and 13.2 Hz, 2H, –C**H**$_2$–CH=CH_2), 4.41 (d, *J*=7.5 Hz, 1H, H-1′), 4.70 (dd, *J*=7.5 and 10.5 Hz, 1H, H-2′), 4.78 (s, 1H, H-11), 5.08–5.24 (m, 3H, H-13, benzyl–CH_2), 5.34 (dd, *J*=1.6 and 17.2 Hz, 1H, –CH=C**H**$_2$), 5.83–5.93 (m, 1H, –C**H**=CH_2), [7.48–7.50(m, 1H), 7.30 (d, *J*=1.2 and 7.6 Hz, 1H), 7.15–7.26 (m, 2H), benzyl ring]. ^{13}C NMR (100 MHz, $CDCl_3$) δ: 175.2(C-1), 169.7(C-9), 165.3(–**C**OCH_3), 154.6(carbonate), 136.1, 134.4, 133.4, 130.8, 128.9, 128.6, 126.4, 116.4, 99.2, 84.9, 84.2, 82.8, 79.0, 78.4, 75.1, 74.4, 72.6, 71.4, 68.5, 49.4, 44.7, 40.6(–N(**C**$H_3)_2$), 36.9, 36.6, 32.8, 31.0, 25.8, 22.1, 21.1, 20.9, 19.3, 18.8, 15.5, 15.2, 12.8, 10.1, 8.5.

3-*O*-[3-(3′-Quinolyl)-*Z*-1-propenyl]-6-*O*-methylerythromycin A 9-*O*-(2-chlorobenzyl)oxime 11, 12-carbonate (9e)

To a solution of **7**(1.0 g, 1.2 mmol), palladium(II) acetate (53.6 mg, 0.24 mmol) and tri(*o*-tolyl) phosphine (145.36 mg, 0.48 mmol), in acetonitrile (8 ml) were added 3-bromoquinoline (0.324 ml, 2.4 mmol) and triethylamine (0.33 ml, 2.4 mmol). The reaction mixture was flushed with nitrogen and sealed in a pressure tube. The reaction mixture was stirred at 60 °C for 1 h and thereafter at 90 °C for 24 h. The reaction mixture was extracted with ethyl acetate, washed with water and brine and the organic phase was concentrated. The crude mixture was purified by column chromatography on silica gel (15:0.4:0.1 $CH_2Cl_2/C_2H_5OH/NH_3{\cdot}H_2O$) to yield **8e** (216 mg, 19.4%).

The product obtained above (216 mg, 0.22 mmol) was heated to reflux in MeOH (20 ml) for 3 h. After the solvent was evaporated, the crude product was purified by column chromatography (silica gel, 5:5:0.2 petroleum ether/acetone/triethylamine) to yield **9e** (100 mg, 48.4%): MS(MALDI-TOF) ($M+Na^+$) *m/z* 944.7. HRMS (ESI) ($M+H^+$) *m/z* 922.46049, calcd for $C_{50}H_{69}ClN_3O_{11}$ 922.46151. ^1H NMR (400 MHz, $CDCl_3$) δ: 0.85 (t, 3H, 15-CH_3), 0.93 (d, *J*=6.9 Hz, 3H, 8-CH_3), 1.12–1.20 (m, 9H, 4-CH_3, 2-CH_3, 5′-CH_3), 1.22 (d, *J*=6.8 Hz, 3H, 10-CH_3), 1.28 (s, 3H, 6-CH_3), 1.32–1.35 (m, 1H, H-7), 1.42–1.60 (m, 6H, H-7, 12-CH_3, H-14ax, H-4′), 1.88–1.99 (m, 2H, H-4, H-14eq), 2.14–2.17 (m, 7H, –$N(CH_3)_2$, H-3′), 2.47 (q, 1H, H-10), 2.71 (s, 3H, 6-OCH_3), 2.89–2.96 (m, 1H, H-2), 3.12 (dd, *J*=7.2 and 10.1 Hz, 1H, H-2′) 3.33–3.36 (m, 2H, H-5′, 3-*O*–CH=CH–C**H**$_2$–Ar), 3.49–3.55 (m, 2H, -3-*O*–CH=CH–C**H**$_2$–Ar, H-3), 3.66 (d, *J*=2.7 Hz, 1H, H-5), 3.67–3.75 (m, 2H, 2′-OH, H-8), 4.21 (d, *J*=7.3 Hz, 1H, H-1′), 4.62 (q, 1H, 3-*O*–CH=C**H**–CH_2–Ar), 4.83 (s, 1H, H-11), 5.09–5.25 (m, 3H, –C**H**$_2$–PhCl, H-13), 6.25 (d, *J*=6.5 Hz, 1H, 3-*O*–C**H**=CH–CH_2–Ar), [7.19–7.25 (m, 2H), 7.32 (dd, *J*=1.3 and 5.2 Hz, 1H), 7.52–7.54(m, 1H), benzyl ring], [7.52–7.54 (m, 1H), 7.64(m, 1H), 7.75 (d, *J*=8.0 Hz, 1H), 7.94 (s, 1H), 8.05 (d, *J*=8.3 Hz, 1H), 8.82 (d, *J*=2.1 Hz, 1H), quinolyl].

3-*O*-[3-(4′-Isoquinolyl)-*Z*-1-propenyl]-6-*O*-methylerythromycin A 9-*O*-(2-chlorobenzyl)oxime 11,12-carbonate (9f)

By a similar procedure to **9e**, **8f** was prepared as a white solid in 17.1% yield according to the general procedure for the preparation of **8e**, and then deacetylated to give **9f** (38.6%). HRMS (ESI) ($M+H^+$) *m/z* 922.46301, calcd for $C_{50}H_{69}ClN_3O_{11}$ 922.46151. ^1H NMR (400 MHz, $CDCl_3$) δ: 0.85 (t, 3H, 15-CH_3), 0.93 (d, *J*=6.9 Hz, 3H, 8-CH_3), 1.12–1.22 (m, 9H, 4-CH_3, 2-CH_3, 5′-CH_3), 1.23 (d, *J*=6.8 Hz, 3H, 10-CH_3), 1.29 (s, 3H, 6-CH_3), 1.35 (d, 1H, H-7), 1.45 (d, 1H, H-7), 1.51 (s, 3H, 12-CH_3), 1.56 (m, 2H, H-4′, H-14ax), 1.87–1.93 (m, 1H, H-14eq), 1.99–2.03 (m, 1H, H-4), 2.23 (s, 6H, –$N(CH_3)_2$), 2.25–2.26 (m, 1H, H-3′), 2.48 (q, 1H, H-10), 2.71 (s, 3H, 6-OCH_3), 2.95–2.99 (m, 1H, H-2), 3.14 (dd, *J*=7.3 and 10.0 Hz, 1H, H-2′), 3.31–3.35 (m, 2H, H-5′, 2′-OH), 3.55 (d, *J*=10.5 Hz, 1H, H-3), 3.66–3.72 (m, 2H, H-5, 3-*O*–CH=CH–C**H**$_2$–Ar), 3.77 (m, 1H, H-8), 3.94 (dd, *J*=7.6 and 15.6 Hz, 1H, 3-*O*–CH=CH–C**H**$_2$–Ar), 4.26 (d, *J*=7.2 Hz, 1H, H-1′), 4.60 (q, 1H, 3-*O*–CH=C**H**–CH_2–Ar), 4.85 (s, 1H, H-11), 5.10–5.16 (m, 2H, –C**H**$_2$–PhCl, H-13), 5.24 (d, *J*=12.9 Hz, 1H, –C**H**$_2$–PhCl), 6.19 (d, *J*=6.1 Hz, 1H, 3-*O*–C**H**=CH–CH_2–Ar), [7.12–7.25(m, 2H), 7.32 (dd, *J*=1.1 and 7.9 Hz, 1H), 7.53 (dd, *J*=1.3 and 7.5 Hz, 1H), benzyl ring], [7.63 (t, 1H), 7.74 (m, 1H), 7.98 (d, *J*=8.1 Hz, 1H), 8.07 (d, *J*=8.4 Hz, 1H), 8.42 (s, 1H), 9.13 (s, 1H), isoquinolyl]. ^{13}C NMR (100 MHz, $CDCl_3$) δ: 174.4 (C-1), 165.1 (C-9), 154.6 (carbonate), 151.4, 148.1, 142.3, 136.0, 134.5, 133.5, 131.0, 130.3, 130.2, 128.9, 128.7, 128.3, 128.1, 126.9, 126.4, 123.1, 102.1, 101.6, 89.5, 84.9, 82.8, 79.7, 78.4, 77.1, 75.4, 72.6, 70.4, 69.2, 65.6, 49.3, 44.5, 40.2 (–N(**C**$H_3)_2$), 37.1, 36.5, 32.8, 28.4, 25.9, 25.2, 22.1, 21.1, 19.3, 18.8, 15.6, 15.4, 12.8, 10.0, 8.9.

3-*O*-[3-(5′-Isoquinolyl)-*Z*-1-propenyl]-6-*O*-methylerythromycin A 9-*O*-(2-chlorobenzyl)oxime 11,12-carbonate (9g)

By a similar prodedure to **9e**, **8g** was prepared as a white solid in 18.0% yield according to the general procedure for the preparation of **8e**, and then deacetylated to give **9g** (52.3%). HRMS (ESI) ($M+H^+$) *m/z* 922.46176, calcd for $C_{50}H_{69}ClN_3O_{11}$ 922.46151. ^1H NMR (600 MHz, $CDCl_3$) δ: 0.86 (t, 3H, 15-CH_3), 0.94 (d, *J*=7.6 Hz, 3H, 8-CH_3), 1.13 (d, *J*=6.9 Hz, 3H, 4-CH_3), 1.16–1.18 (m, 9H, 2-CH_3, 4-CH_3, 5′-CH_3), 1.21–1.25 (m, 3H, 10-CH_3), 1.31 (s, 3H, 6-CH_3), 1.35–1.31 (m, 1H, H-7), 1.43–1.48 (m, 1H, H-7), 1.51 (s, 3H, 12-CH_3), 1.54–1.61 (m, 2H, H-14ax, H-4′), 1.89–1.93 (m, 1H, H-14eq), 1.97–2.02 (m, 1H, H-4), 2.18 (m, 7H, H-3′, –$N(CH_3)_2$), 2.48 (q, 1H, H-10), 2.71 (s, 3H, 6-OCH_3), 2.92–2.95 (m, 1H, H-2), 3.14 (dd, *J*=6.9 and 10.3 Hz, 1H, H-2′), 3.28–3.32 (m, 2H, 2′-OH, H-5′), 3.53 (d, *J*=10.9 Hz, 1H, H-3), 3.67–3.71 (m, 2H, H-5, 3-*O*–CH=CH–C**H**$_2$–Ar), 3.76–3.78 (m, 1H, H-8), 3.98 (dd, *J*=7.5 and 15.8 Hz, 1H, 3-*O*–CH=CH–C**H**$_2$–Ar), 4.25 (d, *J*=7.5 Hz, 1H, H-1′), 4.57–4.60 (m, 1H, 3-*O*–CH=C**H**–CH_2–Ar), 4.84 (s, 1H, H-11), 5.11–5.29 (m, 2H, H-13, –C**H**$_2$–PhCl), 6.20 (d, *J*=6.2 Hz, 1H, 3-*O*–C**H**=CH–CH_2–Ar), [7.19–7.25 (m, 2H), 7.32 (d, *J*=7.5 Hz, 1H), 7.51–7.54 (m, 1H), benzyl ring], [7.51–7.54 (m, 1H), 7.59 (d, *J*=6.8 Hz, 1H), 7.84 (d, *J*=8.2 Hz, 1H), 7.89 (d, *J*=6.2 Hz, 1H), 8.56(d, *J*=5.5 Hz, 1H), 9.24(s, 1H), isoquinolyl].

3-*O*-[3-(5′-Indolyl)-*E*-2-propenyl]-6-*O*-methylerythromycin A 9-*O*-(2-chlorobenzyl)oxime 11,12-carbonate (9h)

By a similar prodedure to **9e**, **8h** was prepared as a white solid in 21.0% yield according to the general procedure for the preparation of **8e**, and then deacetylated to give **9h** (13.9%). HRMS (ESI) ($M+H^+$) *m/z* 910.46418, calcd for $C_{49}H_{69}ClN_3O_{11}$ 910.46151. ^1H NMR (400 MHz, $CDCl_3$) δ: 0.87 (t, 3H, 15-CH_3), 0.91 (d, *J*=6.9 Hz, 3H, 8-CH_3), 1.09 (d, *J*=7.5 Hz, 3H, 4-CH_3), 1.22–1.19 (m, 6H, 5′-CH_3, 2-CH_3), 1.25–1.34 (m, 6H, 10-CH_3, 6-CH_3), 1.42 (m, 1H, H-7), 1.49(s, 3H, 12-CH_3), 1.56 (m, 3H, H-7, H-14ax, H-4′), 1.92–1.87 (m, 2H, H-14eq, H-4), 2.10 (s, 6H, –$N(CH_3)_2$), 2.37 (br, 1H, H-3′), 2.47(q, 1H, H-10), 2.63 (s, 3H, 6-OCH_3), 2.92–2.87 (m, 1H, H-2), 3.16 (m, 1H, H-2′), 3.28 (s, 1H, 2′-OH), 3.34 (d, *J*=7.8 Hz, 1H, H-3), 3.46 (m, 1H, H-5′), 3.71 (m, 2H, H-8, H-5), 4.23 (dd, *J*=5.3 and 13.2 Hz, 1H, 3-*O*–C**H**$_2$–CH=CH-Ar), 4.48 (d, *J*=5.4 Hz, 1H, H-1′), 4.53 (dd, *J*=9.3 Hz, 1H, 3-*O*–C**H**$_2$–CH=CH–Ar), 4.82 (s, 1H, H-11), 5.08–5.15 (m, 2H, –C**H**$_2$–PhCl, H-13), 5.23 (d, *J*=12.9 Hz, 1H, –C**H**$_2$–PhCl), 6.29 (dt, *J*=15.6 Hz, 1H, 3-*O*–CH_2–C**H**=CH–Ar), 6.78 (d, *J*=15.9 Hz, 1H, 3-*O*–CH_2–CH=C**H**-Ar), [6.52 (m, 1H), 7.12 (m, 1H), 7.20–7.31 (m, 4H), 7.34–7.36 (m, 1H), 7.50–7.53 (m, 1H), 7.62 (s, 1H), 8.19 (s, 1H), benzyl ring, indolyl]. ^{13}C NMR (100 MHz, $CDCl_3$) δ: 175.4 (C-1), 165.3(C-9), 154.8 (carbonate), 136.1,

135.5, 133.5, 133.2, 131.0, 128.9, 128.6, 128.5, 128.1, 126.4, 124.8, 122.6, 120.4, 119.2, 111.1, 102.7, 101.7, 85.0, 83.8, 82.9, 80.2, 78.3, 77.1, 75.0, 74.2, 72.6, 70.5, 69.1, 65.1, 49.3, 44.9, 39.9 (–N(**C**H_3)$_2$), 37.2, 36.9, 32.8, 28.6, 25.9, 22.1, 21.3, 19.4, 18.8, 15.6, 15.5, 12.8, 10.1, 8.8.

3-*O*-[3-(5′-Pyrimidyl)-*Z*-1-propenyl]-6-*O*-methylerythromycin A 9-*O*-(2-chlorobenzyl)oxime 11,12-carbonate (9d)

By a similar prodedure to **9e**, **8d** was prepared as a white solid in 9.4% yield according to the general procedure for the preparation of **8e**, except for the addition of 3eq 5-bromopyrimidine, and then deacetylated to give **9d** (32.3%). HRMS (ESI) (M+H$^+$) *m/z* 873.44271, calcd for $C_{45}H_{66}ClN_4O_{11}$ 873.44111. ^{1}H NMR (400 MHz, $CDCl_3$), *δ*: 0.83 (t, 3H, 15-CH_3), 0.91 (d, 3H, 8-CH_3), 1.04–1.11 (m, 6H, 4-CH_3, 2-CH_3), 1.17–1.24 (m, 7H, 10-CH_3, 5′-CH_3, H-4′ax), 1.27 (s, 3H, 6-CH_3), 1.42–1.28 (m, 2H, H-7), 1.48 (s, 3H, 12-CH_3), 1.61 (m, 2H, H-14ax, H-4′eq), 1.86–1.96 (m, 2H, H-14eq, H-4), 2.25 (s, 6H, –N(CH_3)$_2$), 2.31 (m, 1H, H-3′), 2.46 (q, 1H, H-10), 2.69 (s, 3H, 6-OCH_3), 2.86–2.91 (m, 1H, H-2), 3.14 (dd, *J*=7.3 and 15.9 Hz, 1H, H-2′), 3.25–3.35 (m, 2H, H-5′, 3-*O*–CH=CH–C**H**$_2$–Ar), 3.48–3.52 (m, 2H, 3-*O*–CH=CH–C**H**$_2$–Ar, H-3), 3.61 (d, *J*=2.4 Hz, 1H, H-5), 3.75 (m, 1H, H-8), 4.16 (d, *J*=7.2 Hz, 1H, H-1′), 4.52 (q, 1H, 3-*O*–CH=C**H**–CH_2–Ar), 4.81 (s, 1H, H-11), 4.78–4.81 (m, 2H, –C**H**$_2$–PhCl, H-13), 5.22 (d, *J*=12.9 Hz, 1H, –C**H**$_2$–PhCl), 6.22 (d, *J*=6.0 Hz, 1H, 3-*O*–C**H**=CH–CH_2–Ar), [7.16–7.23 (m, 2H), 7.29–7.31 (m, 1H), 7.50–7.52 (m, 1H), benzyl ring], [8.60 (s, 2H), 9.04 (s, 1H), pyrimidyl]. ^{13}C NMR (100 MHz, $CDCl_3$) *δ*: 174.2 (C-1), 165.1 (C-9), 156.6, 154.6 (carbonate), 149.2, 136.0, 134.4, 133.5, 130.9, 128.9, 128.7, 126.4, 101.8, 100.5, 89.8, 84.8, 82.8, 80.1, 78.4, 77.1, 75.5, 72.6, 70.2, 69.2, 65.8, 49.3, 44.4, 40.2 (–N(**C**H_3)$_2$), 37.1, 36.4, 32.8, 28.4, 25.8, 25.3, 22.1, 21.1, 19.3, 18.7, 15.6, 15.4, 12.8, 10.0, 8.8.

3-*O*-[3-(1′-Phenyl)-*Z*-1-propenyl]-6-*O*-methylerythromycin A 9-*O*-(2-chlorobenzyl)oxime 11,12 -carbonate (9b)

By a similar prodedure to **9e**, **8b** was prepared as a white solid in 51.2% yield according to the general procedure for the preparation of **8e**, and then deacetylated to give **9b** (16.2%). HRMS (ESI) (M+H$^+$) *m/z* 871.45056, calcd for $C_{47}H_{68}ClN_2O_{11}$ 871.45062. ^{1}H NMR (600 MHz, $CDCl_3$) *δ*: 0.83–0.88 (m, 3H, 15-CH_3), 0.91–0.95 (m, 3H, 8-CH_3), 1.09–1.12 (m, 3H, 4-CH_3), 1.18(d, *J*=2.7 Hz, 3H, 2-CH_3), 1.19–1.22 (m, 3H, 5′-CH_3), 1.22–1.24 (m, 3H, 10-CH_3), 1.28 (s, 3H, 6-CH_3), 1.30–1.34 (m, 1H, H-7), 1.43–1.45 (m, 1H, H-7), 1.50 (s, 3H, 12-CH_3), 1.54–1.58 (m, 1H, H-14eq), 1.90–1.92 (m, 1H, H-14ax), 1.96 (q, 1H, H-4), 2.21 (s, 6H, –N(CH_3)$_2$), 2.23–2.27 (m, 1H, H-3′), 2.48 (q, 1H, H-10), 2.71 (s, 3H, 6-OCH_3), 2.87–2.94 (m, 1H, H-2), 3.11–3.13 (m, 1H, H-2′), 3.25–3.38 (m, 3H, 2′-OH, H-5′, 3-*O*–CH=CH–C**H**$_2$–Ar), 3.48 (d, *J*=10.3 Hz, 1H, H-3), 3.54 (dd, *J*=15.8 and 7.6 Hz, 1H, 3-*O*–CH=CH–C**H**$_2$–Ar), 3.67 (d, *J*=2.7 Hz, H-5), 3.75–3.77 (m, 1H, H-8), 4.23 (d, *J*=7.5 Hz, H-1′), 4.53 (q, 1H, 3-*O*–CH=C**H**–CH_2–Ar), 4.83 (s, 1H, H-11), 6.15 (d, *J*=6.2 Hz, 1H, 3-*O*–C**H**=CH–CH_2–Ar), [7.16–7.32 (m, 7H), 7.38 (d, 1H, *J*=7.5 Hz), 7.52–7.54 (m, 1H), benzyl ring, phenyl]. Including 41% **3-*O*-[3-(1′-Phenyl)-*E*-2-propenyl]** isomer, *δ*: 6.71 (d, *J*=15.8 Hz, 1H, 3-*O*–CH_2–CH=C**H**–Ar), 6.24 (dt, 1H, 3-*O*–CH_2–C**H**=CH–Ar).

3-*O*-[3-(3′-Pyridyl)-*Z*-1-propenyl]-6-*O*-methylerythromycin A 9-*O*-(2-chlorobenzyl)oxime 11,12 -carbonate (9c)

By a similar prodedure to **9e**, **8c** was prepared as a white solid in 25.6% yield according to the general procedure for the preparation of **8e**, and then deacetylated to give **9c** (46.7%). HRMS (ESI) (M+H$^+$) *m/z* 872.44808, calcd for $C_{46}H_{67}ClN_3O_{11}$ 872.44586. ^{1}H NMR(400 MHz, $CDCl_3$) *δ*: 0.84 (t, 3H, 15-CH_3), 0.92 (d, 3H, 8-CH_3), 1.15–1.13 (m, 6H, 4-CH_3, 2-CH_3), 1.16 (d, *J*=6.1 Hz, 3H, 5′-CH_3), 1.21 (d, *J*=6.8 Hz, 3H, 10-CH_3), 1.25 (s, 3H, 6-CH_3), 1.27–1.30 (m, 1H, H-7), 1.41–1.45 (m, 1H, H-7), 1.48 (s, 3H, 12-CH_3), 1.51–1.59 (m, 2H, H-14ax, H-4′), 1.86–1.97 (m, 2H, H-14eq, H-4), 2.23 (s, 6H, –N(CH_3)$_2$), 2.28 (m, 1H, H-3′), 2.46 (q, 1H, H-10), 2.70(s, 3H, 6-OCH_3), 2.87–2.94 (m, 1H, H-2), 3.13 (dd, *J*=7.3 and 10.1 Hz, 1H, H-2′), 3.28–3.33 (m, 3H, H-5′, 2′-OH, 3-*O*–CH=CH–C**H**$_2$–Ar), 3.47–3.55 (m, 2H, H-3, 3-*O*–CH=CH–C**H**$_2$–Ar), 3.64 (d, *J*=2.7 Hz, 1H, H-5), 3.74–3.82 (m, 1H, H-8), 4.19 (d, *J*=7.2 Hz, 1H, H-1′), 4.48–4.54 (q, 1H, 3-*O*–CH=C**H**–CH_2–Ar), 4.82 (s, 1H, H-11), 5.24–5.09 (m, 3H, –C**H**$_2$–PhCl, H-13), 6.18 (d, *J*=6.0 Hz, 1H, 3-*O*–C**H**=CH–CH_2–Ar), [7.16–7.26 (m, 3H), 7.30 (dd, *J*=1.2 and 7.7 Hz, 1H), 7.50–7.52 (m, 2H), 8.41–8.47 (m, 2H), benzyl ring, pyridyl]. ^{13}C NMR(100 MHz, $CDCl_3$) *δ*: 174.3 (C-1), 165.1 (C-9), 154.6 (carbonate), 149.7, 148.5, 147.3, 136.6, 136.0, 135.6, 133.5, 130.9, 128.9, 128.6, 126.4, 123.2, 101.9, 101.6, 89.5, 84.8, 82.8, 79.7, 78.4, 75.4, 72.6, 70.3, 69.1, 65.6, 49.3, 44.5, 40.2 (–N(**C**H_3)$_2$), 37.1, 36.4, 32.8, 27.7, 25.8, 22.1, 21.1, 19.3, 18.7, 15.6, 15.4, 12.8, 10.0, 8.8.

3-*O*-allyl-6-*O*-methylerythromycin A 9-*O*-(2-chlorobenzyl)oxime 11,12-carbonate (9a)

Compound **7** was heated to reflux in MeOH for 3 h. After the solvent was evaporated, the crude product was purified by column chromatography (silica gel, 15:0.3:0.1 $CH_2Cl_2/C_2H_5OH/NH_3{\cdot}H_2O$) to give **9a** in 62.1% yield. HRMS (ESI) (M+H$^+$) *m/z* 795.42088, calcd for $C_{41}H_{64}ClN_2O_{11}$ 795.41932. ^{1}H NMR (400 MHz, $CDCl_3$) *δ*: 0.86 (t, 3H, 15-CH_3), 0.92 (d, *J*=7.0 Hz, 3H, 8-CH_3), 1.03 (d, *J*=7.5 Hz, 3H, 4-CH_3), 1.17–1.23 (m, 6H, 10-CH_3, 5′-CH_3), 1.25–1.29 (m, 6H, 2-CH_3, 6-CH_3), 1.32–1.35 (m, 1H, H-7), 1.41–1.44 (m, 1H, H-7), 1.48 (s, 3H, 12-CH_3), 1.51–1.67 (m, 2-3H, H-14ax, H-4′), 1.86–1.92 (m, 2H, H-4, H-14eq), 2.28 (s, 6H, –N(CH_3)$_2$), 2.46–2.50 (m, 2H, H-3′, H-10), 2.72 (s, 3H, 6-CH_3), 2.80–2.89 (m, 1H, H-2), 3.16 (dd, *J*=7.2 and 10.1 Hz, 1H, H-2′), 3.21–3.24 (m, 2H, H-3, 2′-OH), 3.42–3.46 (m, 1H, H-5′), 3.70 (d, *J*=3.2 Hz, 1H, H-5), 3.74–3.78 (m, 1H, H-8), 4.05–4.30 (m, 2H, –C**H**$_2$–CH=CH_2), 4.37 (d, *J*=7.2 Hz, 1H, H-1′), 4.81 (s, 1H, H-11), 5.11–5.26 (m, 5H, H-13, –C**H**$_2$–PhCl, –CH=C**H**$_2$), 5.35 (dd, *J*=1.6 and 17.2 Hz, 1H, –CH=C**H**$_2$) 5.84–5.93(m, 1H, –C**H**=CH_2), [7.17–7.26(m, 2H), 7.32 (dd, *J*=1.2 and 7.8 Hz, 1H), 7.53 (dd, *J*=1.6 and 7.5 Hz, 1H), benzyl ring].

3-*O*-allyl-6-*O*-methylerythromycin A 9-*O*-(2-chlorobenzyl)oxime (12a)

Compound **12a** was synthesized by a similar procedure to **9a** in 70.0% yield. MS(MALDI-TOF) (M+Na$^+$) *m/z* 791.2, calcd for $C_{40}H_{65}ClN_2O_{10}$ 768.4 (M). ^{1}H NMR (400 MHz, $CDCl_3$) *δ*: 0.82 (t, 3H, 15-CH_3), 0.96 (d, 3H, 8-CH_3), 1.05 (d, 3H, 4-CH_3), 1.12 (d, 3H, 10-CH_3), 1.14 (s, 3H, 12-CH_3), 1.20 (d, 3H, 5′-CH_3), 1.25 (d, 3H, 2-CH_3), 1.31 (s, 3H, 6-CH_3), 1.39–1.52 (m, 3H, H-7, H-14ax), 1.62–1.66 (m, 1H, H-4′), 1.92–2.08 (m, 2H, H-4, H-14eq), 2.27 (s, 6H, –N(CH_3)$_2$), 2.45–2.46 (m, 1H, H-3′), 2.57 (q, 1H, H-10), 2.81–2.84 (m, 1H, H-2), 2.85 (s, 3H, 6-CH_3), 3.14–3.27 (m, 4H, H-2′, H-3, 12-OH, 2′-OH), 3.42–3.46 (m, 1H, H-5′), 3.74–3.76 (m, H-5, H-8, H-11), 4.09–4.28 (m, 2H, –C**H**$_2$–CH=CH_2), 4.39 (s, 1H, 11-OH), 4.42 (d, 1H, H-1′), 5.07–5.37 (m, 5H, H-13, –C**H**$_2$–PhCl, –CH=C**H**$_2$), 5.86–5.93 (m, 1H, –C**H**=CH_2), 7.19–7.40 (m, 4H, benzyl ring]. ^{13}C NMR(100 MHz, $CDCl_3$) *δ*: 175.0, 170.8, 135.8, 134.7, 133.2, 129.6, 129.2, 128.7, 126.5, 116.0, 101.2, 84.4, 79.2, 78.3, 76.8, 74.2, 73.9, 72.6, 70.7, 70.3, 68.9, 65.3, 49.9, 44.6, 40.2, 36.9, 33.0, 28.8, 26.4, 21.3, 21.1, 19.4, 18.5, 16.0, 15.3, 15.2, 10.4, 8.6.

3-*O*-[3-(3′-Pyridyl)-*Z*-1-propenyl]-6-*O*-methylerythromycin A 9-*O*-(2-chlorobenzyl)oxime (12c)

Compound **12c** was synthesized by a similar procedure to **9c** (26.3% in two steps). HRMS (ESI) (M+H$^+$) *m/z* 846.4648, calcd for $C_{45}H_{69}ClN_3O_{10}$ 846.4666. ^{1}H NMR(400 MHz, $CDCl_3$) *δ*: 0.81 (t, 3H, 15-CH_3), 0.96 (d, 3H, 8-CH_3), 1.11–1.24 (m, 16H, 4-CH_3, 2-CH_3, 10-CH_3, 5′-CH_3, 12-CH_3, H-4′ax), 1.30 (s, 3H, 6-CH_3), 1.30–2.12 (m, 6H, H-7, H-14ax, H-4′eq, H-14eq, H-4), 2.30 (s, 6H, –N(CH_3)$_2$), 2.31–2.34 (m, 1H, H-3′), 2.56 (q, 1H, H-10), 2.87 (s, 3H, 6-OCH_3), 2.88–2.91 (m, 1H, H-2), 3.31–3.54 (m, 7H, H-5′, H-2′, 12-OH, 2′-OH, 3-*O*–CH=CH–C**H**$_2$–Ar, H-3), 3.67 (m, 3H, H-5, H-8, H-11), 4.22 (d, *J*=7.3 Hz, 1H, H-1′), 4.42 (s, 1H, 11-OH), 4.50 (q, 1H, 3-*O*–CH=C**H**–CH_2–Ar), 5.06–5.21 (m, 3H, –C**H**$_2$–PhCl, H-13), 6.20 (d, *J*=6.1 Hz, 1H, 3-*O*–C**H**=CH–CH_2–Ar), 7.20–8.49 (m, 8H, benzyl ring, pyridyl).

3-*O*-[3-(5′-Pyrimidyl)-*Z*-1-propenyl]-6-*O*-methylerythromycin A 9-*O*-(2-chlorobenzyl)oxime (12d)

Compound **12d** was synthesized by a similar procedure to **9d** (12.2% in two steps). HRMS (ESI) (M+H$^+$) *m/z* 847.4612, calcd for $C_{44}H_{68}ClN_4O_{10}$ 847.4618. ^{1}H NMR (400 MHz, $CDCl_3$), *δ*: 0.81 (t, 3H, 15-CH_3), 0.97 (d, 3H, 8-CH_3), 1.11–1.24 (m, 16H, 4-CH_3, 2-CH_3, 10-CH_3, 5′-CH_3, 12-CH_3, H-4′ax), 1.27 (s, 3H, 6-CH_3), 1.30–2.20 (m, 6H, H-7, H-14ax, H-4′eq, H-14eq, H-4), 2.38

(s, 6H, –$N(CH_3)_2$), 2.46 (m, H-3′), 2.56 (q, 1H, H-10), 2.87 (s, 3H, 6-OCH_3), 2.88–2.91 (m, 1H, H-2), 3.23–3.54 (m, 7H, H-5′, H-2′, 12-OH, 2′-OH, 3-*O*–CH=CH–C**H**$_2$–Ar, H-8), 3.67 (d, *J*=2.8 Hz, 1H, H-5), 3.74–3.76 (m, 2H, H-3, H-11), 4.20 (d, *J*=7.2 Hz, 1H, H-1′), 4.41 (s, 1H, 11-OH), 4.50 (q, 1H, 3-*O*–CH=C**H**–CH_2–Ar), 5.07–5.20 (m, 3H, H-13, –C**H**$_2$–PhCl), 6.25 (d, *J*=6.0 Hz, 1H, 3-*O*–C**H**=CH–CH_2–Ar), 7.19–7.41 (m, 4H, benzyl ring], [8.62 (s, 2H), 9.06 (s, 1H), pyrimidyl].

3-*O*-[3-(3′-Quinolyl)-*Z*-1-propenyl]-6-*O*-methylerythromycin A 9-*O*-(2-chlorobenzyl)oxime (12e)

Compound **12e** was synthesized by a similar procedure to **9e** (45.0% in two steps). HRMS (ESI) ($M+H^+$) *m/z* 896.4802, calcd for $C_{49}H_{71}ClN_3O_{10}$ 896.4822. ^{1}H NMR (400 MHz, $CDCl_3$) δ: 0.82 (t, 3H, 15-CH_3), 0.97 (d, 3H, 8-CH_3), 1.11–1.27 (m, 16H, 4-CH_3, 2-CH_3, 10-CH_3, 5′-CH_3, 12-CH_3, H-4′ax), 1.30 (s, 3H, 6-CH_3), 1.30–2.20 (m, 6H, H-7, H-14ax, H-4′eq, H-14eq, H-4), 2.22–2.32 (m, 7H, –$N(CH_3)_2$, H-3′), 2.57 (q, 1H, H-10), 2.89 (s, 3H, 6-OCH_3), 2.89–2.96 (m, 1H, H-2), 3.17 (dd, 1H, H-2′), 3.26 (s, 1H, 12-OH), 3.28–3.55 (m, 4H, H-5′, 3-*O*–CH=CH–C**H**$_2$–Ar, H-3), 3.71–3.78 (m, 3H, H-5, H-11, H-8), 4.24 (d, *J*=7.4 Hz, 1H, H-1′), 4.43 (s, 1H, 11-OH), 4.59 (q, 1H, 3-*O*–CH=C**H**–CH_2–Ar), 5.07–5.22 (m, 3H, –C**H**$_2$–PhCl, H-13), 6.27 (d, *J*=6.1 Hz, 1H, 3-*O*–C**H**=CH–CH_2–Ar), 7.21–7.42 (m, 4H, benzyl ring), 7.53–8.83(m, 6H, quinolyl).

3-*O*-[3-(4′-Isoquinolyl)-*Z*-1-propenyl]-6-*O*-methylerythromycin A 9-*O*-(2-chlorobenzyl)oxime (12f)

Compound **12f** was synthesized by a similar procedure to **9f** (26.2% in two steps). HRMS (ESI) ($M+H^+$) *m/z* 896.4819, calcd for $C_{49}H_{71}ClN_3O_{10}$ 896.4822. ^{1}H NMR (400 MHz, $CDCl_3$) δ: 0.83 (t, 3H, 15-CH_3), 0.93 (d, *J*=6.9 Hz, 3H, 8-CH_3), 0.97 (d, 3H, 8-CH_3), 1.11–1.27 (m, 16H, 4-CH_3, 2-CH_3, 10-CH_3, 5′-CH_3, 12-CH_3, H-4′ax), 1.32 (s, 3H, 6-CH_3), 1.30–2.20 (m, 6H, H-7, H-14ax, H-4′eq, H-14eq, H-4), 2.23 (s, 6H, –$N(CH_3)_2$), 2.25–2.26 (m, 1H, H-3′), 2.58 (q, 1H, H-10), 2.89 (s, 3H, 6-OCH_3), 2.97–2.99 (m, 1H, H-2), 3.15–3.27 (m, 4H, H-2′, H-5′, 12-OH, 2′-OH), 3.57 (d, *J*=10.2 Hz, 1H, H-3), 3.58–3.98 (m, 5H, H-11, H-5, H-8, 3-*O*–CH=CH–C**H**$_2$–Ar), 4.29 (d, *J*=7.2 Hz, 1H, H-1′), 4.41 (s, 1H, 11-OH), 4.57 (q, 1H, 3-*O*–CH=C**H**–CH_2–Ar), 5.07–5.23 (m, 3H, –C**H**$_2$–PhCl, H-13), 6.22 (d, *J*=6.1 Hz, 1H, 3-*O*–C**H**=CH–CH_2–Ar), 7.21–7.42 (m, 4H, benzyl ring), 7.61–9.14 (m, 6H, isoquinolyl).

Crystallographic data for the structure of **9f** in this paper have been deposited with the Cambridge Crystallographic Data Centre as supplementary publication number CCDC 729701. Copies of the data can be obtained, free of charge, on application to CCDC, 12 Union Road, Cambridge CB2 1EZ, UK [fax: +44 (0) 1223-336033 or E-mail: deposit@ccdc.cam.ac.uk].

ACKNOWLEDGEMENTS

This research was supported by the National Natural Science Foundation of China (20602002). We thank Prof. Xiang Hao and Ms. Tong-Ling Liang, Institute of Chemistry Chinese Academy of Sciences, for single X-ray crystal structure determination.

1 Kurath, P., Jones, P. H., Egan, R. S. & Perun, T. J. Acid degradation of erythromycin A and erythromycin B. *Experientia* **27,** 362 (1971).
2 Watanabe, Y., Morimoto, S., Adachi, T., Kashimura, M. & Asaka, T. Chemical modification of erythromycins. 9. Selective methylation the C-6 hydroxyl group of erythromycin A oxime derivatives and preparation of clarithromycin. *J. Antibiot.* **46,** 647–660 (1993).
3 Plata, D. J. *et al.* The synthesis of ketolide antibiotic ABT-773 (cethromycin). *Tetrahedron* **60,** 10171–10180 (2004).
4 Ma, Z. *et al.* Novel erythromycin derivatives with aryl groups tethered to the C-6 position are potent protein synthesis inhibitors and active against multidrug-resistant respiratory pathogens. *J. Med. Chem.* **44,** 4137–4156 (2001).
5 Clark, R. F. *et al.* Synthesis and antibacterial activity of novel 6-O-substituted erythromycin A derivatives.. *Bioorg. Med. Chem. Lett.* **10,** 815–819 (2000).
6 Agouridas, C. *et al.* Synthesis and antibacterial activity of ketolides (6-O-methyl-3-oxoerythromycin derivatives): a new class of antibacterials highly potent against macrolide-resistant and -susceptible respiratory pathogens. *J. Med. Chem.* **41,** 4080–4100 (1998).
7 Tanikawa, T. *et al.* Synthesis and antibacterial activity of acylides (3-O-acyl-erythromycin derivatives): a novel class of macrolide antibiotics. *J. Med. Chem.* **44,** 4027–4030 (2001).
8 Tang, D. *et al.* Design, synthesis, and antibacterial activities of novel 3,6-bicyclolide oximes: length optimization and zero carbon linker oximes. *Bioorg. Med. Chem. Lett.* **18,** 5078–5082 (2008).
9 Elliott, R. L. *et al.* Anhydrolide macrolides. 1. Synthesis and antibacterial activity of 2,3-anhydro-6-O-methyl 11,12-carbamate erythromycin A analogues. *J. Med. Chem.* **41,** 1651–1659 (1998).
10 Denis, A. *et al.* Beta-keto-ester chemistry and ketolides. Synthesis and antibacterial activity of 2-halogeno, 2-methyl and 2,3 enol-ether ketolides. *Bioorg. Med. Chem. Lett.* **10,** 2019–2022 (2000).
11 Elliott, R. L. *et al.* Novel 3-deoxy-3-descladinosyl-6-O-methyl erythromycin A analogues. Synthesis and in vitro activity. *Bioorg. Med. Chem. Lett.* **7,** 641–646 (1997).
12 Misawa, Y., Asaka, T., Kashimura, M., Morimoto, S. & Hatayama, K. 5-O-desosaminylerythronolide derivative EP 682, 038 24 January (1994).
13 Cheng, H. M. *et al.* Synthesis and SAR of azalide 3,6-ketal aromatic derivatives as potent gram-positive and gram-negative antibacterial agents. *Bioorg. Med. Chem. Lett.* **12,** 2431–2434 (2002).
14 Heggelund, A. & Undheim, K. Descladinosyl erythromycin in phosgene-assisted cyclic 3,6-ether formation. *Tetrahedron Lett.* **49,** 5569–5571 (2008).
15 Douthwaite, S., Hansen, L. H. & Mauwais, P. Macrolide-ketolide inhibition of MLS-resistant ribosomes is improved by alternative drug interaction with domain II of 23S rRNA. *Mol. Microbiol.* **36,** 183–192 (2000).
16 Furuuchi, T. *et al.* Design and synthesis of novel leucomycin analogues modified at the C-3 position. Part II: 3-O-(3-Aryl-2-propenyl)leucomycin analogues. *Bioorg. Med. Chem.* **16,** 4401–4418 (2008).
17 Watanabe, Y. *et al.* Chemical modification of erythromycins. 12. A facile synthesis of clarithromycin (6-O-methylerythromycin A) via 2′-silylethers of erythromycin A derivatives. *J. Antibiot.* **46,** 1163–1167 (1993).
18 Clinical and Laboratory Standards Institute. *Methods for Dilution Antimicrobial Susceptibility Tests for Bacteria that Grow Aerobically. Approved Standard M7-A7*, Seventh Edition, Clinical and Laboratory Standards Institute, Wayne, PA, (2006).

The Journal of Antibiotics (2009) 62, 613–619

www.nature.com/ja

ORIGINAL ARTICLE

Nocardithiocin, a novel thiopeptide antibiotic, produced by pathogenic *Nocardia pseudobrasiliensis* IFM 0757

Akira Mukai[1], Toshio Fukai[2,5], Yasutaka Hoshino[3], Katsukiyo Yazawa[1], Ken-ichi Harada[4] and Yuzuru Mikami[1]

Nocardithiocin is a novel thiopeptide compound produced by the pathogenic *Nocardia pseudobrasiliensis* strain IFM 0757. It shows a strong activity against acid-fast bacilli such as the *Mycobacterium* and *Gordonia* species. Nocardithiocin was highly active against rifampicin-resistant as well as -sensitive *Mycobacterium tuberculosis* strains, and most of the resistant strains were inhibited at concentrations ranging from 0.025 to 1.56 μg ml^{-1}. The structure of the thiopeptide antibiotic containing thiazole, natural and unnatural amino acids was elucidated by MS and NMR spectral analyses.
The Journal of Antibiotics (2009) **62,** 613–619; doi:10.1038/ja.2009.90; published online 11 September 2009

Keywords: *Nocardia*; nocardithiocin; pathogenic actinomycetes; rifampicin-resistant mycobacteria; thiopeptide

INTRODUCTION

Actinomycetes produce numerous secondary metabolites including various biologically active compounds such as antimicrobial, cytotoxic, immunosuppressive and antifungal agents.[1] As the potential to isolate useful new antibiotics from *Streptomyces* sp. is now low and diminishing all the time, we have focused our attention on other sources. Pathogenic actinomycetes are distributed on a limited basis in the natural environment and are difficult to isolate. They can be considered among the rare actinomycetes and represent a relatively unexplored resource for the discovery of new bioactive compounds. We have collected many pathogenic actinomycetes from clinical materials, which mainly belong to the genus of *Nocardia* and may cause human infections called nocardiosis.[2,3] They have produced several biologically active compounds such as antitumor and immunosuppressive ones.[4,5]

During our ongoing research for new metabolites from a *Nocardia* strain (IFM 0757 strain) obtained from a patient at the Health Center, University of Texas, we isolated a new cyclic thiopeptide antibiotic with potent antibacterial activity against rifampicin-resistant *Mycobacterium tuberculosis*, called nocardithiocin (Figure 1), which was classified as a 'series *d*' group peptide antibiotic based on the definition by Bagley *et al.*[6] Cyclic thiopeptides are known as activators of thiostrepton-induced protein A, which is a member of the mercury resistance regulator family, and are active against Gram-positive bacteria.[3,7] In this paper, we describe the fermentation, isolation, structure elucidation and antimicrobial activities of the antibiotic.

RESULTS

Isolation

The separation of the active compounds was monitored by the antimicrobial activity against *Corynebacterium xerosis* IFM 2057.[8] After incubation, the culture broth was centrifuged at 3000 r.p.m. for 10 min. Six hundred milliliters of MeOH was then added to the mycelial cake and stirred for 3 hours. The MeOH fraction was filtered, evaporated to dryness and suspended in distilled water. The active compound was then extracted with EtOAc. The compound was further purified by HPLC. The isolation was carried out under dark conditions because the antibiotic was not stable in the light.

Structure elucidation

The physicochemical data for nocardithiocin are shown in Table 1. The positive ion FAB mass spectrum (JMS-AX500) of nocardithiocin showed a protonated molecule $[M+H]^+$ at *m/z* 1161. HRFAB-MS (JMS-HX110) displayed the $[M+K]^+$ ion at *m/z* 1199.1469 (calcd. 1199.1527). The molecular formula was determined to be $C_{48}H_{48}N_{12}O_{11}S_6$ based on the HRFAB-MS data by considering the number of protons and carbons from the NMR spectra. In the ^{1}H-NMR spectrum, one singlet and four doublet signals assigned to five methyl groups were observed between δ 0.86–1.78, and two singlet signals (δ 3.70 and 3.97) were assigned to methoxyl groups. Amino acid moiety α-proton signals were also observed at δ 4.52 (H-46), 5.11 (H-32) and 5.56 (H-22). Thirteen sp^2 proton signals and amido proton signals were detected between δ 8.06–9.52. The ^{13}C-NMR spectrum showed 48 signals that were assigned to eight methyl, 15

[1]Medical Mycology Research Center, Chiba University, Chuo-ku, Chiba, Japan; [2]School of Pharmaceutical Sciences, Toho University, Funabashi, Chiba, Japan; [3]Department of Bioactive Molecules, National Institute of Infectious Diseases, Shinjuku-ku, Tokyo, Japan and [4]Graduate School of Environmental and Human Science & Faculty of Pharmacy, Meijo University, Tempaku, Nagoya, Japan
[5]Current address: Department of Health Pharmacy, Yokohama College of Pharmacy, 601 Matano-cho, Totsuka-ku, Yokohama, Kanagawa 245-0066, Japan
Correspondence: Dr K-i Harada, Graduate School of Environmental and Human Science & Faculty of Pharmacy, Meijo University, Tempaku, Nagoya 468-8503, Japan.
E-mail: kiharada@ccmfs.meijo-u.ac.jp
Received 18 June 2009; revised 13 August 2009; accepted 13 August 2009; published online 11 September 2009

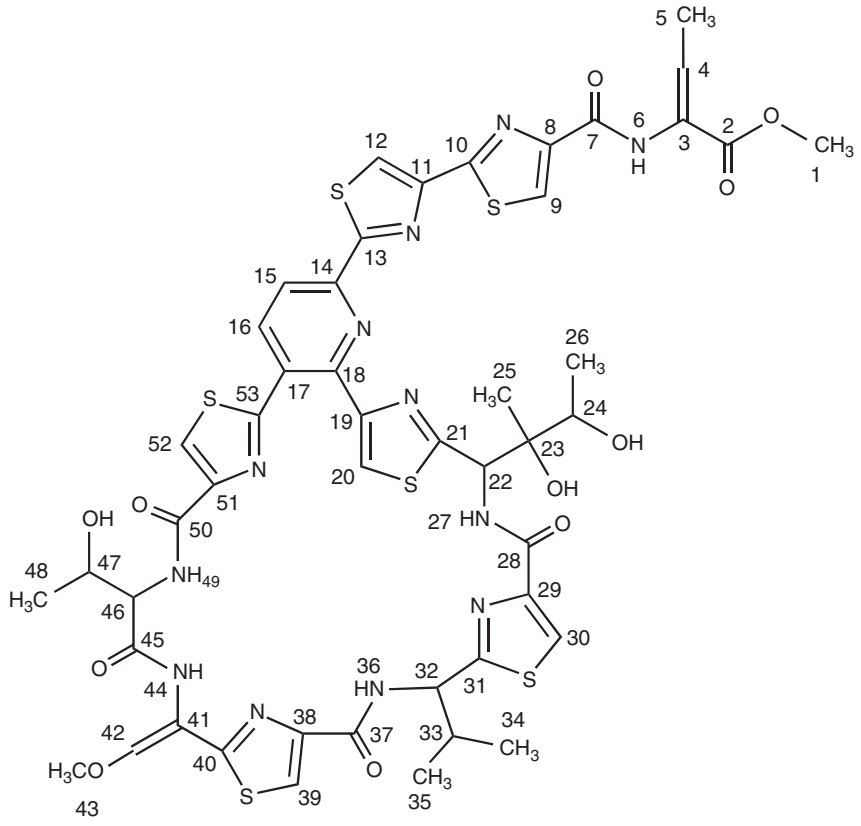

Figure 1 Structure of nocardithiocin.

Table 1 The physicochemical data of nocardithiocin

Appearance	White powder
Molecular weight	1160
Molecular formula	$C_{48}H_{48}N_{12}O_{11}S_6$
HRFAB-MS (m/z)	
Found:	1199.1469 $[M+K]^+$
Calcd.:	1199.1527
IR λ_{max} ($CHCl_3$)	3728, 3699, 3628, 3596, 3383, 3113, 2961, 2269, 1665, 1533, 1477, 1273, 1236, 1273, 1236, 1148, 1067, 743, 675
$[\alpha]_D$ (23.2 °C, MeOH)	+34.0° (c 1 mg ml^{-1}, MeOH)
UV λ_{max} (MeOH) nm (log ε)	344.5 (3.89), 339.5 (3.97), 232.0 (4.25)

methine, and 25 quaternary carbons by heteronuclear multiple quantum coherence and distortionless enhancement by polarization transfer experiments (Table 2). The C–H connectivity and assignment of the signals were confirmed by 2D NMR experiments using ^{1}H–^{1}H COSY and heteronuclear multiple bond coherence (HMBC) techniques as follows:

Thiazole units

The thiazole units were contained in substructures B, C and D (Figure 2), and the whole structure was deduced by comparison with those of the corresponding ^{1}H and ^{13}C chemical shifts with those reported for promoinducin,[9] nocathiacins[10] and radamycin.[11] As a result, six thiazole units were determined by the following long-range correlations; in the HMBC spectrum, the thiazole ring proton signal at δ 8.43 (H-9) showed long-range couplings to carbons at δ 149.8 (C-10) and 161.5 (C-8), H-12 signal at δ 8.56 to δ 149.2 (C-11) and 168.2 (C-13), H-20 signal at δ 8.15 to δ 151.6 (C-19) and 169.0 (C-21), H-30 signal at δ 8.22 to δ 149.1 (C-29) and δ 170.3 (C-31), H-39 signal at δ 8.24 to 146.7 (C-38) and 160.3 (C-40), and H-52 signal at δ 8.14 to δ 149.2 (C-51) and 163.5 (C-53).

Substructure A

Substructure A was a terminal moiety of the side chain (Figure 2). In the COSY spectrum, CH_3-5 (δ 1.78) correlated with the olefinic proton at δ 6.76 (H-4) and showed a long-range correlation to the quaternary carbon at δ 127.3 (C-3). Furthermore, in the HMBC spectrum, the H-4 proton showed a long-range correlation to the carbonyl carbon at δ 164.3 (C-2), which showed a long-range correlation from the *O*-methyl proton at δ 3.70 (CH_3-1). An amide proton (disappearing with the addition of CD_3OD) at δ 9.52 (H-6) was correlated to C-2 and C-4, indicating the presence of substructure A.

Substructure B

Substructure B contained a pyridine ring and four thiazole rings. The *ortho*-coupled aromatic protons at δ 8.34 (H-15) and 8.53 (H-16), respectively, were connected by the COSY spectrum. H-16 showed long-range correlations to δ 149.6 (C-14) and 150.9 (C-18), and a long-range coupling from H-15 to δ 128.6 (C-17) was observed. These data revealed the presence of a pyridine ring. The methyl proton signal at δ 1.00 (H-26) showed long-range couplings to the oxygenated

Table 2 ^{1}H and ^{13}C NMR spectral data of nocardithiocin in DMSO-d_6

Position	*δc*	*δ_H, J (Hz)*	*Position*	*δc*	*δ_H, J (Hz)*
1	51.7	3.70 (s)	27		8.17 (d, 9.5)
2	164.3		28	159.9	
3	127.3		29	149.1	
4	134.0	6.76 (q, 7)	30	124.2	8.22 (s)
5	13.6	1.78 (s)	31	170.3	
6		9.52 (s)	32	55.5	5.11 (dd, 8, 0.5)
7	158.9		33	31.0	2.65 (m)
8	161.5		34	17.8	0.88 (d, 7)
9	125.4	8.43 (s)	35	19.6	0.86 (d, 7)
10	149.8		36		8.48 (d, 9.5)
11	149.2		37	160.1	
12	121.5	8.56 (s)	38	146.7	
13	168.2		39	124.0	8.24 (s)
14	149.6		40	160.3	
15	118.5	8.34 (d, 8)	41	111.5	
16	140.1	8.53 (d, 8)	42	152.0	7.30 (s)
17	128.6		43	61.6	3.97 (s)
18	150.9		44		9.33 (s)
19	151.6		45	169.8	
20	121.7	8.15 (s)	46	58.7	4.52
21	169.0		47	66.9	4.36 (m)
22	54.9	5.56 (d, 9.5)	OH		5.21 (d, 6)
23	75.2		48	20.0	1.27 (d, 6)
OH		4.37 (s)	49		8.06 (d, 8)
24	69.5	3.66 (m, 6)	50	160.1	
OH		4.52 (d, 5.5)	51	149.2	
25	19.5	0.90 (s)	52	125.9	8.14 (s)
26	17.2	1.00 (d, 6.5)	53	163.5	

methine carbon at δ 69.5 (C-24) and oxygenated quaternary carbon at δ 75.2 (C-23). Moreover, long-range correlations from the methyl proton signal at δ 0.90 (CH_3-25) to C-23, C-24 and C-22 (δ 54.9) were observed. The methine proton at δ 5.56 (H-22) was coupled to an amide proton at δ 8.17 (H-27) and showed a long-range correlation to δ 169.0 (C-21), which was a part of the thiazole unit, indicating the presence of the thiostreptin unit.[12] The proton signal of the thiazole unit at δ 8.15 (H-20) showed long-range coupling to δ 150.9 (C-18), which was C-2 of the pyridine unit. Furthermore, long-range coupling from the proton signal of the pyridine unit at δ 8.53 (H-16) to the quaternary carbon of the thiazole unit at δ 163.5 (C-53), and from H-15 at δ 8.34 to δ 168.2 (C-13) was observed. The presence of the long-range couplings from the proton signal of the third thiazole unit at δ 8.56 (H-12) to δ 149.8 (C-10), H-9 (δ 8.43) to the carbonyl carbon at δ 158.9 (C-7), and from the olefinic proton of the fourth thiazole unit at δ 8.14 (H-52) to the carbonyl carbon at δ 160.1 (C-50) indicated the presence of substructure B.

Substructure C

In the COSY spectrum, vicinal coupling signals were detected between the methyl protons at δ 0.86 (CH_3-35)/δ 0.88 (CH_3-34) and the methine proton at δ 2.65 (H-33), H-33 and the methine proton at δ 5.11 (H-32), and the H-32 and the amide proton at δ 8.48 (H-36). Furthermore, the HMBC spectrum revealed the presence of substructure C by the long-range correlations from CH_3-35 to the methyl carbon at δ 17.8 (C-34), H-32 to a quaternary carbon of the thiazole ring at δ 170.3 (C-31), and H-30 to the carbonyl carbon at δ 159.9 (C-28).

Substructure D

Substructure D was determined by the HMBC spectrum, which showed long-range coupling from an oxygenated methyl proton at δ 3.97 (H_3-43) to an olefinic carbon at δ 152.0 (C-42), and long-range correlations from the olefinic proton at δ 7.30 (H-42) to a quaternary carbon of the thiazole ring at δ 160.3 (C-40) and an olefinic carbon at δ 111.5 (C-41), an amide proton at δ 9.33 (H-44) to C-42, and the olefinic proton of the thiazole ring at δ 8.24 (H-39) to δ 160.1 (C-37).

Substructure E

Vicinal coupling signals in the COSY spectrum were observed between the methyl group at δ 1.27 (H-48) and the methine proton at δ 4.36 (H-47), H-47 and the hydroxy proton at δ 5.21,the methine proton at δ 4.52 (H-46) and H-46 and an amide proton at δ 8.06 (H-49). The long-range couplings in the HMBC spectrum from CH_3-48 to C-46 and H-46 to a carbonyl carbon at δ 169.8 (C-45) revealed the presence of the threonine moiety in Substructure E.

Finally, each substructure was connected by the long-range correlations of the HMBC technique from the amide proton (H-6) to the carbonyl carbon (C-7), H-22 to C-28, H-32 to C-37, H-44 to C-45 and H-49 to C-50. Thus, the planar structure of nocardithiocin was determined as shown in Figure 1 and the ^{1}H and ^{13}C-NMR spectral data of nocardithiocin are summarized in Table 2.

Stereochemistry

To determine the absolute configurations of substructures C and E, the advanced Marfy method[13,14] was performed. Nocardithiocin was first hydrolyzed with 6 M HCl and the liberated threonine (substructure E) and the valine-derived thiazole moiety (substructure C) were derivatized with 1-fluoro-2,4-dinitrophenyl-5-L-leucineamide (L-FDLA) and D-FDLA. Figure 3 shows the HPLC chromatograms of the 2,4-dinitrophenyl-5-L-leucineamide (DLA) derivatives ((A) with L-FDLA and (B) with D-FDLA) of the hydrolyzate. Two desired peaks were observed together with large amounts of the residual reagent and related compounds (*). Furthermore, an intense peak was also found at around 4 min. These derivatives were also analyzed by LC/MS at *m/z* 414 and 459 in the positive ion mode (Figure 4).[15] Using the DL-FDLA method,[16] it was possible to conclude that the two amino acids have the L configuration. It was also found that the intense peak observed at around 4 min shown in Figure 3 has a molecular weight of 616. The geometries of the double bonds in substructures A and D and the absolute configuration of substructure B could not be determined in this study.

Antimicrobial activity

Nocardithiocin showed a strong antimicrobial activity against acid-fast bacteria but its activity against other Gram-positive microorganisms was moderate. The MIC values of the antibiotic against *Corynebacterium xerosis* and *Gordonia bronchialis* were <0.0078 and $0.039\,\mu g\,ml^{-1}$, respectively (Table 3). As shown in Table 4, nocardithiocin showed a strong antimicrobial activity against the rifampicin-resistant strains of *M. tuberculosis* as well as the susceptible ones, and their MIC values were $0.025–6.25\,\mu g\,ml^{-1}$ and $0.025–>6.25\,\mu g\,ml^{-1}$, respectively. In the comparison of the antimicrobial activity of nocardithiocin with the reference drug of levofloxacin against rifampicin-susceptible as well as rifampicin-resistant mycobacteria, nocardithiocin was found to show an activity higher than that of levofloxacin. Nocardithiocin did not show any antimicrobial activities against gram-negative bacteria and fungi (Table 3). The cytotoxicity of nocardithiocin against LH-60 was $64\,\mu g\,ml^{-1}$ (data not shown).

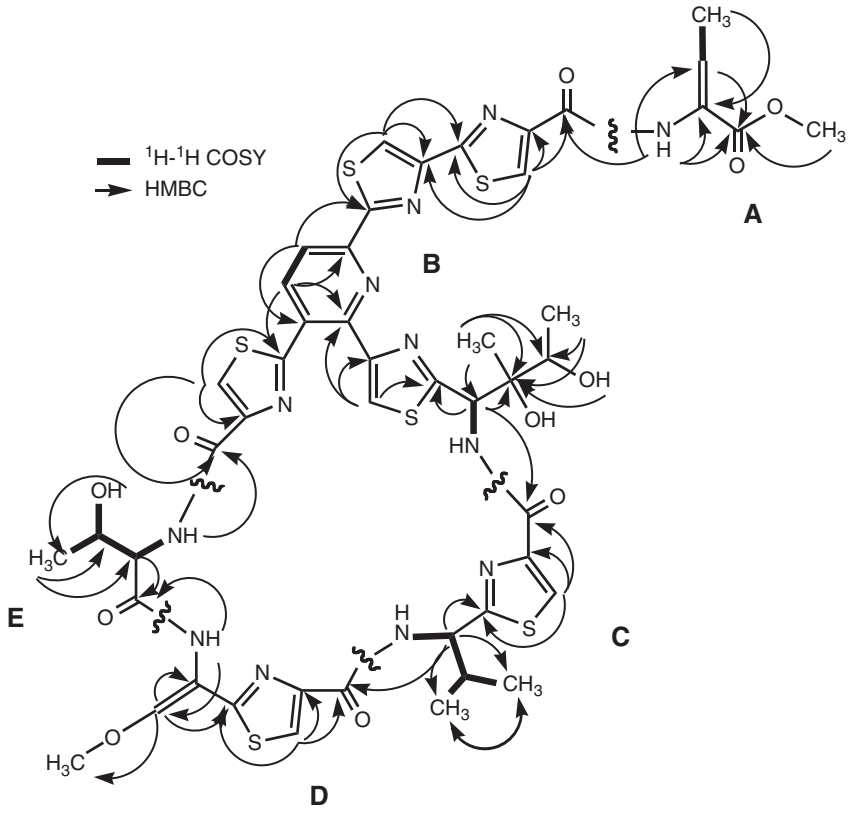

Figure 2 COSY and HMBC correlations of nocardithiocin.

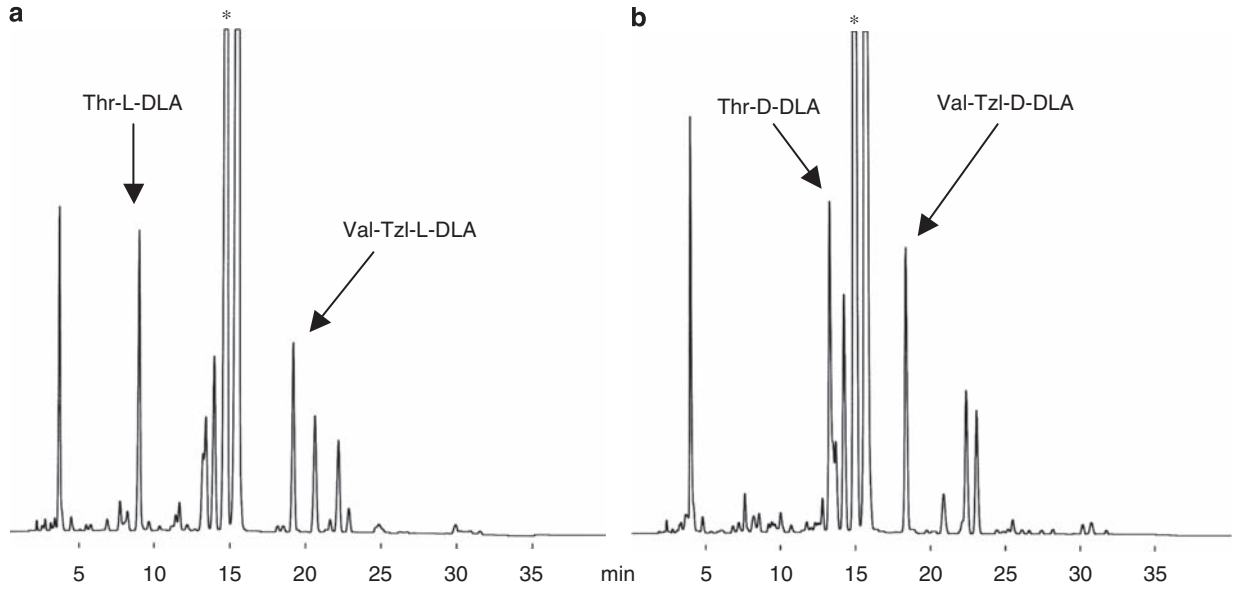

Figure 3 HPLC chromatograms of the DLA (2,4-dinitrophenyl-5-L-leucineamide) derivatives of the reaction mixture with (**a**) L-FDLA and (**b**) D-FDLA. Asterisks indicate residual reagent and related compounds.

DISCUSSION

During our continuing studies of biologically active compounds from pathogenic actinomycetes, we have isolated many biologically active compounds from the *Nocardia* species. According to a review by Bagley *et al*.,[6] the first thiopeptides produced by the *Nocardia* species to be identified were the nocathiacins, which belonged to series *e* because they possessed a tetrasubstituted hydroxypyridine as the central heterocyclic domain. In this study, *Nocardia pseudobrasiliensis* (IFM 0757) obtained from a patient at the Health Center, University of Texas, was studied. The strain produced several active compounds, of which nocardicyclin A was characterized as a broth metabolite[17] and nocardithiocin as a metabolite associated with the mycelium.

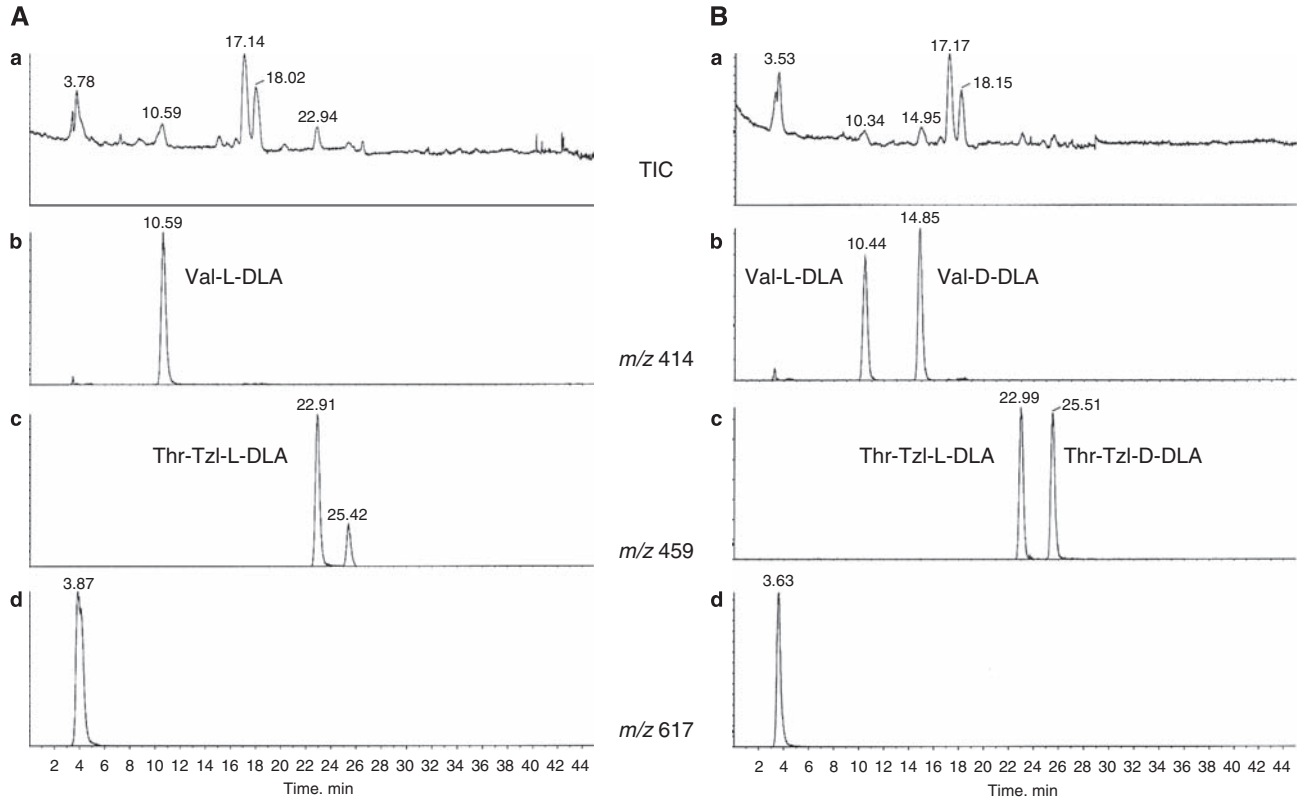

Figure 4 LC/MS data of the DLA derivatives of the reaction mixture with (**A**) L-FDLA and (**B**) L- + D-FDLA: (a) Total ion current chromatogram (TIC); (b) mass chromatogram at *m/z* 414; (c) mass chromatogram at *m/z* 459; (d) mass chromatogram at *m/z* 617.

Table 3 ***In vitro*** **antimicrobial activity of nocardithiocin**

Test organisms	*MIC values* ($\mu g\,ml^{-1}$)
Micrococcus luteus	>133
Bacillus subtilis	>133
Gordonia bronchialis	0.03
Corynebacterium xerosis	<0.0078
Mycobacterium smegmatis	0.062
Nocardia asteroides	0.062
Escherichia. coli	>133
Candida albicans	>133
Cryptococcus neoformans	>133
Aspergillus niger,	>133
Paecilomyces variotii,	>133
Trichophyton mentagrophytes	>133

2% MeOH was added in broth to increase solubility of nocardithiocin.

The latter structurally belongs to the thiopeptide group of antibiotics and was classified into series *d*, because it has a 2,3,6-trisubstituted pyridine domain as shown in Figure 1. The identification of nocardithiocin was the second example of a thiopeptide from a *Nocardia* species. Nocardithiocin has a very similar thiopeptide nucleus to micrococcins P1 and P2 but differs in having a side chain terminating in an *O*-methyl moiety (substructure A) and subtle differences to the thiopeptide ring substructures termed substructures B and D.[6] Although the absolute configurations of C-32, -46 and -47 were firmly determined to be *S*, *S* and *R*, respectively, by advanced Marfey's method, those of C-23 and C-24 still remained unsolved. As mentioned above, the compound was slightly sensitive to light and the cause of this instability is currently under investigation.

During our screening program of antimicrobial compounds, we have found and reported a new anthracycline type antibiotic called nocardicyclin. The structures were characterized by 1- and 8-methyl groups, a 10-carbonyl group and novel carbon-methylated amino sugar constituent.[17] Although the antibiotics exerted a cytotoxic activity against leukemia in mice, they showed anti-Gram-positive bacteria, especially a strong antimycobacterial activity. We also reported a new siderophore and a benzonoid compound called asterobactin and nocaracins, respectively.[18,19] Interestingly, both the siderophore and benzonoid compounds also showed strong antimycobacterial activity. These studies suggested to us that the *Nocardia* strains are useful sources for new antimycobacterial compounds. Indeed, this study showed that a pathogenic *Nocardia* strain produced a unique antibiotic, nocardithiocin. Although the reason for higher productivity of the antimycobacterial substances in *Nocardia* strains is not clear, it may be because of the high similarity of *Nocardia* to *Mycobacterium* strains regarding their physiological characteristics such as cell membrane or cell wall permeability. Both genera belong to a special bacterial group of acid-fast bacteria.

METHODS

Instrumentation

The NMR experiments were performed using JEOL-A400, -EXP-500 and -A600 spectrometers (Tokyo, Japan) in DMSO-d_6 or CD_3OD at 40 °C. The MS spectra were measured by JEOL-HX110 and JEOL-JMS-AX500 spectrometers for the FABMS and a Finnigan MAT TSQ700 (San Jose, CA, USA) for the ESI LC/MS. High-resolution MS spectra were obtained using a JEOL-HX110 under FAB

Table 4 Antimicrobial activities of nocardithiocin against rifampicin-susceptible and -resistant *Mycobaterium tuberculosis*, and *M. avium* and *M. intracellulare*

		MIC ($\mu g\,ml^{-1}$)		
Test organisms	*Strain no.*	*Nocardithiocin*	*LVFX*	*RFP*
M. tuberuclosis	H37Rv	0.78	0.39	0.39
Rifampicin-susceptible	40	0.78	0.2	0.1
	41	0.025	0.1	≦0.006
	43	0.78	3.13	6.25
	47	0.78	3.13	25
	68	1.56	0.39	3.13
	2	1.56	0.2	0.2
	3	1.56	0.39	0.2
	4	1.56	0.39	0.2
	5	6.25	0.2	0.39
	6	6.25	0.39	0.39
	7	6.25	0.39	0.39
	8	1.56	0.2	0.1
	9	3.13	0.39	0.2
Rifampicin-resistant	45	0.78	6.25	>100
	50	0.78	0.39	>100
	51	1.56	3.13	100
	56	0.025	6.25	>100
	71	>6.25	3.13	>100
	97	0.39	6.25	>100
	1	0.78	25	50
	3	1.56	3.13	>100
	4	0.39	6.25	>100
	5	0.025	25	>100
	7	>6.25	3.13	>100
	9	0.39	3.13	>100
	12	1.56	3.13	>100
M. avium	N-357	>6.25	3.13	50
	N-458	>6.25	1.56	>100
	N-444	>6.25	12.5	12.5
	N-472	>6.25	50	25
M. intracellulare	N-294	>6.25	12.5	3.13
	N-313	1.56	6.25	0.78
	N-338	>6.25	12.5	3.13
	N-345	>6.25	25	3.13

Abbreviations: LVFX, levofloxacin; MIC, minimum inhibitory concentration.

conditions. The UV spectra were recorded on a Shimadzu UV-2100 (Kyoto, Japan). The optical rotations were measured by a Jasco DIP-370 polarimeter (Tokyo, Japan). HPLC was carried out using the following two systems: pump; Shimadzu LC-9A, detector, Shimadzu SPD-10A (UV-VIS) or Shimadzu SPD-M10A (diode array) and pump; TOSOH CCPS, detector; TOSOH UV-8020 (Tokyo, Japan).

Fermentation

The seed broth was prepared by inoculating mycelial elements of *Nocardia pseudobrasiliensis* IFM 0757 grown on the Brain Heart Infusion broth (BHI: Difco Laboratories, Detroit, MI, USA) in 10 ml with 2% glucose in a 50 ml Erlenmeyer shake flask. The culture was incubated on a rotary shaker at 250 r.p.m. for 4 days. Ten percent of the inoculum was transferred to a 500 ml Erlenmeyer shake flask containing 100 ml of the production medium (two times concentrated nutrient broth medium, Difco Laboratories) and the culture was incubated on a rotary shaker at 250 r.p.m. for 7 days.

Isolation

After centrifugation of the culture broth (2 l), the mycelia were subjected to extraction by MeOH with stirring. The extract was evaporated and the residue was subjected to liquid–liquid extraction with EtOAc and water. The EtOAc fraction was evaporated and the residue was separated by the following HPLC procedure under dark conditions to provide nocardithiocin in a pure state (10.5 mg): column, Cosmosil 5C18-ARII (250×10 mm ID, Nacalai Tesque, Kyoto, Japan); mobile phase, MeOH: 0.01% TFA=52:48; flow rate, 1.0 ml min^{-1}; detection; 254 nm.

Advanced Marfey's method

One milligram of nocardithiocin was dissolved in 500 µl of 6 M HCl, and then heated at 110 °C for 1 h under nitrogen. The reaction solution was evaporated to dryness and 150 µl of water and 50 µl of MeOH were added. The solution was divided into two portions and 20 µl of 1 M $NaHCO_3$ and 100 µl of 1% L-FDLA (1-fluoro-2,4-dinitrophenyl-5-L-leucineamide) or D-FDLA acetone solution were added to each portion. The solution was heated at 40 °C for 1 h and the reaction was quenched by the addition of 20 µl of 1 M HCl. After dilution with 220 µl of acetonitrile, 0.1 and 1 µl of the DLA derivatives of all the samples were analyzed by the following HPLC and ESILC/MS, respectively: column; TSK gel ODS-80Ts (150×4.6 mm ID, TOSOH), mobile phase; acetonitrile:0.05% TFA, gradient condition; acetonitrile 30→70%, flow rate; 1.0 ml min^{-1}, detection; 340 nm, column; TSK gel ODS-80Ts (150×2 mm ID, TOSOH), mobile phase; acetonitrile:0.05% TFA, gradient condition; acetonitrile 30→70%, flow rate; 0.2 ml min^{-1}, split ratio; 1:40, detection; MS (positive ion mode).

Antimicrobial activity measurement

The antimicrobial activities were determined by a method described earlier[20] using the microbroth dilution method, except for the determination of MIC values against the slowly growing mycobacteria. The antimicrobial activities against the slowly growing mycobacteria were determined by the agar dilution method using the MIDDLEBROOK 7H10 agar medium (BD, Difco). Inocula were prepared by incubation of the *Mycobacterium* species in MIDDLEBROOK (7H9) liquid medium at 37 °C for 2–3 weeks in a 5% CO_2 incubator. After adjustment of the cell concentration by the optical density measurement, the diluted cell suspensions were inoculated onto the MIDDLEBROOK 7H10 agar medium containing various drug concentrations. After incubation at 37 °C for 14 days (for *Mycobacterium avium* and *Mycobacterium intracellulare*) and 21 days (for *M. tuberculosis*), the MIC values were determined. The *M. tuberculosis* H37Rv strain was used as the standard strain. Rifampicin (REF; Sigma-Aldrich Co., Tokyo, Japan) and levofloxacin (Daiichi Seiyaku Co., Tokyo, Japan) were used as the reference drugs in this study.

ACKNOWLEDGEMENTS

This work was partially supported by a Grant from Daiichi Pharmaceutical Co. (presently Daiichi-Sankyo Pharmaceutical Co.) Ltd, Chiba, Japan.

1 Bérdy, J. Bioactive microbial metabolites: a personal view. *J. Antibiot.* **58,** 1–26 (2005).
2 Beaman, B. L. & Beaman, L. *Nocardia* species: host-parasite relationships. *Clin. Microbiol. Rev.* **7,** 213–264 (1994).
3 Kageyama, A. *et al.* Nocardial infections in Japan from 1992 to 2001, including the first report of infection by *Nocardia transvalensis*. *Eur. J. Epidemiol.* **19,** 383–389 (2004).
4 Tsuda, M. *et al.* Brasilibactin A, a cytotoxic compound from actinomycete *Nocardia brasiliensis*. *J. Nat. Prod.* **68,** 462–464 (2005).
5 Komatsu, K., Tsuda, M., Tanaka, Y., Mikami, Y. & Kobayashi, J. SAR studies of brasilicardin A for immunosuppressive and cytotoxic activities. *Bioorg. Med. Chem.* **13,** 1507–1513 (2005).
6 Bagley, M. C., Dale, J. W., Merritt, E. A. & Xiong, X. Thiopeptide antibiotics. *Chem. Rev.* **105,** 685–714 (2005).

7 Holmes, D. J., Caso, J. L. & Thompson, C. J. Autogenous transcriptional activation of a thiostrepton-induced gene in *Streptomyces lividans*. *EMBO J.* **12,** 3183–3191 (1993).
8 Mai, T. *et al.* Productivity of antimicrobial substances in pathogenic actinomycetes *Nocardia brasiliensis*. *Microbiol. Cult. Coll.* **13,** 103–108 (1997).
9 Yun, B. S. & Seto, H. Promoinducin, a novel thiopeptide produced by *Streptomyces* sp. SF2741. *Biosci. Biotechnol. Biochem.* **59,** 876–880 (1995).
10 Leet, J. E. *et al.* Nocathiacins, new thiazolyl peptide antibiotics from *Nocardia* sp. II. Isolation, characterization, and structure determination. *J. Antibiot.* **56,** 232–242 (2003).
11 Rodríguez, J. C., Holgado, G. G., Sánchez, R. I. S. & Cañedo, L. M. Radamycin, a novel thiopeptide produced by *Streptomyces* sp. RSP9. II. Physico-chemical properties and structure determination. *J. Antibiot.* **55,** 391–395 (2002).
12 Muramatsu, I., Motoki, Y., Aoyama, M. & Suzuki, H. Amino acids and derivatives of thiazole-4-carboxylic acid as constituents of thiopeptin B. *J. Antibiot.* **30,** 383–387 (1977).
13 Fujii, K. *et al.* A nonempirical method using LC/MS for determination of the absolute configuration of constituent amino acids in a peptide: elucidation of limitations of Marfey's method and of its separation mechanism. *Anal. Chem.* **69,** 3346–3352 (1997).
14 Fujii, K., Ikai, Y., Oka, H., Suzuki, M. & Harada, K.-I. A nonempirical method using LC/MS for determination of the absolute configuration of constituent amino acids in a peptide: combination of Marfey's method with mass spectrometry and its practical application. *Anal. Chem.* **69,** 5146–5151 (1997).
15 Fujii, K. *et al.* Simultaneous detection and determination of the absolute configuration of thiazole-containing amino acids in a peptide. *Tetrahedron* **58,** 6873–6879 (2002).
16 Harada, K.-I. *et al.* Application of D, L-FDLA derivatization to determination of absolute configuration of constituent amino acids in peptide by advanced Marfey's method. *Tetrahedron Lett.* **37,** 3001–3004 (1996).
17 Tanaka, Y., Gräfe, U., Yazawa, K., Mikami, Y. & Ritzau, M. Nocardicyclins A and B: new anthracycline antibiotics produced by *Nocardia psedobrasiliensis*. *J. Antibiot.* **50,** 822–827 (1997).
18 Tsuda, M. *et al.* Nocaracins A-C, and brasiliquinone D, new metabolites from the actinomycete *Nocardia brasiliensis*. *J. Nat. Prod.* **62,** 1640–1642 (1999).
19 Nemoto, A. *et al.* Asterobactins, a new siderophore group antibiotic from *Nocardia asteroides*. *J. Antibiot.* **55,** 593–597 (2002).
20 Kaneda, S. *et al.* Biological activities of newly prepared saframycins. *J Antibiot.* **40,** 1640–1642 (1987).

The Journal of Antibiotics (2009) 62, 621–624

www.nature.com/ja

ORIGINAL ARTICLE

6-Hydroxymethyl-1-phenazine-carboxamide and 1,6-phenazinedimethanol from a marine bacterium, *Brevibacterium* sp. KMD 003, associated with marine purple vase sponge

Eun Ju Choi[1,2], Hak Cheol Kwon[1], Jungyeob Ham[1] and Hyun Ok Yang[1]

Two new antibacterial phenazines were isolated from the culture broth of *Brevibacterium* sp. KMD 003 obtained from a marine purple vase sponge of the genus *Callyspongia*, collected in Kyeongpo, Gangwondo, Korea. The structures of these compounds were determined to be 6-hydroxymethyl-1-phenazine-carboxamide (1) and 1,6-phenazinedimethanol (2) through analyses of HR–EI–MS and NMR data. Compounds 1 and 2 showed antibacterial activities against *Enterococcus hirae* and *Micrococcus luteus* with 5 μM MIC values.
The Journal of Antibiotics (2009) **62,** 621–624; doi:10.1038/ja.2009.92; published online 2 October 2009

Keywords: antibacterial activity; *Brevibacterium*; 6-Hydroxymethyl-1-phenazine-carboxamide; phenazine; 1,6-phenazinedimethanol; sponge

INTRODUCTION

Marine sponges are animals belonging to the phylum porifera and are known to be an abundant source of bioactive secondary metabolites. They are host organisms for various microorganisms, and a number of cytotoxic, anti-microfouling and antimicrobial metabolites have been reported from bacteria associated with marine sponges.[1–4] Marine sponges of genus *Callyspongia* have been shown to contain bioactive secondary metabolites such as pyridine alkaloids,[5] polyacetylenes,[6] peptides,[7] sulfated meroterpenoids[8] and polyketide.[9] However, little is known about the secondary metabolite production of microbes derived from *Callyspongia*. To date, only two cultured microbes, a carotenoid-producing *Streptomyces* sp.[10] and a macrolide-producing fungus *Cladosporium herbarum*,[11] have been isolated from *Callyspongia diffusa* and *C. aerizusa*, respectively.

In an effort to investigate the chemical potential of microbes growing in marine environments, we initiated the investigation of the microbial diversity associated with marine sponges and their secondary metabolites production. During this survey, we isolated a dark green-pigmented bacterium, *Brevibacterium* sp. KMD 003, from the marine purple vase sponge, *Callyspongia* sp. From the liquid culture of KMD 003, we isolated two new antimicrobial phenazines, 6-hydroxymethyl-1-phenazine-carboxamide (**1**) and 1,6-phenazinedimethanol (**2**). Compounds **1** and **2** displayed potent antimicrobial activity against *Enterococcus hirae* and *Micrococcus luteus*.

Phenazine-related compounds have been shown to display a variety of biological activities such as antibiotic, antitumor, antimalaria and antiparasitic activities.[12–15] Phenazines have also attracted great interest due to their physiological roles related to pigment production, quorum sensing and biofilm formation in microbial communities.[16] Here, we report the isolation, structure elucidation and antimicrobial activity of two new phenazines (**1** and **2**) isolated from *Callyspongia*-derived *Brevibacterium* sp.

RESULTS AND DISCUSSION

The sequence analysis of the 16S rRNA gene placed the strain KMD 003 within the genus *Brevibacterium* on the basis of the 99.9 and 99.7% sequence identity with *Brevibacterium sanguinis*[17] and *B. celere*,[18] respectively. The cultured strain KMD 003 was deposited with Korean Culture Center of Microorganisms (KCCM 90080). *B. sanguinis* and *B. celere*, the nearest neighbors of strain KMD 003 in the phylogenetic tree, were isolated from blood cultures of a patient with human immunodeficiency virus and degraded thallus of a brown alga, respectively. A few *Brevibacterium* species have previously been shown to produce the antibiotic phenazine pigments, 1,6-dihydroxyphenazine-5-oxide,[19] 1,6-dihydroxyphenazine-5,10-oxide,[20] iodinin[21] and 1,6-dihydroxyphenazine.[21] However, no biologically valuable organic compounds have been reported from the bacterial strains, *B. sanguinis* and *B. celere*.

[1]Natural Products Research Center, Korea Institute of Science and Technology, Gangneung, Gangwon-do, Korea and [2]Division of Applied Marine Biotechnology and Engineering, Faculty of Marine Bioscience and Technology, Gangneung-Wonju National University, Gangneung, Gangwon-do, Korea
Correspondence: Dr HC Kwon, Natural Products Research Center, Korea Institute of Science and Technology, 290 Daejeon-dong, Gangneung 210-340, Republic of Korea.
E-mail: hkwon@kist.re.kr
Received 12 July 2009; revised 25 August 2009; accepted 27 August 2009; published online 2 October 2009

To investigate secondary metabolite production by KMD 003, the strain was cultured in 10 1-l Erlenmeyer flasks each containing 500 ml of TCG liquid medium (total 5 l) ((3 g tryptone (Difco, Sparks, MD, USA), 5 g casitone (Difco) and 4 g glucose (Difco) in 1 l filtered seawater). Metabolite production in the culture broth was monitored daily by HPLC analysis using an Agilent 1100 LC-MS system (Agilent Technologies Inc., Santa Clara, CA, USA) with a Phenomenex Luna 5 C18(2) analytical column (Phenomenex Inc., Torrance, CA, USA) (4.6×150 mm, flow rate 0.7 ml min^{-1}) and a gradient elution of 10–100% acetonitrile in water for 30 min. Two major peaks were observed at retention time 11.3 and 12.2 min on the fourth day of culture. At the end of the culture period (day 7), the cultured broth of the strain KMD 003 was extracted with Amberlite XAD-7 resin (Sigma-Aldrich, St Louis, MO, USA) (20 g l^{-1}) and acetone. The crude extract was subjected to preparative HPLC using C18 column and gradient elution of 10–100% aqueous acetonitrile for the separation of the two major peaks. The subfraction including the major peaks was purified by repeated HPLC using a silica column and an isocratic elution of methylene chloride–methanol (50:1) to afford compounds **1** and **2**.

Compound **1** was isolated as a yellow amorphous powder. The molecular formula was assigned to be $C_{14}H_{11}N_3O_2$ by HR–EI–MS ($(M)^+$=253.0848) (Table 1 and Supplementary Figure S1). The UV spectrum of **1** showing maximal absorptions at 204, 251 and 367 nm was similar to those of the core phenazine structure, which was confirmed by comparison analysis with our in-house HPLC–UV database (Supplementary Figure S2). The ^{1}H NMR spectrum (Supplementary Figure S3) showed six aromatic protons signals at δ_H 8.04 (×2), 8.06, 8.28, 8.43 and 8.68, and one oxymethylene doublet signal at δ_H 5.32. Two-dimensional (2D) NMR analysis, using heteronuclear multiple bond correlation (HMBC) and heteronuclear single quantum coherence (HSQC) experiments, showed that these proton signals correlated with ^{13}C NMR signals at δ_C 132.5, 127.8, 130.6, 127.9, 131.1, 134.5 and 58.8. Other characteristic features of the ^{1}H NMR spectrum of **1** were the presence of a primary alcohol at δ_H 5.49 (1H, t, J=5.0 Hz) and two protons of a primary amide at δ_H 8.12 (1H, br s) and 9.77 (1H, br s). As expected, the amide carbon signal was observed at δ_C 166.1 in the ^{13}C NMR spectrum (Supplementary Figure S4). In addition, the ^{13}C NMR spectrum of **1** showed additional signals attributed to six aromatic quaternary carbons at δ_C 133.7, 140.5, 140.9, 141.5, 141.7 and 142.2. Comprehensive collation of 2D NMR data (Supplementary Figures S5–S7) from ^{1}H-^{1}H COSY, HSQC and HMBC experiments led to the construction of a phenazine structure with a primary amide and a hydroxymethyl functionality. The HMBC correlations between H-2 (δ_H 8.68) and C-1′ (δ_C 166.1), and between 1′-NH (δ_H 8.12) and C-1 (δ_C 131.1) allowed the amide group to be positioned at C-1. The position of the hydroxymethlene group was also determined to be C-6 by the HMBC correlation of a methylene proton signal at δ_H 5.32 with C-6 (δ_C 141.7) and C-7 (δ_C 127.8). In addition, the NOE correlation between 1′-NH at δ_H 9.77 and H-9 (δ_H 8.28), in 2D NOESY experiment with 700 ms mixing time (Supplementary Figure S8), further supported that the functionalities were not at C-1 and C-9, but compound **1** was 1,6-disubstituted phenazines. These data allowed us to assign the structure of compound **1** as 6-hydroxymethyl-1-phenazine-carboxamide (Figure 1).

Compound **2** was obtained as a yellow amorphous powder that was determined to have the molecular formula $C_{14}H_{12}N_2O_2$ by interpretation of HR–EI–MS ($(M)^+$=240.0900) (Supplementary Figure S9) and NMR data (Table 1). The UV and IR spectra (Supplementary Figures S10 and S11) of **2** displayed similar absorption bands with those of compound **1**, indicating that **2** contains a phenazine component. Proton NMR spectral data analysis (Supplementary Figures S12 and S13) indicated signals attributable to a 1,2,3-trisubstitued phenyl group (δ_H 7.95 (1H, dd, J=8.5, 7.0 Hz), 7.98 (1H, br dd, J=7.0, 2.0 Hz) and 8.12 (1H br dd, J=8.5, 2.0 Hz)) and a hydroxymethyl group (δ_H 5.31 (2H, d, J=5.0 Hz) and 5.43 (1H, t, J=5.0 Hz, OH)). The HSQC spectrum (Supplementary Figure S14) showed that these three aromatic protons signals at δ_H 7.95, 7.98 and 8.12 correlated with carbon signals at δ_C 131.2, 127.1 and 128.1, respectively The HSQC spectrum also showed the correlation between the hydroxylmethyl proton signal at δ_H 5.31 and an oxymethylene carbon signal at δ_C 59.5. The ^{13}C NMR spectrum (Supplementary Figure S15) of **2** showed additional signals attributed to three aromatic quaternary carbons at δ_C 140.9, 141.4 and 142.0. Key HMBC correlations allowed the hydroxymethyl group to be positioned at C-1 (δ_C 141.4) (Supplementary Figure S16). Overall analysis of the NMR data for compound **1** indicated a molecular formula of C_7H_6NO, exactly one-half of the molecular formula, $C_{14}H_{12}N_2O_2$, determined by HRMS. Thus, it became clear that compound **1** is a symmetrical phenazine composed

Table 1 The physicochemical and spectral properties of 6-hydroxymethyl-1-phenazine-carboxamide (1) and 1,6-phenazinedimethanol (2)

	1	*2*
Appearance	Yellow amorphous powder	Yellow amorphous powder
Molecular formula	$C_{14}H_{11}O_2N_3$	$C_{14}H_{12}O_2N_2$
HR-EI-MS m/z		
Calcd for	253.0851	240.0899
Found	253.0848	240.0900
UV λ_{max} (CH_3OH) nm (log ε)	204 (4.41), 251 (4.63), 367 (3.95)	203 (4.46), 253 (4.96), 363 (4.11)
IR (neat, $CHCl_3$) ν_{max} cm^{-1}	2922, 2851, 1729, 1452, 1271, 1122, 1072, 854, 805, 752, 699, 617, 575	2923, 2853, 1732, 1667, 1561, 1458, 1380, 1281, 1125, 1073, 746, 699, 617, 575, 544

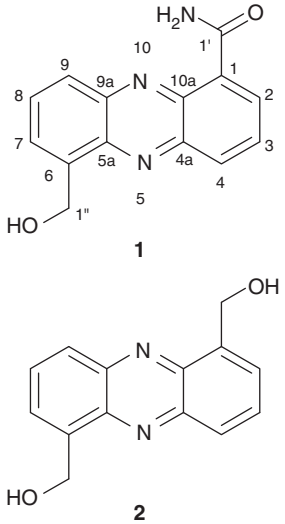

Figure 1 Structures of compounds **1** and **2**.

of two identical 1-hydroxymethyl phenyl groups. The substituted position of two hydroxymehtyl group, 1,6- or 1,9-substitution, was determined to be C-1 and C-6 by NOE correlation between hydroxymethyl (δ_H 5.31) and H-9 signal (δ_H 8.12) in 2D NOESY experiment with 700 ms mixing time (Supplementary Figure S17). These data allowed us to assign the structure of compound **2** as 1,6-phenazinedimethanol (Figure 1).

Although compounds **1** and **2** seem quite simple, small modifications of the core phenazine structure give rise to a dynamic change of color, redox potential and solubility.[16] Moreover, phenazine-1-carboxamide (PCN) and phenazine-1-carboxylic acid (PCA), the structural neighbors of 6-hydroxymethyl-1-phenazinecarboxylic acid (**1**), have important physiological roles, including Fe acquisition,[22] and contribute to pathogen inhibition[23] and microbial biofilm formation.[24] Compound **1** is composed of two functionalities, a hydroxymethyl and a carboxamide, whereas compound **2** includes two hydroxymethyl functionalities, the first examples of these structural compositions. Mono-functionalized phenazine structures including a hydroxymethyl or a carboxamide can be found in 1-phenazinemethanol or PCN. This class of compounds has a variety of ecological functions and therapeutic potential. 1-Phenazinemethanol possesses antifungal activity against *Gaeumannomyces graminis* var. *tritici* and *Pythium* spp.,[25] and PCN displayed antimicrobial activity especially against plant pathogenic Gram-positive bacteria and fungi.[23] PCN is synthesized in *Pseudomonas aeruginosa* by the conversion of PCA in the pyocyanin biosynthetic pathway, which consists of two core loci responsible for the synthesis of PCA and three additional genes encoding unique enzymes involved in the conversion of PCA to pyocyanin, 1-hydroxyphenazine and PCN.[26] In addition, PCN has important physiological roles, including Fe acquisition, due to its redox-activity like other phenazines such as pyocyanin, PCA and 1-hydroxyphenazine *inter alia*.[22] PCA, along with its hydroxylated analog, 2-hydroxy-PCA, contributes to pathogen inhibition and microbial biofilm formation.[24] PCA also increases oxidant formation and alters the expression of IL-8 (interleukin-8) and ICAM-1 (intercellular adhesion molecule-1) in human airway epithelial cells by oxidant-dependent mechanisms.[27]

Compounds **1** and **2** showed antimicrobial activity toward three human pathogenic microorganisms (MIC_{50}=20 μM against *B. subtilis*, 5 μM against *E. hirae* and 5 μM against *M. luteus*). In previously reported literature,[23] the structural neighbors of compound **1**, PCA and PCN, efficiently inhibited the growth of *Bacillus cereus* (MIC <2 μM), whereas showed only modest antimicrobial activity against *M. luteus* (MIC 20 μM). Compounds **1** and **2** were only weakly cytotoxic against eukaryotic cell lines with an IC_{50} value 205.8 and 174.3 μM on HL-60 human leukemia cell lines, respectively, whereas showed no cytotoxicity against five human solid tumor cell lines.

METHODS

General experimental procedures

UV spectra were obtained on an Agilent 8453 UV-Spectrophotometer. FT-IR spectra were measured on a Bruker Tensor27 Spectrophotometer (Bruker, Ettlingen, Germany) at Kangnung-Wonju National University. ^{1}H-, ^{13}C NMR and 2D NMR spectra were obtained in DMSO-d_6 (δ_H 2.55 and δ_C 39.5) on a Varian Unity Plus 500 MHz NMR System (Varian, Palo Alto, CA, USA). Low-resolution ESI–MS was measured on an Agilent Technologies VS/Agilent 1100 system at Kangnung-Wonju National University. HR–EI–MS was measured on a Hewlett-Packard 5890A (Hewlett-Packard, Palo Alto, CA, USA) at the National Center for Inter-University Facilities of Seoul National University. Lichroprep RP-18 (Merck, Darmstadt, Germany, 40–63 μm) was used for column chromatography. A Gilson 321 HPLC system (Gilson, Middleton, WI, USA), with a Delta pak C18 (300×30.00 mm, 15 μm), a Luna C18(2) column (250×10.00 mm, 10 μm) and UV detector (254 nm) was used for preparative HPLC. A Waters 1525 system (Waters, Milford, MA, USA) with PDA detector and a Luna C18(2) column (150×4.6 mm, 5 μm) were used for HPLC analysis.

Isolation of KMD 003 strain, cultivation, extraction

The bacterial strain, *Brevibacterium* sp. KMD 003, was isolated from the tissue of the marine purple vase sponge, *Callyspongia* sp., collected at a depth of 12 m near Kyung-Po beach in Korea (June 2007). The sponge was washed with autoclaved seawater and the tissues ground and diluted with autoclaved seawater (1:10). The diluted suspension (100 μl) was spread on a TCG agar plate. The TCG agar medium contained 3 g tryptone (Difco), 5 g casitone (Difco), 4 g glucose (Difco) and 18 g agar (Difco) in 1 l filtered seawater (pH 7.0). The plate was incubated for 2 weeks at 25 °C under aerobic conditions. KMD 003 was isolated as a dark green-pigmented colony and it was on a TCG agar plate before secondary culturing in TCG liquid medium (25 ml) while shaking at 200 r.p.m. for 7 days at 25 °C. Stocks of the isolated bacterial strain were generated and stored at −80 °C in liquid culture medium containing 15% (v/v) glycerol.

The strain was further cultured in 10 1-l Erlenmeyer flasks each containing 500 ml of TCG liquid medium (total 5 l). The culture flasks were incubated at 25 °C for 7 days with shaking at 200 r.p.m. At the end of the culture period (day 7), Amberlite XAD-7 resin (20 g l^{-1}) was added to each flask, followed by shaking for one additional hour. The resin was collected by filtration through cheesecloth, washed with deionized water and eluted twice with acetone. The acetone solution was then concentrated under reduced pressure to yield 150 mg of crude extract.

Taxonomy

The strain KMD 003 was identified based on 16S rRNA gene sequencing analysis. The chromosomal DNA of strain KMD 003 was extracted using the G-spin Genomic DNA Extraction Kit (iNtRON Biotechnology, Daejoen, Korea). The 16S rRNA gene of strain KMD 003 was amplified by PCR using universal primers 27f and 1492r corresponding to positions 27 in the forward direction and 1492 in the reverse direction of the *Eschrichia coli* 16S rRNA gene.[28] The DNA sequencing reaction was carried out by using an ABI Prism Bigdye terminator cycle sequencing ready reaction kit V.3.1 (Applied Biosystems, Foster City, CA, USA). The PCR cycle-sequencing product was purified by using Montage dye remove kit (Millipore, Bedford, TX, USA) according to the manufacturer's protocol. 16S rRNA gene sequence was determined on a Perkin-Elmer model ABI 3730XL capillary DNA sequencer (Applied Biosystems). The 16S rRNA gene sequence of strain KMD 003 was compared with primary sequence information within the GenBank/EMBL/DDBJ nucleotide sequence database using the BLAST algorithm.[29]

Isolation and purification of phenazines 1 and 2

The crude extract was subjected to preparative HPLC using gradient elution of 10–100% aqueous acetonitrile for 1 h (flow rate 12 ml min^{-1}, Waters Delta pak C18 column 15 μm 300×30 mm) to yield eight subfractions (fractions I–VIII). Fraction VI (33.6 mg) was fractionated by reversed-phase HPLC using a gradient elution of 30–100% aqueous methanol for 1 h (flow rate 4 ml/min, column: Phenomenex Luna C18(2) 10 μm 250×10 mm) to give 15 subfractions (fraction VI-1–VI-15). Compound **1** (5.4 mg) was purified from subfraction VI-9 (9.6 mg) by repeated HPLC using a Phenomenex Luna Silica (2) column (250×10 mm, 10 μm) and an isocratic elution of methylene chloride–methanol (50:1). Compound **2** (5.0 mg) purified from subfraction VI-10 (7.8 mg) was purified by repeated HPLC in the same manner as the purification of compound **1**.

6-Hydroxymethyl-1-phenazine-carboxamide (1)

^{1}H-NMR[a] (500 MHz, DMSO-d_6) δ 5.32. (2H, d, J=5.0 Hz, H$_2$-1″), 5.49 (1H, t, J=5.0 Hz, 1″-OH), 8.04 (2H, m[b], H-8 and H-7), 8.06 (1H, dd, J=8.5, 7.0 Hz, H-3), 8.12 (1H, br s, amide NH$_2$), 8.28 (1H, m[b], H-9), 8.43 (1H, dd, J=8.5, 1.5 Hz, H-4), 8.68 (1H, dd, J=7.0, 1.5 Hz, H-2), 9.77 (1H, br s, amide NH$_2$). [a]The reference for chemical shifts: the signal of DMSO-d_6 (δ_H 2.55). [b]Resonance multiplicity was not able to be assigned due to peak overlapping and second-order effects; ^{13}C NMR[a] (125 MHz, DMSO-d_6) δ 58.8 (C-1″), 127.8

(C-7), 127.9 (C-9), 130.6 (C-3), 131.1(C-1), 132.5 (C-8), 133.7 (C-4), 134.5 (C-2), 140.5 (C-10a), 140.9 (C-5a), 141.5 (C-9a), 141.7 (C-6), 142.2 (C-4a), 166.1 (C-1′). [a]The reference for chemical shifts: the signal of DMSO-d_6 (δ_C 39.5).

1,6-Phenazinedimethanol (2)

^{1}H-NMR[a] (500 MHz, DMSO-d_6) δ 5.31. (4H, d, J=5.0 Hz, H_2-1′ and H_2-1″), 5.43 (2H, t, J=5.0 Hz, 1′-OH and 1″-OH), 7.95 (2H, dd, J=8.5, 7.0 Hz, H-3 and H-8), 7.98 (2H, br dd, J=7.0, 2.0 Hz, H-2 and H-7), 8.12 (2H, br dd, J=8.5, 2.0 Hz, H-4 and H-9); ^{13}C NMR[a] (125 MHz, DMSO-d_6) δ 59.5 (C-1′ and C-1″), 127.1 (C-2 and C-7), 128.1 (C-4 and C-9), 131.2 (C-3 and C-8), 140.9 (C-5a and C-10a), 141.4 (C-1 and C-6), 142.0 (C-4a and C-9a). [a]The reference for chemical shifts: the signals of DMSO-d_6 (δ_H 2.55 and δ_C 39.5).

Antibacterial activity

The antibacterial activity of compounds **1** and **2** were tested in a range of 1.25–10 μg ml^{-1} against six pathogenic microorganisms, *Escherichia coli* (KCTC 2593), *Bacillus subtilis* (KCTC 1021), *Staphylococcus aureus* (KCTC 1916), Methicillin resistance *S. aureus* MRSA 2659, *M. luteus* (KCCM 11548) and *E. hirae* (KCCM 11768). All strains except for *B. subtilis* were grown at 37 °C, and *B. subtilis* was grown at 30 °C in nutrient agar (Difco, USA). Antibacterial activity was determined when the density of the growth control reached an absorbance of 0.150–0.200 at 600 nm. Each pathogenic microorganism was seeded in 96-well plates at 100 μl per well, and incubated for 24 h. Compounds **1** and **2** (1.25, 2.5, 5 and 10 μg ml^{-1}) were then inoculated and incubated in 96-well plates at 30 °C for *B. subtilis* and 37 °C for other pathogens. Growth density was checked every 6 h (0–42 h) at 600 nm.

Cell lines and cytotoxicity

Cytotoxicity was measured by the MTT colorimetric method against HCT116, A549, AGS, MCF-7, HepG2 and HL-60 tumor cell lines. Each cancer cell was seeded in 96-well plates at a density of 10^4 cells per well, and incubated in 5% CO_2 for 24 h at 37 °C. The cells were then treated with varying concentrations (1.56, 3.13, 6.25, 12.5, 25 and 50 μg ml^{-1}) of compounds and incubated in 5% CO_2 for 24 h at 37 °C. After 24 h, cells were incubated in 5% CO_2 for 1 h at 37 °C with 10 μl of WST-8 (2-(2-methoxy-4-nitrophenyl)-3-(4-nitrophenyl)-3-(4-nitrophenyl)-5-(2,4-disulfophenyl)-2H-tetrazolium, monosodium salt) solution to each well of the plate. Absorbance was then measured at 450 nm using a microplate reader, and experiments were performed in triplicate for each concentration of compounds.

ACKNOWLEDGEMENTS

This research is a result of financial support from the Korea Institute of Science and Technology Institute under grant 2Z03270, and from the Marine Biotechnology Program funded by the Ministry of Land, Transport and Maritime Affairs, Republic of Korea. We thank Dr W. Strangman at the University of British Columbia, for scientific advice and English revision.

1 Tanaka, J. *et al*. Diverse metabolites of coral reef organisms. *Pure Appl. Chem.* **77,** 83–89 (2005).
2 Wang, G. Y. S. *et al*. Three novel anti-microfouling nitroalkyl pyridine alkaloids from the okunawan marine sponge *Callyspongia* sp. *Tetrahedron Lett.* **37,** 1813–1816 (1996).
3 Umeyama, A., Nagano, C. & Arihara, S. Three novel C21 polyacetylenes from the marine sponge *Callyspongia* sp. *J. Nat. Prod.* **60,** 131–133 (1997).
4 Gray, C. A. *et al*. Sulfated meroterpenoids from the Brazilian sponge *Callyspongia* sp. are inhibitors of the antileishmaniasis target adenosine phosphoribosyl transferase. *J. Org. Chem.* **71,** 8685–8690 (2006).
5 (a)Buchanan, M. S. *et al*. Niphatoxin C, a cytotoxic tripyridine alkaloid from *Callyspongia* sp. *J. Nat. Prod.* **70,** 2040–2041 (2007). (b) Davies-Coleman, M.T. *et al*. A new EGF-active polymeric pyridinium alkaloid from the sponge *Callyspongia fibrosa*. *J. Org. Chem.* **58**, 5925–5930 (1993). (c) Wang, G.-Y.-S., Kuramoto, M. & Uemura, D. Three novel anti-microfouling nitroalkyl pyridine alkaloids from the Okinawan marine sponge *Callyspongia* sp. *Tetrahedron Lett*. **37**, 1813–1816 (1996).
6 (a)Youssef, D. T. A. Van Soest, R. W. M. & Fusetani, N. Callyspongamide A, a new cytotoxic polyacetylenic amide from the Red Sea sponge *Callyspongia fistularis*. *J. Nat. Prod.* **66,** 861–862 (2003). (b) Nakao, Y., Uehara, T., Matunaga, S., Fusetani, N. & Van Soest, R.W.M. Callyspongynic acid, a polyacetylenic acid which inhibits α glucosidase, from the marine sponge *Callyspongia truncate*. *J. Nat. Prod.* **65**, 922–924 (2002). (c) Uno, M., Ohta, S., Ohta, E. & Ikegami, S. Callyspongins A and B: novel polyacetylene sulfates from the marine sponge *Callyspongia truncata* that inhibit fertilization of starfish gametes. *J. Nat. Prod.* **59**, 1146–1148 (1996).
7 (a)Capon, R. J. *et al*. Phoriospongin A and B: two new nematocidal depsipeptides from the Australian marine sponges *Phoriospongia* sp. and *Callyspongia bilamellata*. *J. Nat. Prod.* **65,** 358–363 (2002). (b) Berer, N., Rudi, A., Goldberg, I., Benayahu, Y. & Kashman, Y. Callynormine A, a new marine cyclic peptide of a novel class. *Org. Lett.* **6**, 2543–2545 (2004).
8 Gray, C. A. *et al*. Sulfated meroterpenoids from the Brazilian sponge *Callyspongia* sp. are inhibitors of the antileishmaniasis target adenosine phosphoribosyl transferase. *J. Org. Chem.* **71,** 8685–8690 (2006).
9 Kobayashi, M., Higuchi, K., Murakami, N., Tajima, H. & Aoki, S. Callystatin A, a potent cytotoxic polyketide from the marine sponge, *Callyspongia truncata*. *Tetrahedron Lett.* **38,** 2859–2862 (1997).
10 Dharmaraj, S., Ashokkumar, B. & Dhevendaran, K. Food-grade pigments from *Streptomyces* sp. isolated from the marine sponge *Callyspongia diffusa*. *Food Res. Int.* **42,** 487–492 (2009).
11 Jadulco, R. *et al*. New macrolides and furan carboxylic acid derivative from the sponge-derived fungus *Cladosporium herbarum*. *J. Nat. Prod.* **64,** 527–530 (2001).
12 Singh, M. P. *et al*. Biological and mechanistic activities of phenazine antibiotics produced by culture LL-14I352. *J. Antibiot.* **50,** 785–787 (1997).
13 Giddens, S. R. & Bean, D. C. Investigations intothe *in vitro* antimicrobial activity and mode of action of the phenazine antibiotic D-alanylgriseoluteic acid. *Int. J. Antimicrob. Agents* **29,** 93–97 (2007).
14 Laursen, J. B. & Nielsen, J. Phenazine natural products: biosynthesis, synthetic analogues, and biological activity. *Chem. Rev.* **104,** 1663–1685 (2004).
15 de Andrade-Neto, V. F. *et al*. Antimalarial activity of phenazines from lapachol β-lapachone and its derivatives against *Plasmodium falciparum in vitro* and *Plasmodium berghei in vivo*. *Bioorg. Med. Chem. Lett.* **14,** 1145–1149 (2004).
16 Price-Whelan, A., Dietrich, L. E. P. & Newman, D. K. Rethinking 'secondary' metabolism: physiological roles for phenazine antibiotics. *Nat. Chem. Biol.* **2,** 71–78 (2006).
17 Wauters, G. *et al*. Identification of a novel *Brevibacterium* species isolated from humans and description of *Brevibacterium sanguinis* sp. nov. *J. Clin. Microbiol.* **42,** 2829–2832 (2004).
18 Ivanova, E. P. *et al*. *Brevibacterium celere* sp. nov., isolated from degraded thallus of a brown alga. *Int. J. Syst. Evol. Microbiol.* **54,** 2107–2111 (2004).
19 Gerber, N. N. & Lechevalier, M. P. 1,6-phenazinediol-5-oxide from microorganisms. *Biochemistry* **4,** 176–180 (1965).
20 Clemo, G. R. & Daglish, A. F. Structure of the pigment of *Chromobacterium iodinum*. *Nature* **162,** 776 (1948).
21 Irie, T., Kurosawa, E. & Nagaoka, J. The constitution of the pigments of *Brevibacterium crystalloiodinum*, Sasaki, Yoshida et Sasaki. *Bull. Chem. Soc. Jpn.* **33,** 1057–1059 (1960).
22 (a)Wang, Y. & Newman, D. K. Redox reactions of phenazine antibiotics with ferric (Hydr)oxides and molecular oxygen. *Environ. Sci. Technol.* **42,** 2380–2386 (2008). (b) Hernandez, M.E., Kappler, A. & Newman, D.K. Phenazines and other redox-active antibiotics promote microbial mineral reduction. *Appl. Environ. Microbiol.* **70**, 921–928 (2004).
23 Jayatilake, G. S., Thornton, M. P., Leonard, A. C., Grimwade, J. E. & Baker, B. J. Metabolites from an Antarctic sponge-associated bacterium, *Pseudomonas aeruginosa*. *J. Nat. Prod.* **59,** 293–296 (2006).
24 Maddula, V. S. R. K., Pierson, E. A. & Pierson, L. S. Altering the ratio of phenazines in *Pseudomonas chlororaphis* (*aureofaciens*) Strain 30–84: effects on biofilm formation and pathogen inhibition. *J. Bacteriol.* **190,** 2759–2766 (2008).
25 Gurusiddaiah, S., Weller, D. M., Sarkar, A. & Cook, R. J. Characterization of an antibiotic produced by a strain of *Pseudomonas fluorescens* inhibitory to *Gaeuman nomyces graminis* var. *tritici* and *Pythium* spp. *Antimicrob. Agents Chemother.* **29,** 488–495 (1986).
26 Mavrodi, D. V. *et al*. Functional analysis of genes for biosynthesis of pyocyanin and phenazine-1-carboxamide from *Pseudomonas aeruginosa* PA01. *J. Bacteriol.* **183,** 6454–6465 (2001).
27 Look, D. C. *et al*. Pyocyanin and its precursor phenazine-1-carboxylic acid increase IL-8 and intercellular adhesion molecule-1 expression in human airway epithelial cells by oxidant-dependent mechanisms. *J. Immunol.* **175,** 4017–4023 (2005).
28 Brosius, J., Palmer, M. L., Kennedy, P. J. & Noller, H. F. Complete nucleotide sequence of a 16S ribosomal RNA gene from *Escherichia coli*. *Proc. Natl. Acad. Sci. USA* **75,** 4801–4805 (1978).
29 Altschul, S. F., Gish, W., Miller, W., Myers, E. W. & Lipman, D. J. Basic local alignment search tool. *J. Mol. Biol.* **215,** 403–410 (1990).

Supplementary Information accompanies the paper on The Journal of Antibiotics website (http://www.nature.com/ja)

The Journal of Antibiotics (2009) 62, 625–629

www.nature.com/ja

ORIGINAL ARTICLE

Screening and evaluation of new inhibitors of hepatic glucose production

Junko Hashimoto[1], Keiichiro Motohashi[1], Kazutoshi Sakamoto[2], Seiichi Hashimoto[3], Maasa Yamanouchi[4], Hiroshi Tanaka[4], Takashi Takahashi[4], Motoki Takagi[1] and Kazuo Shin-ya[5]

In the course of our screening program for inhibitors of hepatic glucose production in rat hepatoma H4IIE-C3 cells, which were used as model liver cells, five naphtoquinone derivatives—javanicin, solaniol, 9-*O*-methylfusarubin, 5,10-dihydroxy-1,7-dimethoxy-3-methyl-1H-naphtho[2,3-c]pyran-6,9-dione, 9-*O*-methylbostrycoidin—and vanillin were selected from our natural product library. These naphtoquinone derivatives inhibited hepatic glucose production at IC_{50} values of 3.8–29 μM, but showed cytotoxicity against hepatic cells after incubation for 48 h. However, vanillin showed an IC_{50} value of 32 μM without exhibiting cytotoxicity at 50 μM. Therefore, we examined 12 vanillin derivatives to investigate their inhibitory activities against glucose production. Among these analogs, 4-hydro-3-methoxyacetophenone and 5-nitrosalicylaldehyde exhibited stronger inhibition than the other compounds at IC_{50} values of 25 and 24 μM, respectively, with no cytotoxicity at a concentration of 50 μM. Hence, 4-hydro-3-methoxyacetophenone and 5-nitrosalicylaldehyde may be useful as a lead compound of anti-type 2 diabetic drugs.
The Journal of Antibiotics (2009) **62,** 625–629; doi:10.1038/ja.2009.93; published online 25 September 2009

Keywords: diabetes; hepatic glucose production; vanillin

Type-2 diabetes is a severe disease that is prevalent in the developed world, and the incidence of diabetes is increasing even in developing countries. Type-2 diabetes is associated with impaired glucose clearance by the liver with elevated glucose production in the postprandial state and is characterized by insulin resistance.[1] Rigid control of plasma glucose levels is known to decrease the incidence and progression of diabetic complications. The liver maintains blood glucose homeostasis by the absorption of glucose in the postprandial state and by the production of glucose from glycogenolysis and gluconeogenesis in the postabsorptive state. In normal tissues, insulin stimulates glucose uptake by muscles and adipose tissue, and inhibits hepatic glucose production. However, this response to insulin is defective in patients with type-2 diabetes, resulting in long-term hyperglycemia. Therefore, the key to treating diabetes is to reverse or bypass the deficient insulin-signaling pathway in patients with type-2 diabetes. Agents that can inhibit hepatic glucose production through a signaling pathway that is distinct from the insulin-signaling pathway may provide new avenues for inhibiting the elevated glucose production caused by insulin resistance in the case of type-2 diabetes.

Several popular classes of oral therapeutic drugs for diabetes that are available in the market (for example, sulphonylureas and peroxisome proliferator-activated receptor-γ agonists) lower plasma glucose levels by increasing glucose metabolism either through enhanced insulin secretion or improved sensitivity to insulin. Metformin is the only drug that acts primarily by reducing endogenous glucose production without exhibiting a major effect on insulin signaling.[2] Metformin lowers glucose levels without resulting in weight gain. Thus, it is often used to treat patients with type-2 diabetes despite the well-known safety concerns in certain diabetic patient populations and the overall high incidence of gastrointestinal intolerance associated with its use. Hence, agents such as metformin are expected to inhibit hepatic glucose production. We screened inhibitors from our natural product library for their effects on glucose production in the rat liver cell line H4IIE-C3 and selected five naphtoquinone derivatives and vanillin as inhibitors. Further, we also evaluated commercially available and synthesized vanillin derivatives for their inhibitory effects on glucose production.

MATERIALS AND METHODS

General experimental procedures

UV and IR spectra were measured on a DU730 spectrophotometer (Beckman Coulter, Fullerton, CA, USA) and an FT-720 spectrophotometer (Horiba, Kyoto, Japan), respectively. High-resolution electrospray ionization-mass spectrometric (HR-ESI-MS) data were recorded on an LCT-Premier XE mass spectrometer (Waters, Milford, MA, USA). NMR spectra were measured on an NMR System 500 NB CL (Varian, Palo Alto, CA, USA) in $CDCl_3$ with the residual solvent

[1]Biomedicinal Information Research Center (BIRC), Japan Biological Informatics Consortium (JBIC), Koto-ku, Tokyo, Japan; [2]Fermentation Research Labs, Astellas Pharma, Toukoudai, Tsukuba-shi, Ibaraki, Japan; [3]Japan Science and Technology Agency (JST), 4–1–8, Honcho, Kawaguchi-shi, Saitama, Japan; [4]Department of Applied Chemistry, Graduate School of Science and Engineering, Tokyo Institute of Technology, 2–12–1-S1–35 Ookayama, Meguro, Tokyo, Japan and [5]Biomedicinal Information Research Center (BIRC), National Institute of Advanced Industrial Science and Technology (AIST), 2–42 Aomi, Koto-ku, Tokyo, Japan
Correspondence: Dr M Takagi, Biomedicinal Information Research Centre (BIRC), Japan Biological Informatics Consortium (JBIC), 2-42 Aomi, Koto-ku, Tokyo 135-0064, Japan. E-mail: motoki-takagi@aist.go.jp or Dr K Shin-ya, Biomedicinal Information Research Centre (BIRC), National Institute of Advanced Industrial Science and Technology (AIST), 2-42 Aomi, Koto-ku, Tokyo 135-0064, Japan. E-mail: k-shinya@aist.go.jp
Received 7 August 2009; revised 25 August 2009; accepted 31 August 2009; published online 25 September 2009

peak as an internal standard (δ_H 7.24 p.p.m.). Normal-phase medium-pressure liquid chromatography (MPLC) was performed using a Purif-pack SI-60 column (Moritex, Tokyo, Japan). Analytical reverse-phase HPLC was performed on an L-column2 ODS column (4.6 i.d.×150 mm, Chemical Evaluation and Research Institute, Tokyo, Japan) with a 2996 photodiode array detector (Waters) and a 3100 mass detector (Waters). Preparative reverse-phase HPLC was performed on an L-column2 ODS (20 i.d.×150 mm) with an L-2455 photodiode array detector (Hitachi High Technologies, Tokyo, Japan). The reagents and solvents used in our study were of the highest grade available.

Cell culture

Rat hepatoma cell line H4IIE-C3 was used in this study. The cells were grown at 37 °C in an atmosphere containing 5% CO_2 in Minimum Essential Medium Eagle (Sigma, Saint Louis, MO, USA). This medium consisted of 10% fetal bovine serum (Sigma), a 100-μM solution of non-essential amino acid (Invitrogen, Carlsbad, CA, USA), 1 mM sodium pyruvate solution (Invitrogen), supplemented with penicillin (100 U ml^{-1}) and streptomycin (100 μg ml^{-1}).

Assay of glucose production in hepatic cells

For performing the screening, H4IIE-C3 cells were inoculated onto a 384-well plate (Cat. No.781182, Greiner Bio-one, Frickenhausen, Germany) at a density of 1.2×10^4 cells per well and incubated overnight in the serum-containing medium. They were then transferred to a serum-free medium and incubated overnight. Next, the medium was replaced with a glucose-free medium—20 μl of Dulbecco's Modified Eagle's Base—which did not contain L-glutamine, glucose, phenol red, sodium pyruvate and sodium bicarbonate (Sigma), supplemented with 3.7 mg l^{-1} sodium bicarbonate and 20 mM pyruvic acid. The samples (0.2 μl) to be screened were then added to the medium by using Multi-dispenser ADS-384–8 (BioTec, Tokyo, Japan) and incubated for 5 h. Subsequently, 10 μl of the medium was transferred to 384-well black plates (Cat. No.784900, Greiner) by using ADS-384–8, and the amount of glucose accumulated in the wells was detected by mixing the contents of the well with 10 μl of Amplex Red Glucose Assay kit solution (Invitrogen).

To confirm the activities of the hit samples, the cells were inoculated into a 96-well plate (Cat. No.353072; BD Biosciences, San Jose, CA, USA) at a density of 6×10^4 cells per 100 μl for each well and incubated as described above. After treatment with the hit samples at various concentrations, 40 μl of the medium was transferred to a 96-well black plate (Cat. No. 3916; Corning Inc., Corning, NY, USA), and the amount of glucose accumulated was determined by mixing 40 μl of the Amplex Red Glucose Assay kit solution.

Cytotoxicity assay

Cytotoxic activities were evaluated by WST-8 (2-(2-methoxy-4-nitrophenyl)-3-(4-nitrophenyl)-5-(2,4-disulfophenyl)-2H-tetrazolium, monosodium salt) colorimetric assay. The 96-well plate was inoculated with H4IIE-C3 cells at a density of 1×10^4 cells per well; these were subsequently treated with compounds at various concentrations and incubated for 48 h. Next, 10 μl of the WST-8 reagent (Cell Counting Kit; Dojindo, Kumamoto, Japan) was added and the cells were incubated for 1 h at 37 °C in a humidified atmosphere containing 5% CO_2. Absorbance of the formazan dye formed was measured at 450 nm.

Natural product library

Our in-house natural product library was used as the source of samples for screening. The library contained 40 508 diverse samples of crude metabolites of actinomycetes (20 608 samples), bacteria (6336 samples) other than actinomycetes and fungi (12 672 samples). It also included plant extracts (252 samples) and metabolites isolated from microorganisms (640 samples). All the samples were dissolved in dimethyl sulfoxide.

Compounds

Javanicin[3] (**1**) and solaniol[4] (**2**) were purified from the culture of *Fusarium* sp. no. 351386, which was isolated from a soil sample collected from Tanzawa, Kanagawa Prefecture, Japan, with MPLC and HPLC by activity-guided separation.

9-*O*-Methylfusarubin[5] (**3**), 5,10-dihydroxy-1,7-dimethoxy-3-methyl-1H-naphtho[2,3-c]pyran-6,9-dione[6] (**4**), 9-*O*-methylbostrycoidin[5] (**5**) and vanillin (**6**) were selected as hit samples from our purified natural product library. These samples were of fungal origin.

Isovanillin (3-hydroxy-4-methoxybenzaldehyde) (**8**), 4-hydroxy-3-methoxyacetophenone (**9**), 4-hydroxy-3,5-dimethoxyacetophenone (**10**), 5-chlorosalicylaldehyde (**12**), 5-nitrosalicylaldehyde (**13**) and 2,4-dihydroxybenzaldehyde (**14**) were purchased from Tokyo Chemical Industry (Tokyo, Japan); vanillic acid (**7**) and 5-bromosalicylaldehyde (**11**) were purchased from Wako Pure Chemical (Osaka, Japan); 2,4,6-trihydroxybenzaldehyde (**15**) was purchased from Aldrich (Saint Louis, MO, USA).

Hydroxy-4,6-dimethoxybenzaldehyde (16)

Oxalyl chloride (16.0 ml, 183 mmol, 2.00 equiv.) in CH_2Cl_2 (44.0 ml) was added dropwise to a solution of *N*,*N*-dimethylformamide (DMF) (18.9 ml, 244 mmol, 2.60 equiv.) in CH_2Cl_2 (90 ml) at room temperature under argon. After the reaction mixture was stirred at the same temperature for 1 h, it was cooled to −15 °C. A solution of 3,5-dimethoxyphenol (14.5 g, 93.8 mmol, 1.00 equiv.) in CH_2Cl_2 (58 ml) was added dropwise to the above reaction mixture for over 45 min. This mixture was stirred at −15 °C for 30 min and then at room temperature for 30 min. Next, 1 M aqueous HCl (130 ml) was added at 0 °C. The mixture was heated to 40 °C after stirring for 2 h at room temperature. After 3 h of stirring at the same temperature, the reaction mixture was added to a mixture of brine and EtOAc at 0 °C. The aqueous layer was extracted with two portions of EtOAc. The combined organic layers were washed with brine, dried over $MgSO_4$ and concentrated *in vacuo*. The residue was re-crystallized from CH_2Cl_2-hexane to afford **16** as a white solid.[7]

Thin-layer chromatography, R*f*=0.57 (hexane/ethyl acetate=1/1); ^{1}H NMR ($CDCl_3$) 12.5 (s, 1H), 10.1 (s, 1H), 6.00 (d, *J*=2.2 Hz, 1H), 5.91 (d, *J*=2.2Hz, 1H), 3.84 (s, 3H), 3.83 (s, 3H); ^{13}C NMR ($CDCl_3$) 191.9, 168.2, 166.4, 163.6, 106.1, 93.0, 90.6, 55.8; FT-IR (solid) 2984, 1624, 1498, 1475, 1211, 1157, 1111, 1045 cm^{-1}.

4,6-Bis(benzyloxy)-2-hydroxybenzaldehyde (17)

K_2CO_3 (9.10 g, 65.8 mmol, 2.40 equiv.) was added to a solution of 2,4,6-trihydroxybenzaldehyde (5.30 g, 27.9 mmol, 1.00 equiv.) in DMF (70 ml) at room temperature under argon. The mixture was stirred at the same temperature for 5 min, after which benzyl bromide (6.64 g, 55.8 mmol, 2.00 equiv.) was added to it. After stirring for 5 h, the reaction mixture was added to a mixture of 1 M aqueous HCl and EtOAc at 0 °C. The aqueous layer was extracted with two portions of EtOAc. The combined organic layers were washed with three portions of H_2O and brine, dried over $MgSO_4$ and concentrated *in vacuo*. The residue was re-crystallized from CH_2Cl_2-hexane to afford **17** as a white solid.[8]

RESULTS AND DISCUSSION

Screening for inhibitors of glucose production in hepatic cells

We have developed a cell-based assay system for detecting hepatic glucose production by using the rat hepatoma cell line H4IIE-C3, which mimics *in vivo* liver function.[9,10] In this system, after culturing overnight in the serum-free medium, the cells were incubated in a glucose-free medium for 5 h and the amount of glucose accumulated in the medium was detected by glucose oxidase reaction. Glucose oxidase catalyzes the formation of D-gluconolactone and H_2O_2 from D-glucose; and H_2O_2 reacts with the Amplex Red reagent in the presence of horseradish peroxidase to generate a red fluorescent oxidation product, resorufin. Resorufin was quantified using a fluorescence microplate reader (Figure 1a). In this system, H4IIE-C3 cells produced glucose, which was accumulated in the medium at a concentration of 25 μM. When metformin was added into the glucose-free medium as a positive control for inhibition of hepatic glucose production, metformin inhibited the production of glucose in the medium with an IC_{50} value of 1.7 mM without cytotoxicity (IC_{50} >100 mM) (Figure 1b). This result suggests that this system is effective for screening inhibitors of glucose production.

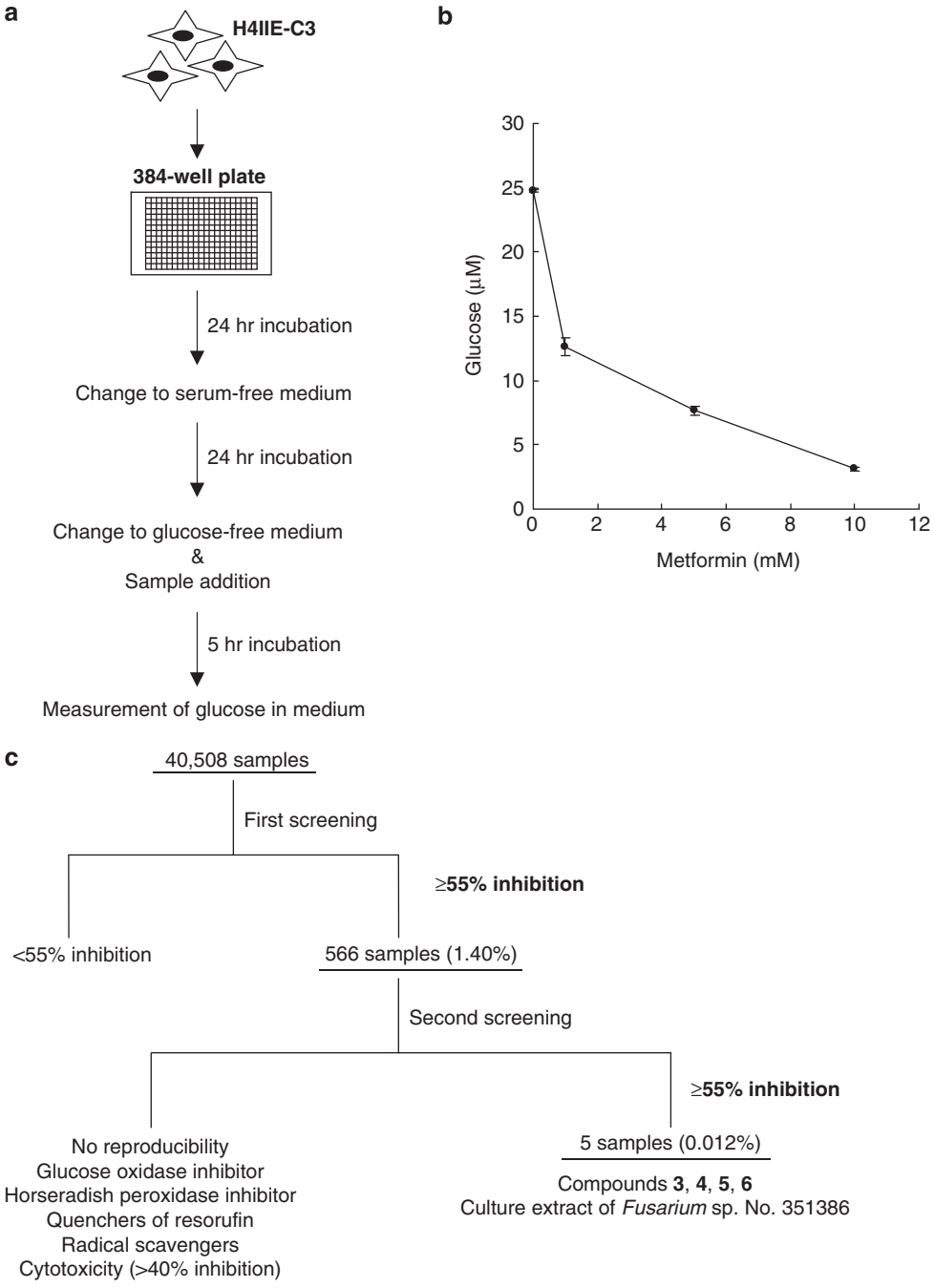

Figure 1 Assay system and the screening of inhibitors of hepatic glucose production. (**a**) Flow chart of the assay system of glucose production in rat liver cells. (**b**) Inhibitory effect of metformin on glucose production. (**c**) Use of this system in screening inhibitors of glucose production from the natural product library.

In the screening process, samples to be screened were added in the glucose-free medium. The samples that showed ⩾55% inhibition of glucose production compared with the glucose production in the medium to which samples were not added were selected as inhibitors of glucose production. A total of 40 508 natural product samples were used for the primary screening. We screened all the samples at a final concentration of 1% in a volume of 20 μl per well using a 384-well format. The first screenings yielded 566 hit samples (1.40%). Among the 566 hit samples, some of them probably behaved as inhibitors of glucose oxidase and horseradish peroxidase in the glucose assay system, some acted as quenchers of resorufin, and some as scavengers of H_2O_2. Hence, we excluded samples that caused a decrease in the fluorescence intensity when 50 μM of glucose solution was separately added into the same assay system (fluorescence intensity, <70%). Furthermore, we excluded samples that showed cytotoxicity during 5 h of incubation (cytotoxicity, >40%). After performing additional reproducible and dose-dependent tests, we finally selected five samples (0.012%) as inhibitors of glucose production. Four of these were **3**[5], **4**[6], **5**[5] and **6**, which were selected from the library of isolated microbial metabolites. The remaining sample was obtained from the culture extract of *Fusarium* sp. no. 351386. Therefore, we cultured this fungus in fermentation media and isolated two active compounds—**1**[3] and **2**[4]—from its culture extract.

Identification of 1 and 2

The structures of the active compounds, **1** and **2**, were determined by HR-ESI-MS, UV and ^{1}H NMR spectra as follows: Javanicin, ^{1}H NMR ($CDCl_3$): δ 13.24. (s, 1H), 12.84 (s, 1H), 6.19 (s, 1H), 3.92 (s, 3H), 3.89 (s, 2H), 2.28 (s, 3H), 2.22 (s, 3H). UV λ_{max} 536, 501, 472, 303; HR-MS *m/z* 291.0868 (calcd for $C_{15}H_{15}O_6$, $[M+H]^+$ 291.0869). Solaniol, ^{1}H NMR δ ($CDCl_3$): 13.31 (s, 1H), 13.04 (s, 1H), 6.19 (s, 1H), 4.11 (m, 1H), 3.91 (s, 3H), 2.93 (d, 2H, *J*=5.5 Hz), 2.33 (s, 3H), 1.30 (d, 3H, *J*=6.0 Hz). UV λ_{max} 540, 504, 475, 307; HR-MS *m/z* 293.1052 (calcd for $C_{15}H_{17}O_6$, $[M+H]^+$ 293.1025).

Table 1 Structures and IC_{50} values for anti-glucose production activity and cytotoxicity of 1–5

Compound	*Structure*	*Glucose production (μM)*	*Cytotoxicity (μM)*
1	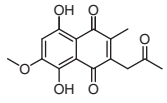	3.8	3.3
2	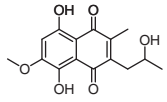	4.4	9.5
3	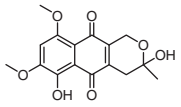	4.8	2.5
4	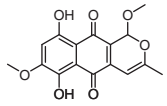	6.3	8.8
5	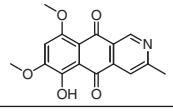	30	>50[a]

[a]**5** showed 30% inhibition of cell growth at a concentration of 50 μM.

Inhibition of hepatic glucose production by naphthoquinone derivatives

We tested the activities of five naphthoquinone derivatives with regard to inhibition of hepatic glucose production. The structures of **3–5** revealed that they were derivatives of **1** and **2**, as shown in Table 1. All these compounds exhibited inhibitory effects on glucose production. Thus, the naphthoquinone moiety, common to all these compounds, may be essential for their inhibitory activities. The compounds **1–4** showed similar degrees of inhibition (IC_{50}=3.8–6.8 μM); however, the inhibitory activity of **5** (IC_{50}=30 μM) was approximately sixfold lower than the inhibitory activities of **1–4**. Therefore, the pyridine moiety of **5** may have a significant role in inhibiting glucose production. In addition, these compounds, except **5**, exhibited cytotoxic effects (IC_{50}=3.3–8.8 μM) on H4IIE-C3 cells during 48 h of incubation, and **5** resulted in 30% inhibition of cell growth at a concentration of 50 μM. Hence, the IC_{50} values for the cytotoxic activity of these compounds were comparable with those of the inhibitory activity against hepatic glucose production (Table 1). On the basis of these results, it was concluded that these compounds are unsuitable candidates for use in anti-diabetic drugs.

Inhibition of hepatic glucose production by vanillin derivatives

Additional screening showed that **6** from our library was also an inhibitor of glucose production. To examine structure–activity relationship, we compared the inhibitory effects of **6** derivatives **7–17** on glucose production (Table 2). All **6** derivatives inhibited hepatic glucose production and their IC_{50} values (IC_{50}=24–190 μM) were lower than that of metformin (IC_{50}=1.7 mM). In particular, **9** and **13** showed strong inhibitory activities. Moreover, these compounds did not exhibit cytotoxic effects on H4IIE-C3 cells at 50 μM after 48 h of incubation. Thus, **6** derivatives can be considered as suitable

Table 2 Structures of vanillin analogs

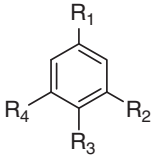

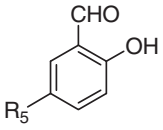

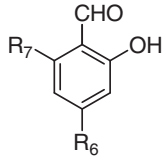

R_1	R_2	R_3	R_4	
CHO	OCH_3	OH	H	vanillin (4-hydroxy-3-methoxybenzaldehyde) (**6**)
COOH	OCH_3	OH	H	vanillic acid (4-hydroxy-3-methoxybenzoic acid) (**7**)
CHO	OH	OCH_3	H	isovanillin (3-hydroxy-4-methoxybenzaldehyde) (**8**)
$COCH_3$	OCH_3	OH	H	4-hydroxy-3-methoxyacetophenone (**9**)
$COCH_3$	OCH_3	OH	OCH_3	4-hydroxy-3,5-dimethoxyacetophenone (**10**)

R_5		R_6	R_7	
Br	5-bromosalicylaldehyde (**11**)	OH	H	2,4-dihydroxybenzaldehyde (**14**)
Cl	5-chlorosalicylaldehyde (**12**)	OH	OH	2,4,6-trihydroxybenzaldehyde (**15**)
NO_2	5-nitrosalicylaldehyde (**13**)	OCH_3	OCH_3	2-hydroxy-4,6-dimethoxybenzaldehyde (**16**)
		OBn	OBn	4,6-bis(benzyloxy)-2-hydroxybenzaldehyde (**17**)

Table 3 IC_{50} values for anti-glucose production activity of 6 to 17

Compound	*Glucose production (μM)*
6	32
7	190
8	75
9	25
10	39
11	31
12	49
13	24
14	43
15	61
16	49
17	59

candidates for use in anti-diabetic drugs, as opposed to the naphthoquinone derivatives examined here.

The inhibitory activity of **7** (IC_{50}=190 μM) against glucose production was weaker than that of **6** (IC_{50}=32 μM), **8** (IC_{50}=75 μM), **9** (IC_{50}=25 μM) and **10** (IC_{50}=39 μM) (Table 3). These results suggest that the absence of a carboxyl group in their structure was important for the inhibitory activity. On comparing the inhibitory activities of 5-halogenated salicylaldehydes (**11**, **12**) and 5-nitrosalicylaldehyde (**13**), it was found that **13**, which contains a 5-nitro group, showed the strongest inhibitory activity at an IC_{50} value of 24 μM. The activities of **14**, **15**, **16** and **17** were lower than those of **6**, **11** and **13**. Accordingly, in the case of benzaldehyde, 4-hydroxy-3-methoxy or 2,5-disubstituted moieties may have important roles in the inhibitory activities of these compounds against glucose production.

In this study, we developed a screening system for inhibitors of glucose production. Using the rat hepatoma cell line H4IIE-C3, we screened a total of 40 508 samples and evaluated 12 vanillin derivatives. We found that **9** or **13** inhibits glucose production in hepatic cells without exhibiting cytotoxic effects. In addition to these characteristics, these compounds also satisfy Lipinski's rule of 5[11] for oral drug-like properties as follows: a molecular weight of a compound is <500, hydrogen bond donors are <5, hydrogen bond accepters are <10 and an octanol–water partition co-efficient log *P* is <5. Therefore, **9** or **13** may have the potential to become leading oral anti-diabetic drugs.

CONFLICT OF INTEREST

The authors declare no conflict of interest.

ACKNOWLEDGEMENTS

This work was supported by a grant from the New Energy and Industrial Technology Development Organization (NEDO), Japan.

1 Agius, L. New hepatic targets for glycaemic control in diabetes. *Best Pract. Res. Clin. Endocrinol. Metab.* **21,** 587–605 (2007).
2 Scarpello, J. H. & Howlett, H. C. Metformin therapy and clinical uses. *Diab. Vasc. Dis. Res.* **5,** 157–167 (2008).
3 Arnstein, H. R. V. & Cook, A. H. Production of antibiotics by fungi. Part III. Javanicin. An antibacterial pigment from *Fusarium javanicum*. *J. Chem. Soc.* 1021–1028 (1947).
4 Arsenault, G. P. Fungal metabolites- III Quinones from *Fusarium solani* D_2 purple and structure of (+)-solaniol. *Tetrahedron* **24,** 4745–4749 (1968).
5 Tatum, J. H., Baker, R. A. & Berry, R. E. Naphthoquinones produced by *Fusarium oxysporum* isolated from citrus. *Phytochemistry* **24,** 457–459 (1985).
6 Tatum, J. H., Baker, R. A. & Berry, R. E. Metabolites of *Fusarium solani*. *Phytochemistry* **28,** 283–284 (1989).
7 Roelens, F. *et al.* Regioselective synthesis and estrogenicity of (±)-8-alkyl-5,7-dihydroxy-4-(4-hydroxyphenyl)-3,4-dihydrocoumarins. *Eur. J. Med. Chem.* **40,** 1042–1051 (2005).
8 Anderson, J. C., Headley, C., Stapleton, P. D. & Taylor, P. D. Asymmetric total synthesis of B-ring modified ()-epicatechin gallate analogues and their modulation of â-lactam resistance in *Staphylococcus aureus*. *Tetrahedron* **61,** 7703–7711 (2005).
9 Hofmann, C., Marsh, J. W., Miller, B. & Steiner, D. F. Cultured hepatoma cells as a model system for studying insulin processing and biologic responsiveness. *Diabetes* **29,** 865–874 (1980).
10 de Raemy-Schenk, A. M. *et al.* A cellular assay for measuring the modulation of glucose production in H4IIE cells. *Assay Drug Dev. Technol.* **4,** 525–533 (2006).
11 Lipinski, C. A., Lombardo, F., Dominy, B. W. & Feeney, P. J. Experimental and computational approaches to estimate solubility and permeability in drug discovery and development settings. *Adv Drug Deliv. Rev.* **46,** 3–26 (2001).

The Journal of Antibiotics (2009) 62, 631–634

www.nature.com/ja

ORIGINAL ARTICLE

Phellinins A1 and A2, new styrylpyrones from the culture broth of *Phellinus* sp. KACC93057P: I. Fermentation, taxonomy, isolation and biological properties

In-Kyoung Lee[1], Geon-Sik Seo[2], Nak Beom Jeon[3], Hee-Wan Kang[4] and Bong-Sik Yun[1]

Novel styrylpyrones, phellinins A1 and A2, were isolated together with known styrylpyrone compounds, hispidin and 1,1-distyrylpyrylethan, from the cultured broth of *Phellinus* sp. KACC93057P. These compounds were purified by solvent partition, Sephadex LH-20 column chromatography, C_{18}-solid phase extraction and finally by reversed-phase (ODS) TLC. To identify the phellinin producer *Phellinus* sp. KACC93057P, the ribosomal DNA (rDNA) internal transcribed space regions containing 5.8 rDNA were sequenced and compared with those of the known *Phellinus* isolates. *Phellinus* sp. KACC93057P was 94.8% identical to *P. baumii* and *P. linteus*, all of which did not produce phellinins A1 and A2. These compounds significantly scavenged free radicals such as 1,1-diphenyl-2-picrylhydrazyl, 2,2′-azinobis-(3-ethylbenzothiazoline-6-sulfonic acid) and superoxide.
The Journal of Antibiotics (2009) **62,** 631–634; doi:10.1038/ja.2009.82; published online 28 August 2009

Keywords: free radical scavenger; fungal metabolite; *Phellinus* sp. KACC93057P; phellinins A1 and A2; styrylpyrone

INTRODUCTION

Several mushrooms including the genera *Phellinus* and *Inonotus* are used as traditional medicines and produce natural pigments, styrylpyrones, which have important roles in their biological activity. The pharmacological activities of styrylpyrones isolated from mushrooms, including antioxidant, anti-inflammation, anticancer and anti-platelet aggregation activities, have been reported.[1–3] To date, a number of styrylpyrone metabolites have been isolated from *Phellinus* and *Inonotus*,[4–6] and the metabolites from the fruiting body were more complex and had greater structural diversity when compared with metabolites isolated from mycelial culture.[7] It is known that the fungal ligninolytic enzymes, laccase and peroxidase, catalyze the polymerization of styrylpyrone monomers and transformation of many phenolic compounds into polymeric structures.[8,9]

In a continuous search for novel styrylpyrones from the cultured broths of *Phellinus* isolates, we found that *Phellinus* sp. KACC93057P produced novel free radical scavengers, phellinins A1 and A2 (**1**, Figure 1), together with the known compounds, hispidin (**2**) and 1,1-distyrylpyrylethan (**3**). Compound **1** was obtained as an inseparable mixture of isomers (A1 and A2) with the same ratio. In this study, the identification and fermentation of the microorganism *Phellinus* sp. KACC93057P and the isolation and antioxidant activity of **1** are described. The physicochemical properties and structure determination of **1** will be described in an accompanying study.[10]

RESULTS

HPLC analysis of styrylpyrones

It is known that ethyl acetate extracts of the cultured broths of the medicinal fungi *Inonotus xeranticus* and *P. linteus* show potent antioxidant activity because of the presence of styrylpyrones.[7] To identify novel antioxidant styrylpyrones from *Phellinus* spp. isolates, the ethyl acetate layer of four cultured broths was analyzed by reversed-phase HPLC equipped with a photodiode array detector. The styrylpyrones showed characteristic UV absorption maxima at 380–420 and 245–255 nm. In general, both hispidin and its dimmers, hypholomine B, 3,14′-bihispidinyl and 1,1-distyrylpyrylethan, are found in the genera *Phellinus* and *Inonotus*.[7,11] The constituents and content of styrylpyrones from *Phellinus* spp. 52370, 52387 and 52391 and *I. xeranticus* BS064 were similar on the basis of their HPLC profiles (Figure 2). The *phellinus* sp. KACC93057P, however, had a different HPLC profile in which the peaks corresponding to hypholomine B and 3,14′-bihispidinyl seemed relatively small and several unidentified peaks were

[1]Division of Biotechnology, College of Environmental and Bioresource Sciences, Chonbuk National University, Iksan, Jeonbuk, Korea; [2]Korea National Agriculture College, Hwaseong, Kyonggi, Korea; [3]Incheon International Airport Branch, National Plant Quarantine Service, Seoul, Korea and [4]Graduate School of Biotechnology and Information Technology, Hankyong National University, Ansung, Kyonggi, Korea
Correspondence: Professor H-W Kang, Graduate School of Biotechnology and Information Technology, Hankyong National University, Ansung, Kyonggi 456-749, Korea and Professor B-S Yun, Division of Biotechnology, College of Environmental and Bioresource Sciences, Chonbuk National University, Iksan, Jeonbuk 570-752, Korea.
E-mail: bsyun@chonbuk.ac.kr
Received 29 June 2009; revised 20 July 2009; accepted 27 July 2009; published online 28 August 2009

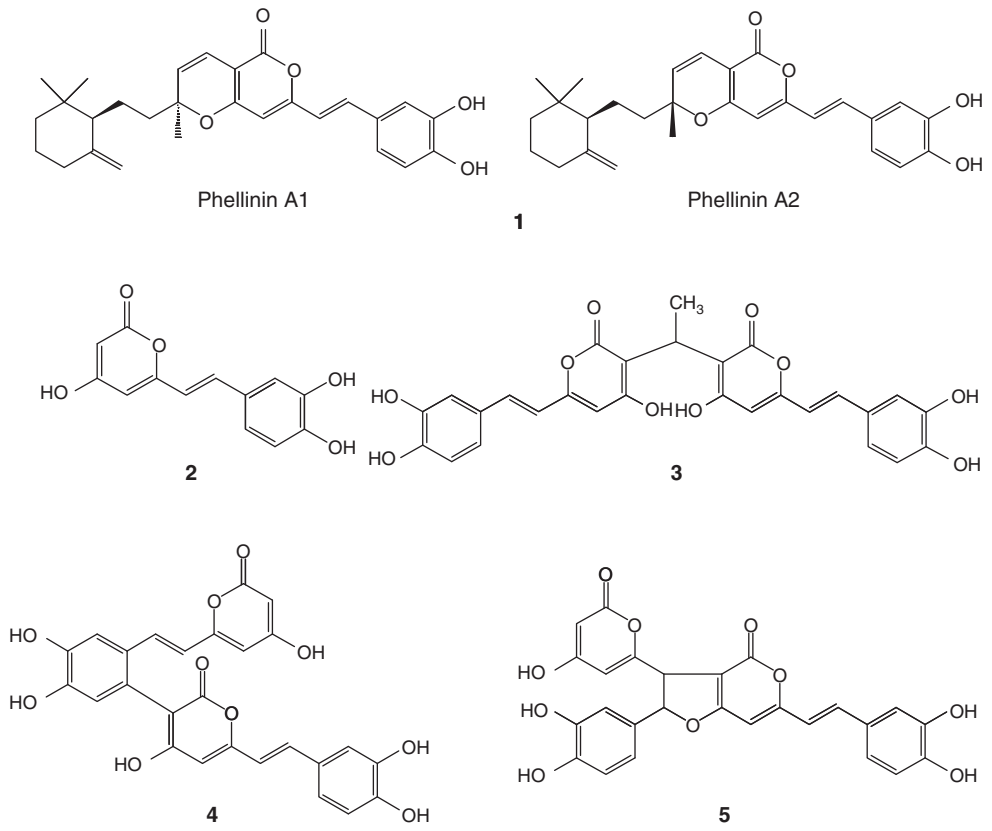

Figure 1 Structures of phellinins A1 and A2 (**1**), hispidin (**2**), 1,1-distyrylpyrylethan (**3**), 3,14′-bihispidinyl (**4**), hypholomine B (**5**).

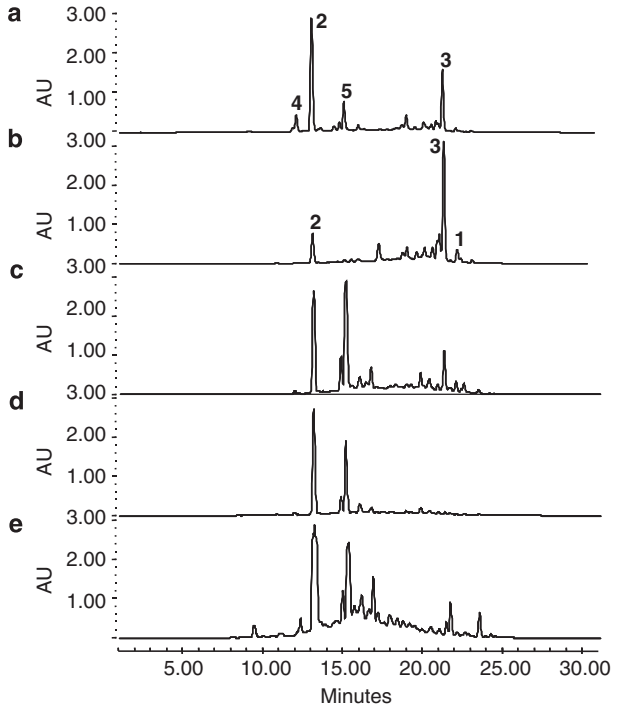

Figure 2 HPLC chromatograms of the ethyl acetate layer of cultured broths of *Inonotus xeranticus* BS064 (**a**), *Phellinus* sp. KACC93057P (**b**), *Phellinus* sp. 52387 (**c**), *Phellinus* sp. 52391 (**d**), *Phellinus* sp. 52370 (**e**) strains. The elution profile was established by monitoring UV absorbance at 380 nm. **1** phellinins A1 and A2; **2** hispidin; **3** 1,1-distyrylpyrylethan; **4** 3,14′-bihispidinyl; **5** hypholomine B.

observed. To identify these new peaks, the fungus *phellinus* sp. KACC93057P was mass cultured.

Taxonomy of *Phellinus* sp. KACC93057P

Nuclear ribosomal DNA (rDNA) has been used to analyze major evolutionary events. This is especially true for the internal transcribed space (ITS) region, which has been established as a useful tool for identifying fungi at the species level. Thus, rDNA ITS regions containing 5.8 rDNA were sequenced to investigate the genetic relatedness among *Phellinus* spp. Alignment of these ITS sequences revealed a close genetic relationship among *P. baumii* and *P. linteus*, and *Phellinus* sp. KACC93057P was found to be 94.8% identical to *P. baumii* and *P. linteus* (Figure 3).

Therefore, the morphological and physiological characteristics of *Phellinus* sp. KACC93057P were compared with *P. baumii* and *P. linteus*. The mycelial growth of *Phellinus* sp. KACC93057P was excellent on YGM broth, which grew more than twice as fast as the other strains of *Phellinus* spp. In addition, KACC93057P had a mycelial colony color of bright yellow and abundant aerial mycelium on potato dextrose agar (PDA) media that was distinguishable from *P. baumii* and *P. linteus* (Figure 4). Earlier, a specific PCR primer set with PLSPF2 (5′-ACTTATTCCATCGCAGGTTA-3′) and PLSPR1 (5′-CTCGTACCTCGTCATCAAGT-3′) was developed for differentiating *P. linteus* from other closely related *Phellinus* spp.[12] However, the primer set did not produce PCR amplicon from genomic DNA of *Phellinus* sp. KACC93057P, indicating that at least KACC93057P was not *P. linteus*. In conclusion, *Phellinus* sp. KACC93057P is likely a variant in the *P. linteus* complex and could also not be excluded from the novel *Phellinus* species in morphological and physiological difference, ITS rDNA data and PCR detection.

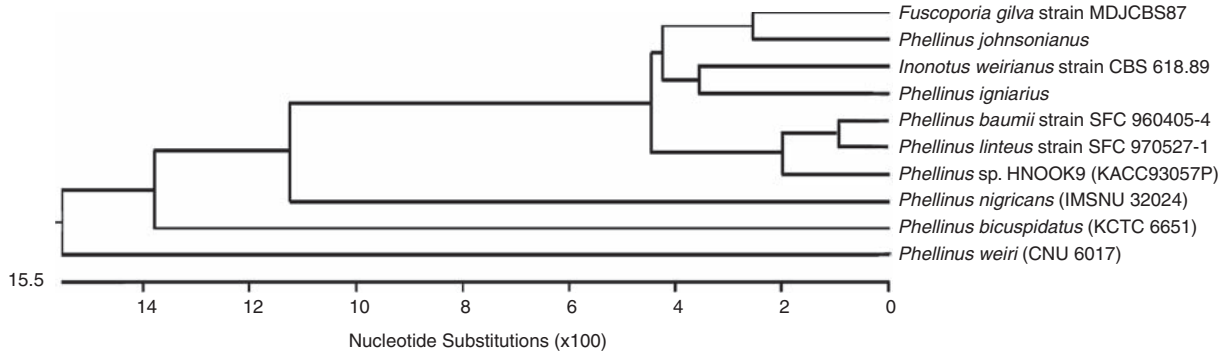

Figure 3 Genetic relationship of *Phellinus* sp. KACC93057P based on rDNA ITS sequences.

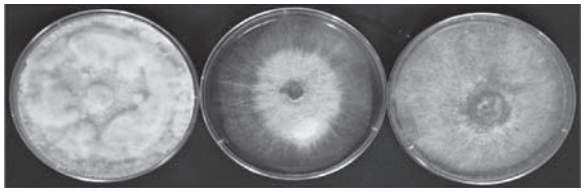

Figure 4 Morphological characteristics of mycelial mats of *Phellinus* sp. KACC93057P, *P. baumii* and *P. linteus* on PDA media after 14 days of culture.

Isolation and purification

The procedure used for isolating the styrylpyrones to assess their antioxidant activity was summarized in Figure 5. In total, 2 l of culture broth was filtered to separate the broth filtrate and the mycelium. Mycelium was extracted with 0.5 l of 80% acetone. The acetone extracts were filtered and the filtrate was evaporated under reduced pressure to remove acetone. The resulting residue was extracted with ethyl acetate twice and then subjected to Sephadex LH-20 (Pharmacia, Uppsala, Sweden) column chromatography using MeOH as the elution solvent. Using this approach, two active fractions were observed. One of the fractions was further purified by C_{18} Sep-Pak cartridge (Waters, Milford, MA, USA) extraction in which the eluting phase was a gradient of increasing methanol (40–90%) in water. The active fraction, which eluted at 70–80% aqueous MeOH, was purified on a column of Sephadex LH-20 with 70% aqueous MeOH, followed by reversed-phase (ODS) TLC developed with 90% aqueous MeOH to give **1** (2.5 mg). The other fraction was chromatographed on a Sephadex LH-20 column with 70% aqueous MeOH, followed by reversed-phase TLC developed with 70% aqueous MeOH to give **2** (3 mg) and **3** (5 mg). Details of the structure of compound **1** will be presented in an accompanying paper.

Free radical scavenging activity

The main property of an antioxidant is its ability to scavenge free radicals. The free radical scavenging efficacies of **1**–**3** were evaluated using the 1,1-diphenyl-2-picrylhydrazyl (DPPH) radical, 2,2′-azinobis-(3-ethylbenzothiazoline-6-sulfonic acid (ABTS) radical anion and superoxide radical cation scavenging assay methods. In the DPPH and ABTS radical scavenging activity assay, the results were expressed in terms of trolox equivalent antioxidant capacity (IC_{50} of μM compound per IC_{50} of μM trolox). Results from the free radical scavenging assay are presented in Table 1, in which all the compounds were capable of scavenging DPPH, ABTS and superoxide radicals, in a concentration-dependent manner and all of the tested compounds showed potent activity comparable with the positive control, caffeic acid and butylated hydroxyanisole (BHA).

METHODS

Fungi and fermentation

To search novel antioxidant styrylpyrones from *Phellinus* spp., the fungal strains (52387, 52391 and 52370) of *Phellinus* sp. were obtained from the Rural Development Administration in Korea, and the strain of *Phellinus* sp. KACC93057P was obtained by tissue culture from the fruiting body of an unidentified fungus belonging to *Phellinus* sp. In brief, a small piece of fresh mushroom was incubated on a Petri dish containing PDA medium. After incubation at 28 °C for 5 days, the mycelium grown was used to obtain axenic culture of *Phellinus* sp. KACC93057P.

For analysis of the styrylpyrone isolated from cultured broths, three strains of *Phellinus* were grown in potato dextrose broth medium at 28 °C for 10 days and a strain of *Phellinus* sp. KACC93057P was cultured in stationary position at 25 °C for 14 days in tissue culture bottle (500 ml with 200 μm filter cap) and containing 120 ml of YGM medium (yeast extract 1%, glucose 0.4% and malt extract 0.4%). The morphological and cultural characteristics were investigated using PDA medium at 25 °C for 14 days.

HPLC analysis of styrylpyrones

The styrylpyrone constituents in the cultured broths were detected using a method reported earlier.[7] In brief, the ethyl acetate layer of the cultured broths of fungi *Phellinus* spp. was analyzed by analytical reversed-phase HPLC (Hitachi L-2000 series, Hitachi, Tokyo, Japan), which consisted of an autosampler, a pump, a photodiode array detector and a reversed-phase C_{18} column (150×4.6 mm i.d.; Cosmosil, Nacalai tesque, Kyoto, Japan).[6] A linear gradient containing water acidified with 0.04% trifluoroacetic acid (vv) and methanol was used at a flow rate of 1 ml min^{-1}. HPLC detection was initiated with a 5 min flow at 30% methanol, which reached 90% methanol within 23 min. The column was washed with 90% methanol for 3 min and then equilibrated at 30% methanol for 4 min.

ITS rDNA analysis

Genomic DNA of *Phellinus* sp. KACC93057P grown in malt-yeast broth (2% malt extract and 0.2% yeast extract) was extracted as described by Graham *et al.*[13] A total of 200 mg of mycelia were transferred to a 1.5 ml test tube and 400 μl of lysis buffer (200 mM Tris-HCl (pH 8.0), 100 mM NaCl, 25 mM EDTA and 0.5% SDS) containing proteinase K (50 μg) was added to the tube. The tube was placed in a 65 °C water bath for 15 min and then extracted with chloroform–isoamyl alcohol (24:1, v/v) and centrifuged at 12 000 r.p.m. for 10 min. The upper phase was transferred to a new tube and DNA was precipitated with a 0.7 volume of isopropanol, washed with 70% ethanol, dried and resuspended in 50 μl of TE buffer (10 mM Tris-HCl and 1 M EDTA, pH 8.0). The rDNA regions, including ITS 1, 2 and the 5.8S ribosomal gene, were amplified from the genomic DNA using the universal primers ITS 1 (5′-TCCGTAGGTGAACCTCGGC-3′) and ITS 2 (5′-TCCTCCGCTTATTGATATGC-3′).[14] The PCR products containing the ITS region were purified using a Wizard PCR prep kit (Promega, Madison, WI, USA) and were directly sequenced with a BigDye terminator cycling sequencing kit (Applied Biosystem Inc, Foster City, CA, USA). The ITS sequences from *Phellinus* sp. KACC93057P of this study and different *Phellinus* spp. retrieved from GenBank were aligned using the MegAlign program of the DNA star software

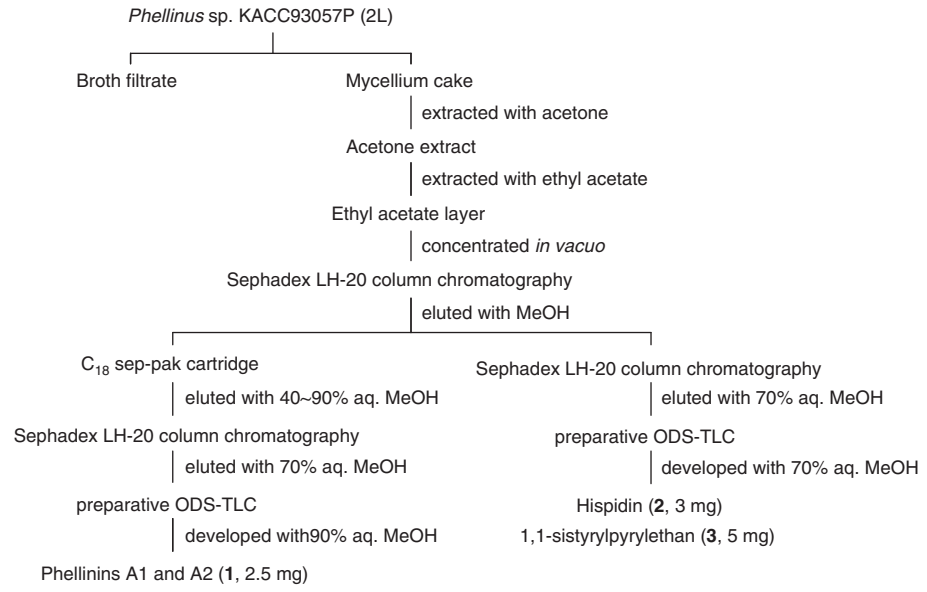

Figure 5 Isolation procedures of compounds **1–3**.

Table 1 Free radical scavenging activity of the compounds isolated

	TEAC[a,b]		
Compounds	*DPPH*	*ABTS*	*Superoxide*[c] *IC_{50} (μM)*[b]
Phellinin A (**1**)	0.76	0.47	47.3 ± 3.3
Hispidin (**2**)	1.31	2.27	34.9 ± 4.0
1,1-distyrylpyrylethan (**3**)	0.37	0.18	32.0 ± 1.1
Caffeic acid	0.11	0.18	16.5 ± 2.3
BHA	0.34	0.12	>500

Abbreviations: ABTS, 2,2′-azinobis-(3-ethylbenzothiazoline-6-sulfonic acid); BHA, butylated hydroxyanisole; DPPH, 1,1-diphenyl-2-picrylhydrazyl; TEAC, trolox equivalent antioxidant capacity.
[a]Expressed as IC_{50} of μM compound per IC_{50} of μM of trolox.
[b]Results presented as the mean (n=3) ± s.d.
[c]Xanthine/xanthine oxidase.

(Madison, WI, USA). The phylogenic tree was constructed using the neighbor-joining program of MEGA (Tempe, AZ, USA).

Free radical scavenging activity assay

The ability of the samples to scavenge free radical was determined using the DPPH radical, ABTS radical cation and superoxide radical anion scavenging assay methods.[7] In detail, 5 μl of each sample was combined with 95 μl of 150 μM methanolic DPPH in triplicate. After incubation at room temperature for 30 min, the absorbance at 517 nm was read using a Molecular Devices Spectromax microplate reader (Sunnyvale, CA, USA).

The ABTS was dissolved in water to a concentration of 7 mM. The ABTS cation radical was produced by reacting the ABTS stock solution with 2.45 mM potassium persulfate and by allowing the mixture to stand in the dark for 12 h. After adding 95 μl of the ABTS radical cation solution to 5 μl of antioxidant compounds in methanol, the absorbance was measured by a microplate reader at 734 nm after mixing for up to 6 min.

The superoxide radical anion scavenging activity was evaluated using the xanthine/xanthine oxidase method. In brief, each well of a 96-well plate contained 100 μl of the following reagents: 50 mM potassium phosphate buffer (pH 7.8), 1 mM EDTA, 0.04 mM NBT (nitroblue tetrazolium), 0.18 mM xanthine, 250 mU ml^{-1} xanthine oxidase and the sample at different concentrations. The reaction was incubated for 30 min at 37 °C in the dark. The xanthine oxidase catalyzes the oxidation of xanthine to uric acid and superoxide, and the superoxide reduces NBT to blue formazan. The reduction of NBT to blue formazan was measured at 560 nm in a microplate reader. BHA, trolox and caffeic acid were used as a reference.

ACKNOWLEDGEMENTS

This work was supported by a grant (20080401-034-069) from the BioGreen 21 Program of the Rural Development Administration (RDA), Republic of Korea.

1 Kim, S. D. *et al*. The mechanism of anti-platelet activity of davallialactone: Involvement of intracellular calcium ions, extracellular signal-regulated kinase 2 and p38 mitogen-activated protein kinase. *Eur. J. Pharmacol.* **584,** 361–367 (2008).
2 Lee, Y. G. *et al*. Src kinase-targeted anti-inflammatory activity of davallialactone from *Inonotusxeranticus* in lipopolysaccharide-activated RAW264.7 cells. *Br. J. Pharmacol.* **154,** 852–863 (2008).
3 Lee, I. K. & Yun, B. S. Highly oxygenated and unsaturated metabolites providing a diversity of hispidin class antioxidants in the medicinal mushrooms *Inonotus* and *Phellinus*. *Bioorg. Med. Chem.* **15,** 3309–3314 (2007).
4 Lee, I. K. & Yun, B. S. Hispidin analogs from the mushroom *Inonotus xeranticus* and their free radical scavenging activity. *Bioorg. Med. Chem. Lett.* **16,** 2376–2379 (2007).
5 Lee, I. K., Kim, Y. S., Jang, Y. W., Jung, J. Y. & Yun, B. S. New antioxidant polyphenols from the medicinal mushroom *Inonotusobliquus*. *Bioorg. Med. Chem. Lett.* **17,** 6678–6681 (2007).
6 Lee, I. K., Seok, S. J., Kim, W. K. & Yun, B. S. Hispidin derivatives from the mushroom *Inonotus xeranticus* and their antioxidant activity. *J. Nat. Prod.* **69,** 299–301 (2006).
7 Jung, J. Y. *et al*. Antioxidant polyphenols from the mycelia culture of the medicinal fungi *Inonotusxeranticus* and *Phellinuslinteus*. *J. Appl. Microbiol.* **104,** 1824–1832 (2008).
8 Ward, G., Hadar, Y., Bilkis, I., Konstantinovsky, L. & Dosoretz, C. G. Initial steps of ferulic acid polymerization by lignin peroxidase. *J. Biol. Chem.* **276,** 18734–18741 (2001).
9 Lee, I. K. & Yun, B. S. Peroxidase-mediated formation of the fungal polyphenol 3,14′-bihispidinyl. *J. Microbiol. Biotechnol.* **18,** 107–109 (2008).
10 Lee, I. K., Jung, J. Y., Kim, Y. H. & Yun, B. S. Phellinins A1 and A2, new styrylpyrones from the culture broth of *Phellinus* sp. KACC93057P: II. Physicochemical properties and structure elucidation. *J. Antibiot.* **62,** 635–637 (2009).
11 Fiasson, J. L. Distribution of styrylpyrones in the basidiocarps of various Hymenochaetaceae. *Biochem. Syst. Ecol.* **10,** 289–296 (1982).
12 Kang, H. W. *et al*. PCR based detection of *Phellinus linteus* using specific primers generated from universal rice primer (URP) derived PCR polymorphic band. *Mycobiology* **30,** 202–207 (2002).
13 Graham, G. C., Mayer, S. P. & Henry, R. J. Amplified method for the preparation of fungal genomic DNA for PCR and RAPD analysis. *Biotechniques* **16,** 175–269 (1994).
14 Park, D. S. *et al*. PCR-based sensitive detection of wood decaying fungus *Phellinus-linteus* by specific primer from rDNA ITS regions. *Mycobiology* **29,** 7–10 (2001).

The Journal of Antibiotics (2009) 62, 635–637

www.nature.com/ja

NOTE

Phellinins A1 and A2, new styrylpyrones from the culture broth of *Phellinus* sp. KACC93057P: II. Physicochemical properties and structure elucidation

In-Kyoung Lee[1], Jin-Young Jung[1], Young-Ho Kim[2] and Bong-Sik Yun[1]

The Journal of Antibiotics (2009) **62,** 635–637; doi:10.1038/ja.2009.83; published online 28 August 2009

Keywords: biosynthesis; chemical structure; phellinins A1 and A2; *Phellinus* sp. KACC93057P

In a continuous search for novel styrylpyrones from the culture broths of *Phellinus* isolates using HPLC analysis and free radical scavenging activity, we found that *Phellinus* sp. KACC93057P produced new styrylpyrones, phellinins A1 and A2 (Figure 1), together with the known compounds, hispidin and 1,1-distyrylpyrylethan. Phellinin A (**1**) was identified as a mixture of isomers (A1 and A2) with the same ratio by NMR experiments. These compounds were structurally related to siccanochromene A and cyclorenierins,[1,2] which are terpenes from the fungus *Helminthosporium siccans* and the sponge *Haliclona* sp., respectively. The identification and fermentation of the producing microorganism *Phellinus* sp. KACC93057P, in addition to the isolation and antioxidant activity of **1**, were described in an earlier paper.[3] This report describes the physicochemical properties and structure determination of **1** using spectroscopic methods including NMR and mass spectrometry.

The physicochemical properties of **1** are summarized in Table 1. Compound **1** was isolated as an orange powder. It was readily soluble in dimethyl sulfoxide and methanol, poorly soluble in $CHCl_3$ and water, and insoluble in hexane. Compound **1** had UV absorption maxima at 257 and 391 nm, which suggested the presence of a characteristic styrylpyrone moiety. The bands at 3444 and 1635 cm^{-1} in the IR spectrum indicated the presence of a hydroxyl group and conjugated carbonyl moiety, respectively. The ESI-mass measurements in the positive and negative modes revealed its molecular mass to be 448. The molecular formula of **1** was determined to be $C_{28}H_{32}O_5$ by high-resolution EI-mass data (Table 1).

The ^{1}H NMR spectrum of **1** revealed two sets of signals at δ 0.91 and 0.92, 0.81 and 0.82, 1.42 and 1.43, 5.44 and 5.48, and 6.39 and 6.40 in the same ratio of intensity, which suggested that **1** was a mixture of two components, A1 and A2, and the mixture could not be separated by HPLC. Thus, a structure analysis of the mixture of A1 and A2 was conducted using NMR. The proton peaks of A1 and A2 in the aromatic region between δ 6.77 and 7.4 perfectly overlapped each other, whereas the methyl groups and sp^2 methines between δ 4.5 and 5.5 appeared as two set of signals. First, we attempted to elucidate the structure of one of the components of the A1/A2 mixture. The ^{1}H NMR spectrum revealed signals attributable to three aromatic protons from a 1,2,4-trisubstituted phenyl moiety at δ 6.77 (d, J=8.4 Hz), 6.95 (dd, J=1.2, 8.4 Hz) and 7.02 (d, J=1.2 Hz), a methine singlet at δ 6.14, a *trans*-disubstituted double bond unit at δ 6.59 (d, J=15.9 Hz) and 7.30 (d, J=15.9 Hz), a *cis*-disubstituted double bond unit at δ 5.44 (d, J=10.5 Hz) and 6.39 (d, J=10.5 Hz), a terminal methylene protons at δ 4.55 (br, s) and 4.79 (br, s), five methylenes at δ 1.50–2.10 that significantly overlapped each other, and three methyl singlets at δ 0.81, 0.91 and 1.42 (Table 2). In the ^{13}C NMR spectrum, many peaks in the aromatic/olefin region were overlapped between the two components, and thus showed a high intensity relative to the separated peaks. However, several methylenes between δ 21 and 42 appeared as two sets of peaks. The heteronuclear multiple quantum coherence (HMQC) spectrum identified all proton-bearing carbons and the ^{1}H–^{1}H COSY spectrum revealed three partial structures, as shown in Figure 2. The connectivity of the partial structures was determined with the aid of the heteronuclear multiple bond coherence (HMBC) spectrum, as shown in Figure 2. The styrylpyrone moiety was assigned by the long-range correlations from H-8 to C-4a, C-7, C-8a and C-1″, H-1″ to C-7, C-8 and C-3″, H-2″ to C-7, C-4″ and C-8″, H-7″ to C-3″, C-5″ and C-6″, and H-8″ to C-2″, C-4″ and C-6″. These proton and carbon chemical shift values were in good agreement with the corresponding proton and carbon chemical shifts of hispidin, a representative styrylpyrone compound.[4] In combination with ^{1}H–^{1}H COSY data, the long-range correlations from two methyl singlets at H-10′ and H-11′ to C-3′, C-4′ and C-5′ revealed the presence of a 1,1-dimethyl-3-methylene-2-ethylcyclohexane moiety. Long-range correlations of H-4 to C-2, C-5 and C-8a, and H-12′ to C-2, C-3 and C-1′

[1]Division of Biotechnology, College of Environmental and Bioresource Sciences, Chonbuk National University, Iksan, Jeonbuk, Korea and [2]College of Pharmacy, Chungnam National University, Daejeon, Korea
Correspondence: Professor B-S Yun, Division of Biotechnology, College of Environmental and Bioresource Sciences, Chonbuk National University, Iksan, Jeonbuk 570-752, Korea.
E-mail: bsyun@chonbuk.ac.kr
Received 29 June 2009; revised 20 July 2009; accepted 21 July 2009; published online 28 August 2009

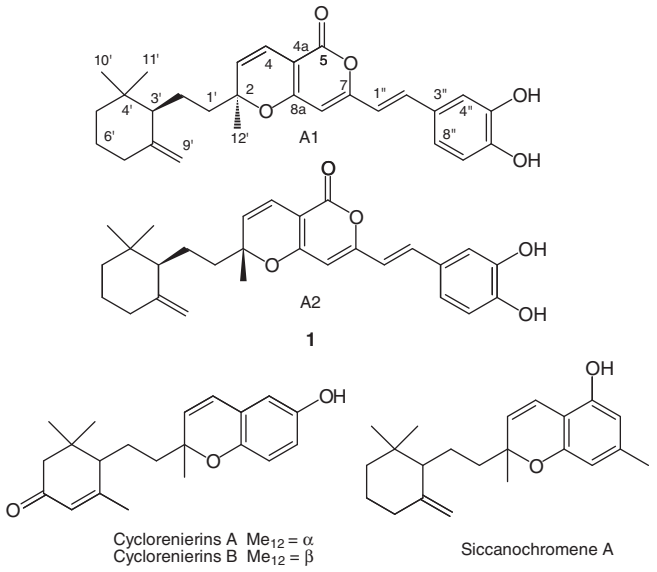

Figure 1 Structures of phellinins A1 and A2 (**1**), cyclorenierins A and B, and siccanochromene A.

Table 1 Physicochemical properties of 1

Appearance	Orange powder
Molecular weight	448
Molecular formula	$C_{28}H_{32}O_5$
ESI mass (*m/z*)	
In negative mode	447.6 $[M-H]^-$
HR-EI mass (*m/z*)	
Found	448.2250
Calcd	448.2250
UV λ_{max}nm (log ε)	
	206 (4.16)
	257 (3.82)
	391 (4.07)
IR ν_{max}(KBr) cm^{-1}	
	3444, 1635, 1458

linked all partial structures. By a process of elimination, C-2 and C-8a were connected by an ethereal linkage, which consequently formed a 2-methylpyran moiety. In addition, HMBC correlations from H-5′ to C-4′, C-10′ and C-11′, H-9′ to C-3′ and C-5′, and H-2′ to C-2 and C-4′ were evident. Therefore, on the basis of its structure, this compound was definitively shown to be a new styrylpyrone compound.

The molecular weight of the other component was the same as the one described above and its ^1H and ^{13}C NMR peaks overlapped significantly with the corresponding signals of the above component, suggesting that this component was an isomer. In the ^1H NMR spectrum, the signals from the styrylpyrone moiety, such as the three aromatic protons attributed to a 1,2,4-trisubstituted phenyl moiety at δ 6.77 (d, J=8.4 Hz), 6.95 (dd, J=1.2, 8.4 Hz) and 7.02 (d, J=1.2 Hz), a methine singlet at δ 6.14 and a *trans*-disubstituted double bond unit at δ 6.59 (d, J=15.9 Hz) and 7.30 (d, J=15.9 Hz), were observed, and these signals completely overlapped with the corresponding signals of the other component. However, the signals from the *cis*-disubstituted double bond at δ 5.48 (d, J=10.5 Hz) and 6.40 (d, J=10.5 Hz) and three singlet methyls at δ 0.82, 0.92 and 1.43 were slightly different

Table 2 ^1H and ^{13}C NMR spectral data for 1 in CD_3OD[a]

No.	δ_C	δ_H
2	84.6/84.5	
3	126.0/125.9	5.48/5.44 (1H, d, J=10.5)[b]
4	117.43/117.40	6.40/6.39 (1H, d, J=10.5)
4a	99.4	
5	163.9	
7	161.4	
8	101.1	6.14 (1H, s)
8a	166.7	
1′	41.6	1.57 (1H, m), 1.35 (1H, m)
2′	21.5	1.60 (1H, m), 1.50 (1H, m)
3′	55.4	1.65 (1H, m)
4′	35.9/35.8	
5′	37.2	1.45 (1H, m), 1.19 (1H, m)
6′	24.7	1.50 (2H, m)
7′	33.4	2.02 (2H, m)
8′	150.4	
9′	110.0	4.79 (1H, br s), 4.55 (1H, br s)
10′	28.8	0.92/0.91 (3H, s)
11′	26.7	0.82/0.81 (3H, s)
12′	27.9/27.8	1.43/1.42 (3H, s)
1″	116.8	6.59 (1H, d, J=15.9)
2″	137.4	7.30 (1H, d, J=15.9)
3″	128.9	
4″	114.9	7.02 (1H, d, J=1.2)
5″	146.8	
6″	148.8	
7″	116.6	6.77 (1H, d, J=8.4)
8″	122.1	6.95 (1H, dd, J=8.4, 1.2)

[a]NMR data were recorded at 400 MHz for proton and at 100 MHz for carbon.
[b]Proton resonance integral, multiplicity and coupling constant (J=Hz) are in parentheses.

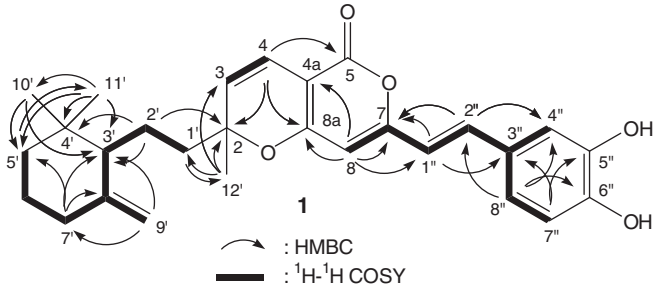

Figure 2 Key correlations in HMBC and ^{1}H-^{1}H COSY experiments of compound **1**.

from those of the earlier component in regard to their chemical shifts (Table 2). In the ^{13}C NMR spectrum, all carbon peaks except for C-2, C-3, C-4, C-4′ and C-12′ overlapped with those of the earlier component. The ^1H–^1H COSY spectrum revealed that the structure of this component was identical to the one described above, as shown in Figure 2. The long-range correlations from H-4 to C-2 and from H-10′ and H-11′ to C-3′, C-4′ and C-5′ confirmed that its planar structure was the same as that of the above structure.

To establish the relative stereochemistry and complete NMR assignments, we measured the NOESY spectrum. However, the significant overlapping of signals and very close corresponding signals of both components prevented us from being able to accurately interpret the NOESY spectrum. Phellinin A is a mixture of stereoisomers and these

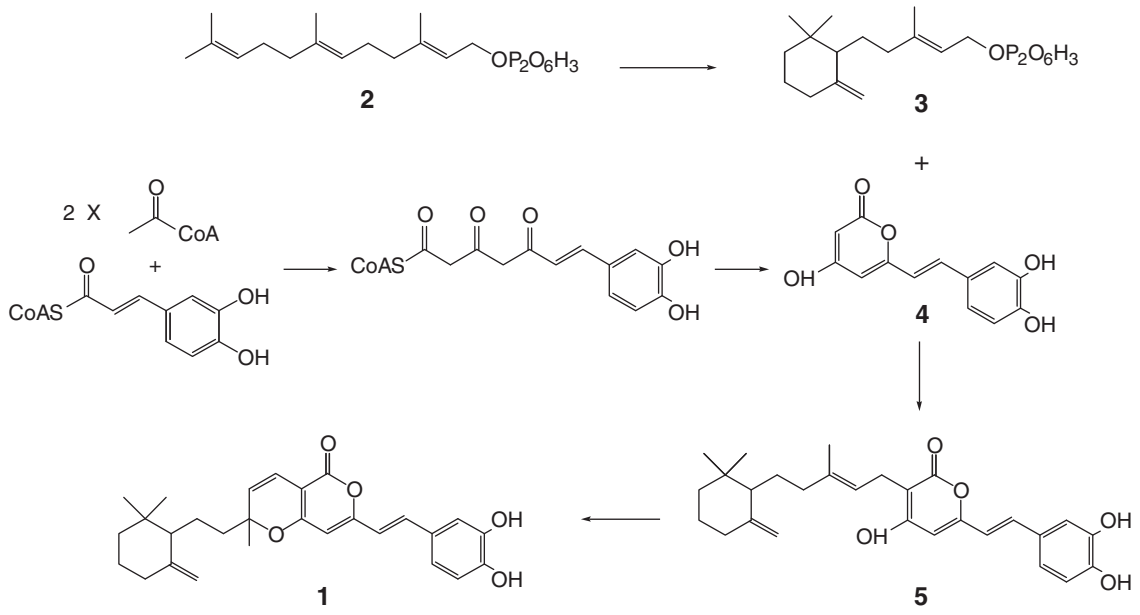

Figure 3 Proposed biosynthesis of phellinins A1 and A2 (**1**).

compounds possess two chiral centers at C-2 and C-3′. Two sets of ^{1}H and ^{13}C NMR peaks should be derived from the α- and β-configuration of C-2 relative to C-3′. Therefore, we designated phellinin A1 as the α-configuration and phellinin A2 as the β-configuration.

Several compounds possessing closely related structures have been identified earlier, including siccanochromene A from the pathogenic fungus *H. siccans*[1] and cyclorenierins A and B from the sponge *Haliclona* sp.[2] Cyclorenierins A and B, sesquiterpenoid quinols, were obtained as a mixture of inseparable α and β isomers, respectively. The comparison of phellinin A with siccanochromene A made it possible to propose a biogenetic pathway.[5] The siccanochromene A was assumed to be a possible intermediate in the biosynthesis of the terpenoid, siccanin. The proposed biosynthesis of siccanochromene A was supported by experiments with both cell-free and intact cell systems of *H. siccans* Drechsler from farnesyl pyrophosphate (**2**).[6] As depicted in Figure 3, the biosynthesis of *trans*-γ-monocyclofarnesyl pyrophosphate (**3**) is believed to proceed stereoselectively by cyclization of *trans,trans*-farnesyl pyrophosphate (**2**). Hispidin (**4**) was shown to be synthesized from phenylalanine through a cinnamyl derivative that was combined with malonate through the polyketide pathway in a cultured fungal strain.[7,8] The condensation of *trans*-γ-monocyclofarnesyl pyrophosphate with hispidin would yield compound **5**, and the oxidative and nonstereoselective cyclization of **5** might form isomers of phellinin A (**1**). To the best of our knowledge, this is the first case of condensation of hispidin and of an isoprene unit and represents a new group of a natural polyketide-isoprenoid hybrid compound with antioxidant activity.

ACKNOWLEDGEMENTS

This work was supported by a grant (20080401-034-069) from the BioGreen 21 Program of Rural Development Administration (RDA), Republic of Korea.

1 Nozoe, S. & Suzuki, K. T. The isolation and structure of siccanochromenes. *Tetrahedron* **27,** 6063–6071 (1971).
2 Jaspars, M., Horton, P. A., Madrid, L. H. & Crews, P. The cyclorenierins, sesquiterpenoid quinols from the sponge *Haliclona* sp. collected in Vanuatu. *J. Nat. Prod.* **58,** 609–612 (1995).
3 Lee, I. K., Seo, G. S., Jeon, N. B., Kang, H. W. & Yun, B. S. Phellinins A1 and A2, new styrylpyrones from the culture broth of *Phellinus* sp. KACC93057P: I. Fermentation, taxonomy, isolation and biological activities. *J. Antibiot.* **62,** 631–634 (2009).
4 Lee, I. K. & Yun, B. S. Highly oxygenated and unsaturated metabolites providing a diversity of hispidin class antioxidants in the medicinal mushrooms *Inonotus* and *Phellinus*. *Bioorg. Med. Chem.* **15,** 3309–3314 (2007).
5 Trost, B. M., Shen, H. C. & Surivet, J. P. Biomimetic enantioselective total synthesis of (−)-siccanin via the Pd-catalyzed asymmetric allylic alkylation (AAA) and sequential radical cyclizations. *J. Am. Chem. Soc.* **126,** 12565–12579 (2004).
6 Suzuki, K. T. & Nozoe, S. Biosynthesis of an antibiotic, siccanin. *Bioorganic Chem.* **3,** 72–80 (1974).
7 Perrin, P. W. & Towers, G. H. N. Hispidin biosynthesis in cultures of *Polyporus hispidus*. *Phytochemistry* **12,** 589–592 (1973).
8 Nambudiri, A. M. D., Vance, C. P. & Towers, G. H. N. Effect of light on enzymes of phenylpropanoid metabolism and hispidin biosynthesis in *Polyporus hispidus*. *Biochem. J.* **134,** 891–897 (1973).

The Journal of Antibiotics (2009) 62, 639–642

www.nature.com/ja

NOTE

Synthesis, structures and anti-HBV activities of derivatives of the glutarimide antibiotic cycloheximide

Hui-fang Guo, Yu-huan Li, Hong Yi, Tian Zhang, Shu-qin Wang, Pei-zhen Tao and Zhuo-rong Li

The Journal of Antibiotics (2009) **62,** 639–642; doi:10.1038/ja.2009.87; published online 28 August 2009

Keywords: anhydrocycloheximide; antiviral activity; crystal structure; cycloheximide

Cycloheximide (CHX) (Figure 1), produced by *Streptomyces griseus*, is a heterocyclic glutarimide antibiotic. It inhibits protein synthesis in most eukaryotic cells and is a well-known tool commonly used in biomedical research.[1] CHX has been reported to significantly inhibit both simian virus 40T antigen and cellular DNA synthesis in CV-1 cells.[2] Research efforts also showed that CHX inhibited RNA production of influenza A,[3] reovirus[4] and arbovirus,[5] and also inhibited hepatitis A virus replication.[6] Recent reports have shown that CHX contributes to the control of human immunodeficiency virus (HIV) by modifying viral protein ratios.[7,8] This observation indicates that CHX may represent an anti-HIV candidate. In this study, the inhibitory activity of CHX against hepatitis B virus (HBV) in 2.2.15 cells was investigated. The results showed that the anti-HBV activity of CHX (IC_{50}=45.5 μg ml^{-1}) was weaker than that of 3TC (Lamivudine) (Table 1). Dehydration of CHX resulted in the formation of two compounds (**1a** and **1b**), which were separated by high pressure liquid chromatography. Compounds **1a** and **1b** significantly inhibited DNA replication of HBV and the IC_{50} values were 1.67 and 2.14 μg ml^{-1}, respectively, with high selectivity indexes (93.0 and 31.1, respectively). The structure of **1a** was elucidated by X-ray diffraction, and that of **1b** was confirmed as the 3″ *S* epimer of **1a** by CD spectroscopy.

Compounds **1a** and **1b** were produced as a mixture from CHX by dehydrating in dichloromethane with BF_3 OEt_2 as the catalyst. Schaeffer and Jain[9] have predicted that the methyl groups in CHX's dehydration product (often known as anhydrocycloheximide) exist as a mixture of both *cis* and *trans* forms. However, no previous study has confirmed whether the geometric structure of the C=C bond in anhydrocycloheximide is *Z* or *E*. The stereo structure (Figure 2) of **1a** was determined by X-ray diffraction, in which C-3″ (C10 in Figure 2b) was found to be *R*, and the double bond between C-2′ and C-1″ (C6 and C4 in Figure 2b) was the *E* configuration. Crystallographic data for the structure of **1a** have been deposited in the Cambridge Crystallographic Data Center with deposition no. CCDC719670.

The C-3″ of CHX was the *S* configuration, whereas the configuration of C-3″ of **1a** was *R*. Consequently, we deduced that **1b** must be the epimer of **1a** with C-3″ in the *S* configuration based on ^{1}H NMR, ^{13}C NMR, MS, IR and NOE spectra. In the NOE experiments, irradiation of 1′-H of **1b** enhanced the intensity of 6″-H_β, and the irradiation of 1′-H of **1a** also enhanced the intensity of 6″-H_β. Moreover, irradiation of 2′-H of compound **1a** or **1b** enhanced the intensity of 1′-H; however, no enhancement of intensity of 6″-H of **1a** or **1b** was observed. The NOE data for **1b** and **1a** indicated that the configuration of the double bond of **1b** was the same as that of **1a**, which was the *E* configuration.

To confirm that **1b** is the 3″ *S* configuration, CD spectra of compounds **1a** and **1b** were acquired (Figure 3). The CD spectra of α, β-unsaturated ketones usually show three CD bands above 180 nm. The two C=C $\pi \rightarrow \pi^*$ bands (200−260 nm) of **1a** and **1b** were similar, but the C-2″ keto $n \rightarrow \pi^*$ bands (260−400 nm) of **1a** and **1b** were opposite. Clearly, **1a** showed a negative Cotton effect, whereas **1b** showed a positive Cotton effect. Both maximum absorption wavelengths of **1a** and **1b** were near 320 nm (**1a**: 327.5 nm, $\Delta\varepsilon = -0.88$ cm^2 mmol^{-1}; **1b**: 323 nm, $\Delta\varepsilon = 0.44$ cm^2 mmol^{-1}). The difference in the CD behavior of the C-2″ keto originated from the different chirality of the C-3″. In conclusion, the data showed that **1b** is 4-[2′-(3″(*S*),5″(*S*)-3″,5″-dimethyl-2″-oxocyclohexylidene)ethyl] piperidine-2,6-dione. During the dehydration process of CHX, keto-enol tautomerization involving the C-2″ keto and the C-3″ proton leads to epimerization at the C-3″. On the basis of quantitative analysis with HPLC, the production of **1a** was ∼1.8 times greater than that of **1b**. Consequently, **1a** seems to be more stable than does **1b**. The total energies of compounds **1a** and **1b** were compared on the basis of calculations using SYBYL (version 7.35, Tripos, St Louis, MO, USA). The results support our hypothesis as the calcd total energy for **1a** was −6.053 kcal mol^{-1} and that of **1b** was −5.747 kcal mol^{-1}.

Alkylation of the nitrogen atom of the glutarimide ring of **1a** afforded compounds **2** and **3**. Reduction of the keto group of **1a** produced compound **4** (Scheme 1). Compounds **2**, **3** and **4** did not inhibit the growth of HBV.

Institute of Medicinal Biotechnology, Chinese Academy of Medical Sciences and Peking Union Medical College, Beijing, China
Correspondence: Professor Z-r Li, Institute of Medicinal Biotechnology, Chinese Academy of Medical Sciences and Peking Union Medical College, No 1, Tiantan Xili, Beijing 100050, PR China.
E-mail: l-z-r@263.net
Received 3 June 2009; revised 16 July 2009; accepted 28 July 2009; published online 28 August 2009

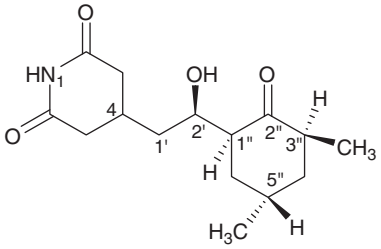

Figure 1 Structure of cycloheximide (CHX).

Table 1 Anti-HBV activities of CHX analogs

Compounds	*CHX*	***1a***	***1b***	***2***	***3***	***4***	***3TC***[a]
$IC_{50}(\mu g\,ml^{-1})$	45.5	1.67	2.14	>200	>200	>200	0.89
SI[b]	4.4	93.0	31.1	/	/	/	1315

Abbreviations: CHX, cycloheximide; HBV, hepatitis B virus; SI, selective index.
[a]3TC: Lamivudine, an antiviral agent used as positive control.
[b]$SI=TC_{50}/IC_{50}$.

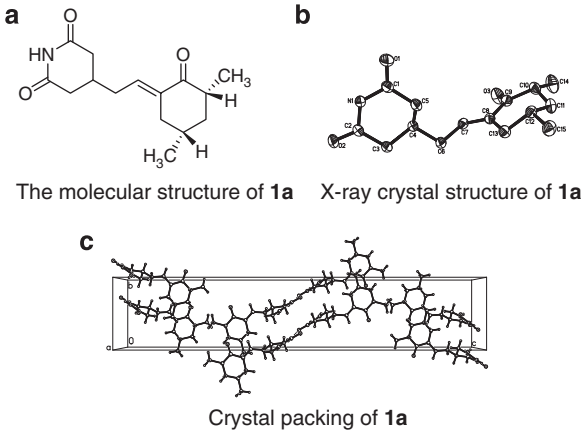

Figure 2 X-ray structures of **1a**. (**a**) The molecular structure of **1a**. (**b**) X-ray crystal structure of **1a**. (**c**) Crystal packing of **1a**.

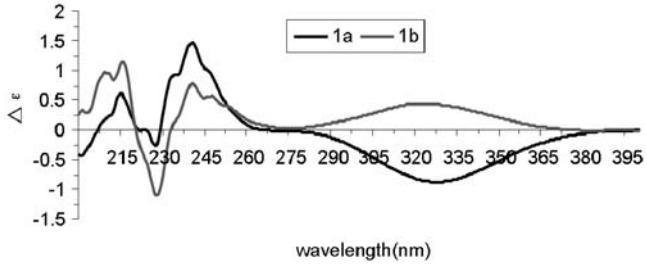

Figure 3 CD spectra of **1a** and **1b** (in chloroform, $c=3.8\times10^{-3}$ M, at 25 °C).

In summary, CHX is a weak inhibitor of HBV in 2.2.15 cells. Under acid-catalyzed dehydration conditions in dichloromethane, the stereo configuration of the C-3″ methyl group in the cyclohexanone ring of CHX was epimerized and the two epimers **1a** and **1b** were formed. Both **1a** and **1b** showed much stronger anti-HBV activities (more than 20-fold higher) and higher selectivity indexes than did CHX. The absolute configuration of compound **1a** was determined by X-ray diffraction, and the structure of **1b** was determined on the basis of ^{1}H NMR, ^{13}C NMR, NOE and CD spectra. Alkylation of the nitrogen atom of the glutarimide ring of **1a** and reduction of the keto group of **1a** lead to the loss of anti-HBV activity. These results showed that the double bond between C-2′ and C-1″, the NH proton and the 2″ carbonyl group in the structure might be essential for anti-HBV activity.

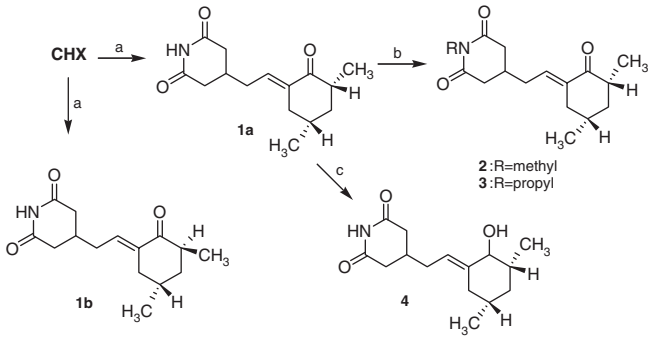

Scheme 1 Reagents and conditions: (**a**) BF_3 OEt_2, CH_2Cl_2; (**b**) CH_3I or $CH_3CH_2CH_2I$, K_2CO_3, CH_3CN, 65 °C; (**c**) $Zn(BH_4)_2$-DME solution, DME. DME, 1,2-dimethoxyethane.

EXPERIMENTAL SECTION

General methods

Melting points were determined using an X_6 microscope melting point apparatus and were uncorrected. ^{1}H NMR, ^{13}C NMR spectra and NOE data were recorded on a Varian Mercury-400 spectrometer (Varian, Beijing, China). HRMS spectra were recorded on an AccuTOF CS mass spectrometer (AccuTOF, Jeol Ltd, Beijing, China). HPLC was performed using a Shimadzu LC-10Avp with a SPD-10Avp UV detector (Shimadzu, Beijing, China) and a Class VP 6.x Workstation (Shimadzu). The column used was a Diamonsil C18 5-μm 250×4.6 mm column (Dikma Technologies, Beijing, China). Preparative liquid chromatography was performed using a Shimadzu LC-6AD *vp* liquid chromatograph instrument (Shimadzu) with a SPD-10Avp UV detector and Class VP 6.x workstation. The column used was a Shim-pack PREP-ODS 20 mm ID ×25 cm column (Shimadzu) with a 100-Å pore diameter and 15-μm particle diameter. Optical rotations were measured on a Perkin Elmer Model 341 LC parameter (Perkin Elmer, Shanghai, China). X-ray data were collected on a MAC DIP-2030K diffractometer. Circular dichroism spectra were recorded on a Jasco J-815 CD spectropolarimeter (Jasco, Tokyo, Japan).

4-[2′-(3″(*R*),5″(*S*)-3″,5″-dimethyl-2″-oxocyclohexylidene)ethyl] piperidine-2,6-dione (1a) and 4-[2′-(3″(*S*),5″(*S*)-3″,5″-dimethyl-2″-oxocyclohexylidene)ethyl]piperidine-2,6-dione (1b)

BF_3 OEt_2 (1.76 ml, 1.4 mmol) was added slowly to an ice-salt cold solution of CHX (2.0 g, 7 mmol) in 20 ml of dichloromethane. After stirring for 5 min, the salt ice-bath was withdrawn and stirring was continued for 3 h at room temperature. The ice-bath was used at the end of the stirring period. The solution was quenched with 20 ml of saturated $NaHCO_3$ solution when the temperature of the solution reached 0 °C. The water layer was extracted with dichloromethane (20 ml×3). The combined organic layer was washed with 60 ml of saturated NaCl and 60 ml of water and then dried over anhydrous magnesium sulfate. The solution was filtered to remove the precipitate and the filtrate was concentrated *in vacuo*. The residue was purified by chromatography using a silica gel column (100:15 dichloromethane/acetone) to afford a mixture of the compounds **1a** and **1b** (1.10 g, yield 55%) as a white powder.

Compounds **1a** and **1b** were separated by preparative liquid chromatography. The chromatography was performed on a Shim-pack PREP-ODS at 25 °C with a mobile phase of water–methanol 50:50 (v/v). The flow rate was 10 ml min^{-1}, and detection was achieved by monitoring the UV absorbance at 231 nm. The sample was dissolved in dimethyl sulfoxide, and sample-loading volumes were 100 μl. The separated solution was concentrated until no

methanol existed and was then dried by vacuum freeze drying. Compounds **1a** and **1b** were isolated and both appeared as a white powder.

Physical data for compound **1a**: m.p. 130–131 °C; $[\alpha]_D^{20}$ =−30.9 °C (*c*=1.25, $CHCl_3$); IR: 3189, 2930 (NH), 1712 (C=O), 1682 (C=O) cm^{-1}; ^1H NMR (400 MHz, $CDCl_3$) δ: 1.05 (3H, d, *J*=5.6 Hz, 5″-Me), 1.13 (3H, d, *J*=6.8 Hz, 3″-Me), 1.22–1.32 (1H, m, 4″-H_α), 1.84–1.93 (2H, m, 5″-H, 6″-H_α), 1.96–2.01 (1H, m, 4″-H_β), 2.16–2.25 (2H, m, 1′-H), 2.27–2.38 (4H, m, 3″-H, 4-H, 3-H_α, 5-H_α), 2.67–2.73 (3H, m, 6″-H_β, 3-H_β, 5-H_β), 6.35 (1H, t, *J*=8.0 Hz, =CH), 7.85 (1H, br, NH); ^{13}C NMR (100 MHz, $CDCl_3$): 15.7 (3″-Me), 22.1 (5″-Me), 30.1 (C-4), 30.3 (C-5″), 32.4 (C-1′), 36.2 (C-6″), 37.4 (C-3), 37.4 (C-5), 40.7 (C-4″), 44.1 (C-3′), 131.6 (C-2′), 139.3 (C-1″), 171.5 (C-2, C-6), 203.2 (C-2″); MS (ESI^+) *m/z*: 286.4 $[M+Na]^+$, HRMS (ESI^+) *m/z*: 286.14183 $[M+Na]^+$, calcd mass for $C_{15}H_{21}NO_3Na$: 286.14191.

Physical data for compound **1b**: m.p. 118–120 °C; $[\alpha]_D^{20}$ =+45.7 °C (*c*=1.03, $CHCl_3$); IR: 3201, 2927 (NH), 1721 (C=O), 1678 (C=O) cm^{-1}; 1H NMR (400 MHz, $CDCl_3$) δ: 1.04 (3H, d, *J*=6.4 Hz, 5″-Me), 1.12 (3H, d, *J*=7.2 Hz, 3″-Me), 1.64–1.77 (2H, m, 4″-H), 2.01–2.11 (2H, m, 4-H, 6″-H_α), 2.19–2.21 (2H, m, 1′-H), 2.28–2.31 (3H, m, 5″-H, 3-H_α, 5-H_α), 2.52–2.59 (2H, m, 3″-H, 6″-H_β), 2.65–2.70 (2H, m, 3-H_β, 5-H_β), 6.40 (1H, t, *J*=7.6 Hz, =CH), 8.47 (1H, br, NH); ^{13}C NMR (100 MHz, $CDCl_3$): 17.1 (3″-Me), 21.1 (5″-Me), 25.9 (C-4), 30.1 (C-5″), 32.4 (C-1′), 34.8 (C-6″), 37.4 (C-3, C-5), 38.2 (C-4″), 40.4 (C-3′), 132.5 (C-2′), 138.4 (C-1″), 171.4 (C-2, C-6), 204.0 (C-2″); MS (ESI^+) *m/z*: 286.4 $[M+Na]^+$, HRMS (ESI^+) *m/z*: 286.14111 $[M+Na]^+$, calcd mass for $C_{15}H_{21}NO_3Na$: 286.14191.

N-methyl-4-[2′-(3″(*R*),5″(*S*)-3″,5″-dimethyl-2″-oxocyclohexylidene)ethyl]piperidine-2,6-dione (2)

Compound **1a** (50 mg, 0.19 mmol), iodomethane (97 mg, 0.57 mmol) and anhydrous potassium carbonate (32 mg, 0.23 mmol) were added to 3 ml of acetonitrile and stirred at 65 °C for 10 h. The solution was filtered to remove potassium carbonate and the filtrate was concentrated. The residue was dissolved in 10 ml of ethyl acetate and washed with water. The organic layer was dried over anhydrous sodium sulfate. The solution was filtered to remove any solids and the filtrate was concentrated under vacuum. The residue was purified by chromatography using a silica gel column (100:7 dichloromethane/methanol) to obtain the title compound **2** (48.5 mg, yield 92%) as a white solid.

Physical data for compound **2**: m.p. 47–49 °C; $[\alpha]_D^{20}$ =−24.9 °C (*c*=0.25, $CHCl_3$); IR: 1720 (C=O), 1671 (C=O) cm^{-1}; ^1H NMR (400 MHz, $CDCl_3$) δ: 1.05 (3H, d, *J*=5.6 Hz, 5″-Me), 1.13 (3H, d, *J*=6.8 Hz, 3″-Me), 1.23–1.32 (1H, m, 4″-H_α), 1.87–1.92 (2H, m, 5″-H, 6″-H_α), 1.96–2.01 (1H, m, 4″-H_β), 2.14–2.26 (3H, m, 1′-H, 4-H), 2.31–2.39 (3H, m, 3″-H, 3-H_α, 5-H_α), 2.70 (1H, d, *J*=13.2 Hz, 6″-H_β), 2.80 (2H, d, *J*=17.2 Hz, 3-H_β, 5-H_β), 3.14 (3H, s, N-Me), 6.35 (1H, t, *J*=7.6 Hz, =CH); ^{13}C NMR (100 MHz, $CDCl_3$): 15.7 (3″-Me), 22.1 (5″-Me), 26.4 (N-C), 29.2 (C-4), 30.3 (C-5″), 32.6 (C-1′), 36.2 (C-6″), 38.4 (C-3), 38.5 (C-5), 40.8 (C-4″), 44.0 (C-3″), 131.8 (C-2′), 139.1 (C-1″), 171.8 (C-2, C-6), 203.5 (C-2″); MS (ESI^+) *m/z*: 278.5 $[M+H]^+$ and 300.5 $[M+Na]^+$, HRMS (ESI^+) *m/z*: 300.15629 $[M+Na]^+$, calcd mass for $C_{16}H_{23}NO_3Na$: 300.15756.

N-propyl-4-[2′-(3″(*R*),5″(*S*)-3″,5″-dimethyl-2″-oxo-cyclohexylidene)-ethyl]piperidine-2,6-dione (3)

The title compound was obtained from **1a** using a procedure similar to that used to prepare compound **2**. The yield was 17% as yellow syrup.

Physical data for compound **3**: $[\alpha]_D^{20}$ =−20.6 °C (*c*=0.56, $CHCl_3$); IR: 1725 (C=O), 1676 (C=O) cm^{-1}; ^1H NMR (400 MHz, $CDCl_3$) δ: 0.88 (3H, t, *J*=7.2 Hz, N-γ-Me), 1.04 (3H, d, *J*=6.0 Hz, 5″-Me), 1.12 (3H, d, *J*=6.8 Hz, 3″-Me), 1.25–1.31(1H, m, 4″-H_α), 1.51(1H, sext, *J*=7.2 Hz, N-β-CH_2), 1.86–1.92 (2H, m, 5″-H, 6″-H_α), 1.96–1.99 (1H, m, 4″-H_β), 2.11–2.27 (3H, m, 1′-H, 4-H), 2.31–2.39 (3H, m, 3-H_α, 5-H_α, 3″-H), 2.70 (1H, d, *J*=13.2 Hz, 6″-H_β), 2.77 (2H, d, *J*=16.8 Hz, 3-H_β, 5-H_β), 3.71 (2H, t, *J*=7.2 Hz, N-α-CH_2), 6.34 (1H, t, *J*=7.6 Hz, =CH); ^{13}C NMR (100 MHz, $CDCl_3$): 11.3 (N-γ-C), 15.7 (3″-Me), 21.2 (N-β-C), 22.1 (5″-Me), 29.2 (C-4), 30.3 (C-5″), 32.5 (C-1′), 36.2 (C-6″), 38.5 (C-3), 38.6 (C-5), 40.8 (C-4″), 41.2 (N-α-C),44.0 (C-3″), 131.9 (C-2′), 139.1 (C-1″), 171.6 (C-2, C-6), 203.2 (C-2″); MS (ESI^+) *m/z*: 306.5 $[M+H]^+$, 328.5 $[M+Na]^+$, HRMS (ESI^+) *m/z*: 328.18554 $[M+Na]^+$, calcd mass for $C_{18}H_{27}NO_3Na$: 328.18886.

4-[2′-(3″(*R*),5″(*S*)-3″,5″-dimethyl-2″-hydroxyl-cyclohexylidene)ethyl]piperidine-2,6-dione (4)

To a solution of **1a** (50 mg, 0.19 mmol) in 3 ml of 1,2-dimethoxyethane (DME), $Zn(BH_4)_2$-DME (4 ml, prepared by the method described by Gensler *et al.*[10]) was added slowly. After stirring at room temperature for 24 h, 4 ml of water and 1 ml of glacial acetic was added to the reaction mixture. The solution was filtered to remove the precipitate and the filtrate was concentrated under vacuum. The residue was purified by chromatography using a silica gel column (150:10 dichloromethane/methanol). The title compound was collected as a white solid (42 mg, yield 84%).

Physical data for compound **4**: m.p. 39–41 °C; $[\alpha]_D^{20}$ =−15.5 °C (*c*=0.47, $CHCl_3$); IR: 3476 (OH), 3198, 3095 (NH), 1681 (C=O) cm^{-1}; ^1H NMR (400 MHz, $CDCl_3$) δ: 0.89–0.92 (m, 4″-H_α), 0.94 (3H, d, *J*=6.0 Hz, 5″-Me), 1.07 (3H, d, *J*=6.4 Hz, 3″-Me), 1.35–1.44 (3H, m, 3″-H, 5″-H, 6″-H_α), 1.56 (s, OH), 1.72–1.76 (1H, m, 4″-H_β), 2.18–2.22 (2H, m, 4-H, 1′-H), 2.28–2.34 (2H, m, 3-H_α, 5-H_α), 2.52 (d, *J*=12.0 Hz, 6″-H_β), 2.67–2.72 (2H, m, 3-H_β, 5-H_β), 3.56 (1H, d, *J*=10.0 Hz, 2″-H), 5.42 (1H, t, *J*=6.8 Hz, =CH), 7.81 (1H, br, NH); ^{13}C NMR (100 MHz, $CDCl_3$): 19.1 (3″-Me), 22.1 (5″-Me), 30.9 (C-4), 31.8 (C-1″), 33.4 (C-5″), 36.5 (C-6″), 37.3 (C-3), 37.4 (C-5), 41.4 (C-3″), 42.5 (C-4″), 77.9 (C-2″), 113.1 (C-2′), 144.0 (C-1″), 172.2 (C-2, C-6); MS (ESI^+) *m/z* : 288.3 $[M+Na]^+$ and 248.3 $[M-H_2O]^+$, HRMS (ESI^+) *m/z*: 288.15935 $[M+Na]^+$, calcd mass for $C_{15}H_{23}NO_3Na$: 288.15756.

Anti-HBV assays

2.2.15 cells in exponential growth phase were seeded into 96-well microplates. A total of 2×10^4 cells per well were used. Test compounds with different concentrations were added, and the cells were cultured in CO_2 incubators at 37 °C. The medium was exchanged every 4 days. The positive control (3TC) and untreated cell negative control groups were established. After 8 days, HBV DNA of the lysed cells was extracted. HBV DNA levels were measured using a quantitative Southern blot hybridization analysis approach.

Cytotoxicity assay

Cytotoxicity induced by the test compounds in the cultures of 2.2.15 cells was also determined. 2.2.15 cells were seeded into 96-well microplates: 1×10^5 cells per ml, 100 µl per well. Cells were treated with test compounds at different concentrations. The control was untreated cells. The culture medium was exchanged every 4 days. After 8 days, cell viability levels were examined. TC_{50} was defined as the concentration that inhibited 50% cellular growth in comparison with untreated controls and was calculated by Reed and Muench analyses.

ACKNOWLEDGEMENTS

This work was supported by the National Natural Science Foundation of China (Grant no. 30472076) and a Grant from the Ministry of Science and Technology of China (863 program 2006AA028414). We thank Professors Yang Lv and Yi-kang Si of the Institute of Materia Medica, Chinese Academy of Medical Sciences and Peking Union Medical College for collecting the crystal and CD data, respectively.

1 Croons, V., Martinet, W., Herman, A. G. & De Meyer, G. R. Differential effect of the protein synthesis inhibitors puromycin and cycloheximide on vascular smooth muscle cell viability. *J. Pharmacol. Exp. Ther.* **325,** 824–832 (2008).
2 Kit, S., Kurimura, T., De Torres, R. A. & Dubbs, D. R. Simian virus 40 deoxyribonucleic acid replication. I. Effect of cycloheximide on the replication of SV40 deoxyribonucleic acid in monkey kidney cells and in heterokaryons of SV40-transformed and susceptible cells. *J. Virol.* **3,** 25–32 (1969).
3 Mark, G. E., Taylor, J. M., Broni, B. & Krug, R. M. Nuclear accumulation of influenza viral RNA transcripts and the effects of cycloheximide, actinomycin D, and alpha-amanitin. *J. Virol.* **29,** 744–752 (1979).
4 Watanabe, Y., Kudo, H. & Graham, A. F. Selective inhibition of reovirus ribonucleic acid synthesis by cycloheximide. *J. Virol.* **1,** 36–44 (1967).
5 Friedman, R. M. & Grimley, P. M. Inhibition of arbovirus assembly by cycloheximide. *J. Virol.* **4,** 292–299 (1969).
6 Crance, J. M., Biziagos, E., Passagot, J., van Cuyck-Gandré, H. & Deloince, R. Inhibition of hepatitis A virus replication in vitro by antiviral compounds. *J. Med. Virol.* **31,** 155–160 (1990).

7 Irvine, J. H., Horsfield, J. A., McKinney, C. Z. & Tate, W. P. A novel strategy to interfere with human immunodeficiency virus type 1 propagation. *N. Z. Med. J.* **111,** 222–224 (1998).
8 Choudhary, S. K. *et al.* CXCR4 tropic human immunodeficiency virus type 1 induces an apoptotic cascade in immature infected thymocytes that resembles thymocyte negative selection. *Virology* **352,** 268–284 (2006).
9 Schaeffer, H. J. & Jain, V. K. Investigation of the stereochemistry of cycloheximide. *J. Pharm. Sci.* **53,** 144–147 (1964).
10 Gensler, W. J., Johnson, F. & David, A. Compounds related to podophyllotoxin. XII. podophyllone and dehydropodophyllotoxin. *J. Am. Chem. Soc.* **82,** 6074–6081 (1960).

The Journal of Antibiotics (2009) 62, 643–646

www.nature.com/ja

NOTE

Enzymatic preparation of neomycin C from ribostamycin

Fumitaka Kudo[1], Taiki Kawashima[2], Kenichi Yokoyama[1] and Tadashi Eguchi[2]

The Journal of Antibiotics (2009) **62,** 643–646; doi:10.1038/ja.2009.88; published online 28 August 2009

Keywords: aminoglycoside antibiotics; biosynthesis; dehydrogenase; enzymatic synthesis; neomycin C; neosamine C

The high regio- and stereospecificities of enzymes and their ability to catalyze reactions in the absence of organic solvents make enzymatic synthesis of antibiotics an attractive way to prepare complex natural products. Enzymatic total syntheses of several complex natural products have been recently achieved, which illustrates the power of this synthetic methodology.[1,2] Combinations of biosynthetic enzymes and substrates, including unnatural types, can afford structurally diverse natural product-like compounds.[3]

In this study, we report the enzymatic synthesis of the aminoglycoside antibiotic neomycin C from ribostamycin by the use of four neomycin biosynthetic enzymes. So far, all nine enzymes for ribostamycin biosynthesis from D-glucose 6-phosphate have been characterized using the enzymes derived from the butirosin producer *Bacillus circulans* and the neomycin producer *Streptomyces fradiae*.[4] Furthermore, two neomycin biosynthetic enzymes NeoF and NeoD were recently found to catalyze the glycosylation of ribostamycin using

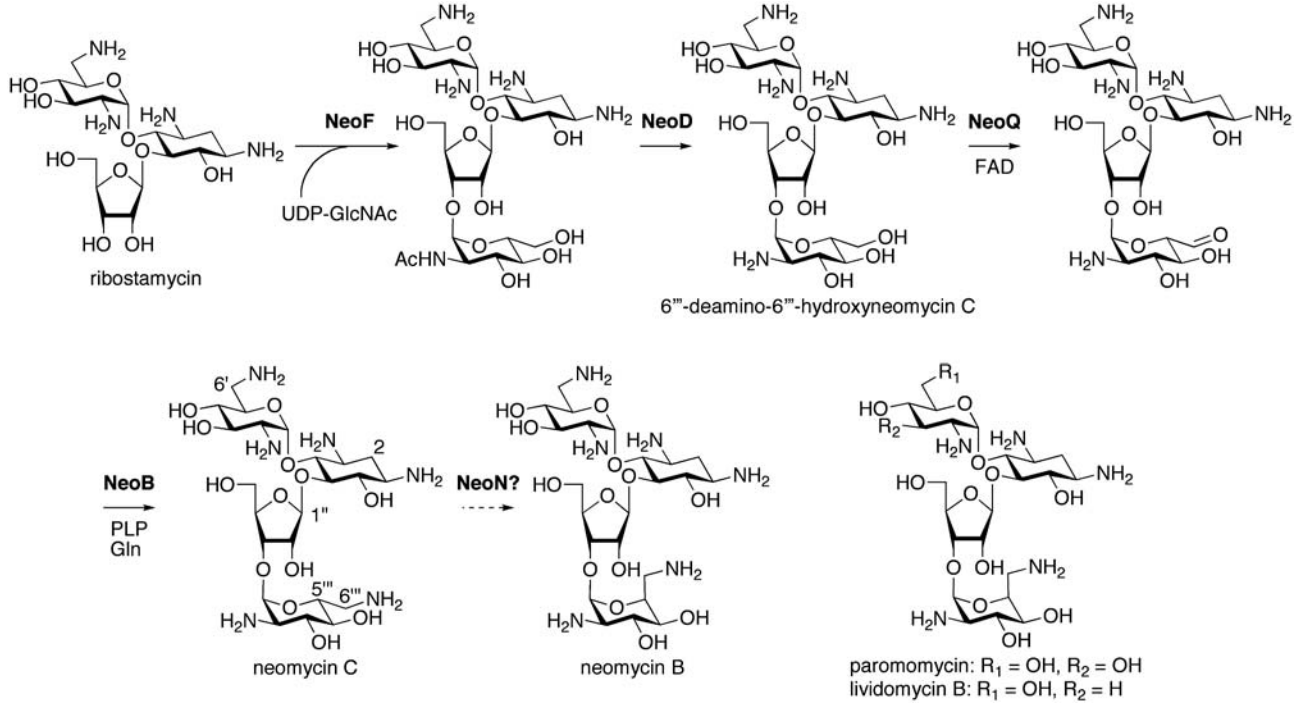

Figure 1 Biosynthesis of neomycin C from ribostamycin.

[1]Department of Chemistry, Tokyo Institute of Technology, Tokyo, Japan and [2]Department of Chemistry and Materials Science, Tokyo Institute of Technology, Tokyo, Japan
Correspondence: Professor T Eguchi, Department of Chemistry and Materials Science, Tokyo Institute of Technology, 2-12-2 O-okayama, Meguro-ku, Tokyo 152-8551, Japan.
E-mail: eguchi@cms.titech.ac.jp
Received 25 June 2009; revised 1 August 2009; accepted 3 August 2009; published online 28 August 2009

UDP-*N*-acetylglucosamine (UDP-GlcNAc) as a sugar donor and the subsequent deacetylation to afford 6‴-deamino-6‴-hydroxyneomycin C (Figure 1).[5] (As the biosynthetic gene cluster for neomycin was deposited with different symbols in DNA databases by multiple groups, we here use the butirosin biosynthetic *btr* gene-based code names, which are systematically utilized by the Piepersberg *et al*.[6] and also in our recent review.[7]) NeoB has also been reported to catalyze two transaminations: the conversion of neomycin C to 6‴-oxoneomycin C, which is a reverse reaction of the postulated *in vivo* biosynthetic reaction (Figure 1), and the conversion of 6′-oxoparo-

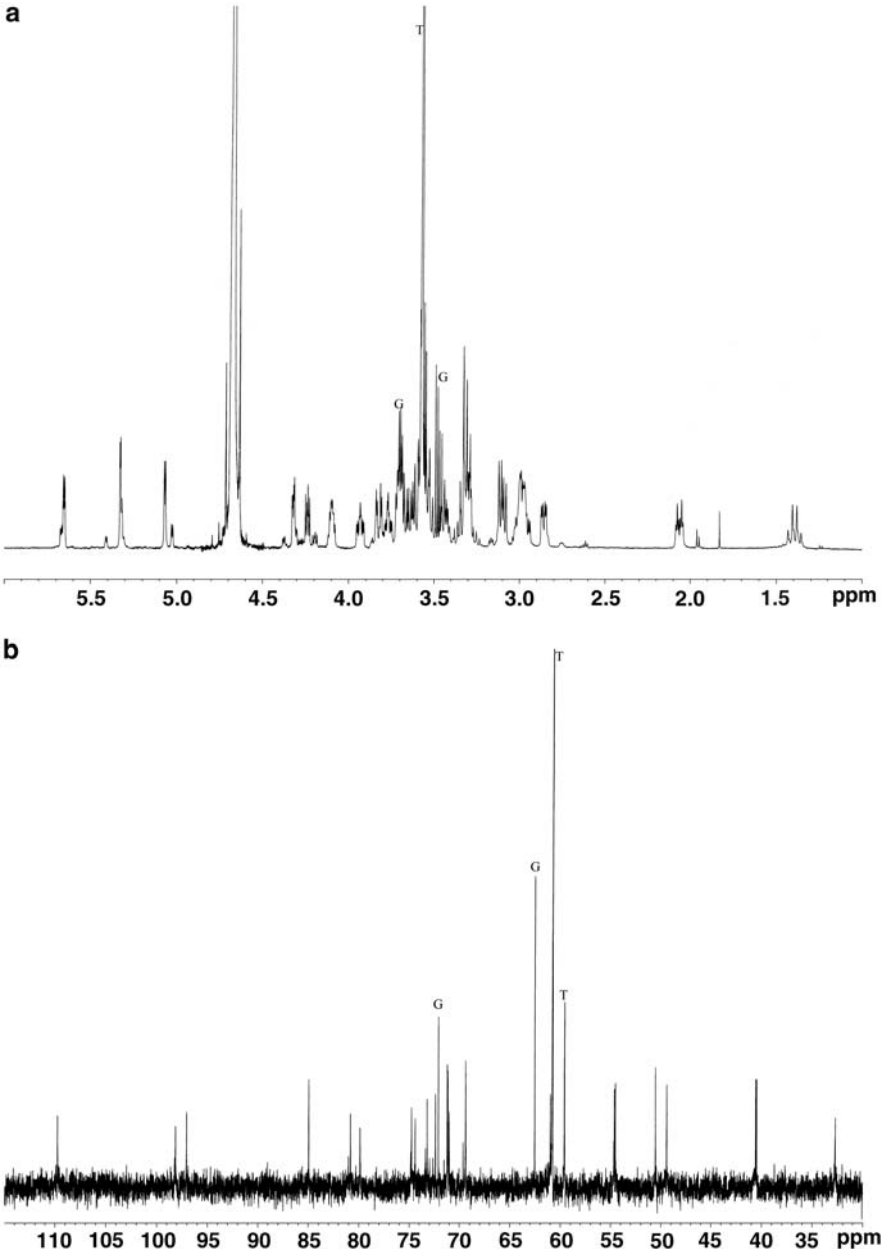

Figure 2 NMR spectra of neomycin C in D_2O synthesized with biosynthetic enzymes. (**a**) ^{1}H-NMR (500 MHz) and (**b**) ^{13}C-NMR (125 MHz) were recorded on DRX500 (Bruker, Rheinstetten, Germany). Auto reference for the D_2O solvent was used for both spectra. Small amounts of Tris buffer and glycerol were contaminated from the purification process of the proteins. 2D-NMRs including ^{1}H-^{1}H COSY and TOCSY spectra (data not shown) were also recorded to determine the structure of neomycin C. The signals were assigned by comparison with those of 6‴-deamino-6‴-hydroxyneomycin C 5 and neomycin B.[11] ^{1}H NMR (500 MHz, D_2O): δ 1.39 (q, J=12.7 Hz, 1H, H-2ax), 2.06 (dt, J=12.7, 4.1 Hz, 1H, H-2eq), 2.86 (dd, J=3.6, 10.2 Hz, 1H, H-2‴), 2.98 (m, 3H, H-1, H-3, H-2′), 3.10 (dd, J=7.3, 13.5 Hz, 2H, H-6′, H-6‴), 3.32 (m, 4H, H-4′, H-6′, H-4‴, H-6‴), 3.44 (m, H-4 or H-6 with glycerol), 3.52 (m, H-4 or H-6 with glycerol), 3.57 (m, H-3‴ with Tris), 3.64 (dd, J=5.0, 12.4 Hz, 1H, H-5″), 3.70 (m, H-5, H-3′ with glycerol), 3.77 (ddd, J=3.1, 7.3, 9.7 Hz, 1H, H-5‴), 3.83 (dd, J=3.2, 12.4 Hz, 1H, H-5″), 3.93 (ddd, J=3.3, 7.3, 10.4 Hz, 1H, H-5′), 4.10 (m, 1H, H-4″), 4.24 (dd, J=4.7, 6.9 Hz, 1H, H-3″), 4.32 (dd, J=2.0, 4.7 Hz, 1H, H-2″), 5.07 (d, J=3.6 Hz, 1H, H-1‴), 5.33 (d, J=2.0 Hz, 1H, H-1″), 5.65 (d, J=3.7 Hz, 1H, H-1′); ^{13}C NMR (125 MHz, D_2O): δ 32.7 (C2), 40.5 (C6′ or C6‴), 40.6 (C6′ or C6‴), 49.4 (C3), 50.5 (C1), 54.5 (C2′ or C2‴), 54.6 (C2′ or C2‴), 61.0 (C5″), 69.4 (C5′ and C4‴), 71.0, 71.1, 71.2, 72.4 (C3′ or C4′ or C3‴ or C5‴), 73.2 (C2″), 74.4 (C3″), 74.8 (C6), 79.9 (C4), 80.8 (C4″), 84.9 (C5), 97.0 (C1′), 98.1 (C1‴) and 109.8 (C1″). Signals at 59.6 and 60.8 p.p.m. were derived from Tris and signals at 62.5 and 72.1 p.p.m. in ^{13}C-NMR were derived from glycerol. The impurities are indicated as T for Tris and G for glycerol, respectively, in spectra.

mamine to neamine using L-glutamate or L-glutamine as an amino donor.[8] NeoQ was characterized as a flavin adenine dinucleotide-dependent dehydrogenase of paromamine to give 6′-oxoparomamine during neamine formation.[8] No dehydrogenase for the oxidation of 6‴-deamino-6‴-hydroxyneomycin C has been identified as yet. As there is no other gene in the biosynthetic gene cluster that can be assigned for the oxidation of 6‴-deamino-6‴-hydroxyneomycin C, the repetitive use of NeoQ has been proposed.[8] Characterization of the NeoQ function and reconstitution of the biosynthetic reactions between ribostamycin and neomycin C is important to elucidate the potential repetitive use of multiple enzymes in the neomycin biosynthetic pathway.

At first, we prepared 6‴-deamino-6‴-hydroxyneomycin C from ribostamycin by incubation with NeoF and NeoD according to earlier methods with minor modifications.[5] Overexpressed NeoF protein was partially purified by anion exchange chromatography with DEAE Sepharose Fast Flow (GE Healthcare, Chalfont St Giles, UK) and the obtained crude enzyme (17 ml, 22 mg as crude enzyme) was directly used for the glycosylation of ribostamycin (56 mg) with UDP-GlcNAc • 2Na (86 mg) at 28 °C for 45 h. Without purification of the glycosylated product, the next deacetylation reaction was carried out by the addition of NeoD (0.3 mg, 0.25 ml) purified by TALON (Clontech, Mountain View, CA, USA) chromatography. After 24 h at 28 °C, the resulting enzymatic solution was heat-treated (100 °C, 2 min) and then applied to a Dowex AG1-X8 (Bio-Rad, Richmond, CA, USA, [OH^-] form, 12 ml) column. The unadsorbed fraction was neutralized with acetic acid and then applied to an Amberlite CG50 (Rohm and Haas Co, Philadelphia, PA, USA, [NH_4^+] form, 8 ml) column. A stepwise gradient of aqueous NH_4OH (0.04 M and then 2 M) eluted 6‴-deamino-6‴-hydroxyneomycin C, which was further passed through Dowex AG1-X8 ([SO_4^{2-}] form, 8 ml) to obtain 6‴-deamino-6‴-hydroxyneomycin C sulfate (45 mg, 2 steps 45% yield).

Next, the probable flavin adenine dinucleotide-dependent dehydrogenation of 6‴-deamino-6‴-hydroxyneomycin C catalyzed by NeoQ with the abovementioned substrate was investigated. When the following conditions for the enzyme reaction and derivatization were used, we observed a time-dependent decrease of the substrate by HPLC analysis (data not shown); NeoQ (0.35 mg ml^{-1}, purified with Ni-NTA His • Bind Resin (Novagen, Darmstadt, Germany)), substrate 2 mM, flavin adenine dinucleotide 0.3 mM in 20 mM Tris buffer (pH 8.0) containing 0.2 M KCl, at 28 °C, followed by derivatization with 2,4-dinitrofluorobenzene for UV detection of aminoglycosides. The result indicated that NeoQ also catalyzes the dehydrogenation of 6‴-deamino-6‴-hydroxy-neomycin C as well as paromamine to give the corresponding aldehyde. The absence of the product is presumably because of a decomposition of the aldehyde compound during the dinitrophenyl derivatization under basic and high temperature (60 °C) conditions. Furthermore, the addition of NeoB (0.6 mg ml^{-1}, purified by Ni-NTA His • Bind Resin chromatography), L-glutamine (Gln, 10 mM) and pyridoxal phosphate (0.2 mM) to the NeoQ reaction mixture followed by the abovementioned derivatization gave a new peak on the HPLC trace, which showed *m/z* 1609.5 corresponding to the MW [M–H]$^-$ of the neomycin C dinitrophenyl derivative (data not shown). A large-scale NeoQ and NeoB reaction (6 mg of NeoQ, 11 mg of NeoB, 17 mg of 6‴-deamino-6‴-hydroxyneomycin C (1 mM), flavin adenine dinucleotide (1 mM), Gln (20 mM) and pyridoxal phosphate (0.4 mM) in the Tris-HCl buffer (pH 8.0) containing 0.2 M of KCl, total 20 ml at 28 °C for 44 h) gave a mixture of starting material and the new product, which was purified by the same procedure as that for the purification of 6‴-deamino-6‴-hydroxyneomycin C. As the preliminary analytical scale experiment suggested the inefficient conversion of this reaction, the mixture was further treated under the same enzymatic conditions for a longer time (44 h) to ensure maximum consumption of the starting material and the resulting aminoglycosides were purified in an identical manner. As a result, 12 mg of the product was obtained and the structure of the main product was confirmed as neomycin C by ^{1}H-NMR, ^{13}C-NMR (Figure 2) and HR-FAB-MS (positive, glycerol) *m/z* 637.3033 (M+Na)$^+$, calcd for $C_{23}H_{46}N_6O_{13}Na$: 637.3020. Despite the use of newly prepared enzymes for both reactions, 10–20% of the starting material remained after the reaction, probably because of the reversibility of the transamination.[8] However, the conversion of 6‴-deamino-6‴-hydroxyneomycin C to neomycin C using purified NeoQ and NeoB strongly suggests a repetitive use of NeoQ and NeoB in neomycin biosynthesis.

The only uncharacterized step in the neomycin B biosynthesis is now the epimerization at the C-5‴ position of neomycin C. As the exact timing of the epimerization is currently unclear,[9] any of the four biosynthetic intermediates in the pathway shown in Figure 1 may be the substrate for the epimerization. The enzymatic synthesis reported here can supply all the possible substrates needed to investigate the corresponding epimerization reaction. A comparison of aminoglycoside biosynthetic gene clusters indicated the involvement of NeoN, a putative radical SAM enzyme that is also encoded in the paromomycin and lividomycin biosynthetic clusters.[5,7] As such an epimerization by a radical SAM enzyme is unprecedented[10] and would be an important tool to synthesize structurally diverse aminoglycosides, the functional characterization of NeoN is important and is currently underway.

In conclusion, we showed the repetitive dehydrogenase activity of NeoQ at the C-6 position of the glucosamine moiety of paromamine and 6‴-deamino-6‴-hydroxyneomycin C, and the transamination activity of NeoB at the corresponding positions. The substrate recognition mechanism of the dehydrogenase, NeoQ, should be interesting, because the C-6′ positions of paromomycin and lividomycin remain as hydroxy groups even though the corresponding enzymes in the biosynthesis of these antibiotics should work for the dehydrogenation at C-6‴. We also achieved the enzymatic synthesis of neomycin C from ribostamycin in a preparative scale. This methodology can be applied for enzymatic synthesis of the other aminoglycoside antibiotics. Thus, the functional characterization of many other biosynthetic enzymes for aminoglycosides such as kanamycin and gentamicin will pave the way for the creation of structurally diverse aminoglycosides, including unnatural types, in the future.

ACKNOWLEDGEMENTS

This work was supported in part by the Mitsubishi Chemical Corporation Fund, the Naito Foundation and KAKENHI 21710224 (FK).

1 Cheng, Q., Xiang, L., Izumikawa, M., Meluzzi, D. & Moore, B. S. Enzymatic total synthesis of enterocin polyketides. *Nat. Chem. Biol.* **3,** 557–558 (2007).
2 Sattely, E. S., Fischbach, M. A. & Walsh, C. T. Total biosynthesis: *In vitro* reconstitution of polyketide and nonribosomal peptide pathways. *Nat. Prod. Rep.* **25,** 757–793 (2008).
3 Kalaitzis, J. A., Cheng, Q., Thomas, P. M., Kelleher, N. L. & Moore, B. S. *In vitro* biosynthesis of unnatural enterocin and wailupemycin polyketides. *J. Nat. Prod.* **72,** 469–472 (2009).
4 Kudo, F. & Eguchi, T. Biosynthetic enzymes for the aminoglycosides butirosin and neomycin. *Methods Enzymol.* **459,** 493–519 (2009).
5 Yokoyama, K., Yamamoto, Y., Kudo, F. & Eguchi, T. Involvement of two distinct *N*-acetylglucosaminyltransferases and a dual-function deacetylase in neomycin biosynthesis. *Chembiochem* **9,** 865–869 (2008).
6 Piepersberg, W., Aboshanab, K. M., Schmidt-Beissner, H. & Wehmeier, U. F. in Aminoglycoside Antibiotics. The biochemistry and genetics of aminoglycoside producers (eds Arya, D. P.) 15–118 (John Wiley & Sons, Inc., Hoboken, NJ, 2007).
7 Kudo, F. & Eguchi, T. Biosynthetic genes for aminoglycoside antibiotics. *J. Antibiot.* **62,** 471–481 (2009).

8 Huang, F. *et al.* Elaboration of neosamine rings in the biosynthesis of neomycin and butirosin. *Chembiochem* **8,** 283–288 (2007).
9 Autissier, D., Barthelemy, P., Mazieres, N., Peyre, M. & Penasse, L. 6‴-Deamino-6‴-hydroxy derivatives, as intermediates in the biosynthesis of neomycin and paromomycin. *J. Antibiot.* **34,** 536–543 (1981).
10 Wang, S. C. & Frey, P. A. S-adenosylmethionine as an oxidant: the radical SAM superfamily. *Trends Biochem. Sci.* **32,** 101–110 (2007).
11 Reid, D. G. & Gajjar, K. A proton and carbon 13 nuclear magnetic resonance study of neomycin B and its interactions with phosphatidylinositol 4,5-bisphosphate. *J. Biol. Chem.* **262,** 7967–7972 (1987).

The Journal of Antibiotics (2009) 62, 647–648

www.nature.com/ja

NOTE

Sannanine, a new cytotoxic alkaloid from *Streptomyces sannanensis*

Yiqing Li[1], Dan Zheng[2], Jun Li[1], Li Han[2], Xiaolong Cui[1], Li Lang[2], Minggang Li[1], Zhanyou Wang[2], Jiangyuan Zhao[1] and Xueshi Huang[2]

The Journal of Antibiotics (2009) **62,** 647–648; doi:10.1038/ja.2009.95; published online 2 October 2009

Keywords: alkaloid; cytotoxicity; sannanine; *Streptomyces sannanensis*

As reported recently, quinoline-5,8-diones have generated a lot of interest as anticancer agents.[1,2] Most of them were obtained by synthesis, and only a few of them, such as streptonigrin, streptonigrone and lavendamycin, were obtained from microbial sources.[2,3] Over the past few decades, major research has focused on the synthesis and biological activities of variously 6,7-functionalized quinoline-5,8-diones.[4–9] In the course of screening for new antitumor bioactive compounds from microbial sources, a new cytotoxic quinoline-5,8-dione derivative, sannanine (**1**), was isolated from the fermentation broth of *Streptomyces sannanensis* (Figure 1). In this paper, we report the fermentation, isolation, structural elucidation and biological activities of **1**.

The producing organism was isolated from a soil sample collected from Dali, Yunnan province, China. The strain was identified as *S. sannanensis* according to phylogenetic analysis. The genomic DNA of the strain was extracted and used as a template for PCR-mediated amplification of 16S rDNA. The amplicons were used for sequencing and the resulting 16S rDNA sequence was compared with those of the type of strains of validly published species in the genus *Streptomyces*. Phylogenetic analysis showed that the strain shared a higher 16S rRNA gene sequence similar to the closely related strains *S. sannanensis* NBRC 14239^T (accession number AB184579). Meanwhile, the strain was examined for a number of key phenotypic properties known to be of value in streptomycete systematics, and the presence of LL-diaminopimelic acid in peptidoglycan, together with its colonial characteristics, supported its assignment to the genus *Streptomyces*.

A slant culture of the strain was inoculated into 500 ml Erlenmeyer flasks containing 100 ml of seed medium composed of yeast extract (0.4%), glucose (0.4%), malt extract (0.5%), multiple vitamins solution (5.0 ml) and trace element solution (1.0 ml), pH was 7.2 with no adjustment, and cultured for 2 days at 28 °C on a rotary shaker at 220 r.p.m. This seed culture was used to inoculate the fermentation medium with 5% volume. Fermentation was carried out in a 500-ml Erlenmeyer flask containing 100 ml of fermentation medium that contained starch (2.4%), beef extract (0.3%), glucose (0.1%), yeast extract (0.5%), peptone (0.3%), $CaCO_3$ (0.4%), pH was 7.0 with no adjustment, and cultured for 6 days at 28 °C on a rotary shaker at 220 r.p.m. for upscale fermentation.

The completed fermentation broth (80 l) was separated into filtrate and mycelium by centrifugation. The culture filtrate was absorbed onto polymeric resin Amberlite XAD-16 (Rohm & Hass, Paris, France). Salt and high molecular materials were washed out with water, and other absorbed organic materials were eluted with MeOH to yield 55 g of dried extract after removing the solvent in vacuum. The dried extract was extracted with petroleum, $CHCl_3$ and EtOAC; the $CHCl_3$ extract fraction (2 g) was applied to gel chromatography on Sephadex LH-20 (Amersham Pharmacia Biotech, Uppsala, Sweden) (MeOH) to produce three fractions. Fraction 1 was then purified by silica gel column chromatography ($CHCl_3$-MeOH 80:1) and yielded 180 mg of a semipure material. Additional preparative HPLC (Waters SunFire C18 10 μm (Milford, MA, USA) 19×250 mm, flow rate: 10 ml min^{-1}), eluted with water–methanol of gradient 6:4, yielded 50 mg of compound **1**. **1** was obtained as an orange amorphous powder. UV (MeOH) λ_{max}=237, 274, 304 nm. IR(KBr) ν_{max}=3376, 3319, 1687, 1608, 1585, 1556, 1506, 1334, 1228 cm^{-1}. ESI-MS *m/z*=217.3 $[M+H]^+$, 239.3 $[M+Na]^+$, 433.4 $[2M+H]^+$, 455.4 $[2M+Na]^+$, 215.3 $[M-H]^-$. For ^1H and ^{13}C NMR data see Table 1.

The molecular formula of **1** was established as $C_{12}H_{12}N_2O_2$ by HRESI-MS at *m/z* 217.0975 $[M+H]^+$ (calcd 217.0977). The IR spectrum of **1** indicated the presence of an amino group (3376 cm^{-1}) and a carbonyl group (1687 cm^{-1}). The ^1H NMR

[1]Laboratory for Conservation and Utilization of Bio-Resources and Key Laboratory for Microbial Resources of the Ministry of Education, Yunnan University, Kunming, PR China and [2]Department of Natural Product Chemistry, Pharmaceutical School, China Medical University, Shenyang, PR China
Correspondence: Dr L Han, Department of Natural Product Chemistry, Pharmaceutical School, China Medical University, BeiEr Road 92, Heping District, Shenyang, Liaoning 110001, PR China.
E-mail: lihan@mail.cmu.edu.cn or Dr Y Li, Laboratory for Conservation and Utilization of Bio-Resources and Key Laboratory for Microbial Resources of the Ministry of Education, Yunnan University, Kunming 650091, PR China
Received 2 August 2009; revised and accepted 27 August 2009; published online 2 October 2009

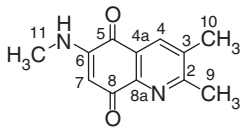

Figure 1 Structure of compound **1**.

Table 1 ^{1}H (300 MHz, $CDCl_3$) and ^{13}C NMR (75 MHz, $CDCl_3$) data of compound 1

No.	δ_C	δ_H	*HMBC*
2	164.4	—	H-4, H-9, H-10
3	135.3	—	H-9, H-10
4	134.2	8.01 (1H, s)	H-10
4a	125.3	—	—
5	181.78 (181.75)[a]	—	H-4
6	148.3	—	H-11
7	101.1	5.83 (1H, s)	H-11
8	181.75 (181.78)[a]	—	H-7
8a	146.7	—	H-4, H-7
9	23.8	2.69 (3H, s)	H-4
10	19.3	2.40 (3H, s)	H-4
11	29.1	2.93 (3H, d, J=5.4 Hz)	—
NH		5.91 (1H, brs)	

[a]Chemical shift were not distinguished.

(Table 1) spectrum of **1** showed two aromatic proton signals at δ=8.01 (1H, s) and 5.83 (1H, s), as well as three methyl signals at δ=2.93 (3H, d, J=5.4 Hz), 2.69 (3H, s) and 2.40 (3H, s). In addition, an active proton was presented at δ=5.91 (1H, brs). ^{13}C NMR and DEPT spectra of **1** (Table 1) indicated the corresponding carbon atoms with ^{1}H NMR data, two aromatic methines (δ=134.2, 101.1) and three methyls (δ=29.1, 23.8, 19.3). Furthermore, seven quaternary carbons were presented, including two ketone carbonyls with nearly the same chemical shifts (δ=181.78, 181.75) and five aromatic quaternary carbons (δ=164.4, 148.3, 146.7, 135.3 and 125.3). ^{1}H and ^{13}C NMR data suggested that **1** possesses quinoline-5, 8-dione skeleton,[1,2] which is the basic structural moiety for a kind of significant compound with wide biological activities.[5–9] By comparing the ^{1}H and ^{13}C data with the known compound 6-amino-2-methyl-quinoline-5,8-dione,[1] two more methyl groups were presented in the molecule of **1**. HMBC correlations were observed between CH_3 (δ=2.40) and C-2 (δ=164.2), C-3 (δ=135.3), C-4 (δ=134.2), CH_3 (δ=2.69) and C-2 (δ=164.2), C-3 (δ=135.3), CH_3 (δ=2.93) and C-6 (δ=148.3), suggesting that two singlet methyls were located at C-2 and C-3, respectively, and the doublet methyl was linked with the amino group. Complete assignments of the ^{1}H and ^{13}C NMR spectra of **1** were achieved with 1D and 2D experiments (Table 1). Therefore, compound **1** was elucidated as 2,3-dimethyl-6-(methylamino)quinoline-5,8-dione, named sannanine. Almost all of the quinoline-5, 8-diones from natural and synthetic sources have no substituent on C-3 and C-4. Sannanine was isolated as a quinoline-5,8-dione derivative with methyl substituted on C-3 first.

To evaluate the cytotoxic activity of **1**, we measured its cytotoxic effects on four human tumor cell lines, including human gastric carcinoma cell line (BGC-823), human pancreatic carcinoma cell line (PANC-1), human hepatocellular liver carcinoma cell line (HepG2) and human large-cell lung carcinoma cell line (H460) grown in RPM1-1640 medium plus 10% heat-inactivated fetal bovine serum with an MTT assay procedure.[10] Assays were performed in 96-well microtiter plates. Compound **1** was dissolved in dimethylsulfoxide and diluted to six different concentrations (10, 3.3, 1.0, 0.33, 0.10 and 0.033 mM), and each solution was 10-fold diluted to six different concentrations using culture medium (1.0, 0.33, 0.10, 0.033, 0.010 and 0.0033 mM); thereafter, 10 µl of each solution was added to 90 µl (about 5000 cells) of culture medium wells. After incubation at 37 °C for 72 h, 10 µl of MTT (5 mg ml^{-1}) was added to each well and incubated for 4 h; thereafter the liquid in the wells was removed. Dimethylsulfoxide (150 µl) was added to each well. Absorbance was recorded on a microplate reader at a wavelength of 590 nm, and IC_{50} was defined as a 50% reduction of absorbance in the control assay. Compound **1** showed cytotoxicity against four human tumor cell lines BGC823, PANC1, HepG2 and H460, with IC_{50} values of 6.6, 5.8, 3.1 and 1.8 µM, respectively.

ACKNOWLEDGEMENTS

This work was funded by the National Natural Science Foundation of China (Grant no. 20602041, 20762012, 30860013, 20462008) and by the Yunnan Provincial Natural Science Foundation (Grant no. 2006C0004M). We thank Professor Jincai Lu and Professor Jinhui Wang (Shenyang Pharmaceutical University, China) for their help in spectral measurement.

1 Choi, H. Y., Kim, D. W., Chi, D. Y., Yoon, E. Y. & Kim, D. J. Preparation of 7-alkylamino-2-methylquinoline-5,8-diones. *J. Org. Chem.* **67,** 5390–5393 (2002).
2 Behforouz, M., Haddad, J., Cai, W. & Gu, Z. X. Chemistry of quinoline-5,8-diones. *J. Org. Chem.* **63,** 343–346 (1998).
3 Herlt, A. J., Rickards, R. W. & Wu, J. P. The structure of streptonigrone, and a comment on the biosynthesis of the streptonigrin antibiotics. *J. Antibiot.* **38,** 516–518 (1985).
4 Yoshida, K., Ishiguro, M., Honda, H., Yamamoto, M. & Kubo, Y. Regioselevtive 6-amination and 6-arylation of 5, 8-quinolinedione promoted by metal irons. *Bull. Chem. Soc. Jpn.* **61,** 4335–4340 (1988).
5 Porter, T. H., Bowman, C. M. & Folkers, K. Antimetabolites of coenzyme Q. 16. new alkylmercaptoquinones having antimalarial curative activity. *J. Med. Chem.* **16,** 115–118 (1973).
6 Take, Y., Oogose, K., Kubo, T. & Inouye, Y. Comparative study on biological activities of heterocyclic quinines and streptonigrin. *J. Antibiot.* **40,** 679–684 (1987).
7 Lazo, J. S. *et al.* Discovery and biological evaluation of a new family of potent inhibitors of the dual specificity protein phosphatase Cdc25. *J. Med. Chem.* **44,** 4042–4049 (2001).
8 Podeszwa, B. *et al.* Investigating the antiproliferative activity of quinoline-5,8-diones and styrylquinolinecarboxylic acids on tumor cell lines. *Bioorg. Med. Chem. Lett.* **17,** 6138–6141 (2007).
9 Hsu, T. S. *et al.* 7-Chloro-6- piperidin-1-yl-quinoline-5,8-dione (PT-262), a novel synthetic compound induces lung carcinoma cell death associated with inhibiting ERK and CDC2 phosphorylation via a p53-independent pathway. *Cancer Chemother. Pharmacol.* **62,** 799–808 (2008).
10 Carmichael, J., DeGraff, W. G., Gazdar, A. F., Minna, J. D. & Mitchell, J. B. Evaluation of a tetrazoliumbased semiautomated colorimetric assay: assessment of chemosensitivity testing. *Cancer Res.* **47,** 936–942 (1987).

The Journal of Antibiotics (2009) 62, 649–650

www.nature.com/ja

MEETING REPORT

Functional molecules from natural sources: Organized by the Royal Society of Chemistry Biotechnology Group, Magdalen College, Oxford, UK, 6–8 July 2009

Stephen K Wrigley

The Journal of Antibiotics (2009) **62,** 649–650; doi:10.1038/ja.2009.94; published online 2 October 2009

Naturally occurring compounds have been, and continue to be, a major source of both new leads and commercially successful products for various industrial sectors, notably pharmaceuticals, agrochemicals and animal health. The last decade has, however, seen many challenges to, and changes in, the industrial use of natural products for new lead finding. Many large company natural product discovery groups are no longer operating, following trends toward discovery based on more 'convenient' synthetic chemical diversity such as combinatorial chemistry. At the same time, a number of small companies dedicated to natural product discovery and development have been founded, with varying degrees of success. Recent years have also been successful in terms of the approval of new classes of natural product-derived drugs, notable examples being the lipopeptide antibacterial agent daptomycin (Cubicin),[1] the first pleuromutilin derivative for human use, Retapamulin,[2] the rapamycin-derived anticancer agents Temsirolimus[3] and Everolimus,[4] and the anticancer epothilone derivative Ixabepilone.[5] This conference followed two earlier meetings organized by the RSC Biotechnology Group[6,7] and aimed to highlight current trends, challenges and successes in the exploitation of natural products.

The opening session set the scene with two contrasting presentations. David Newman (National Cancer Institute, Frederick, MD, USA) started with a summary of the past successes of natural products in providing antitumour drugs with and without chemical modification or by inspiring chemical mimics.[8] He went on to highlight a wide variety of natural product and natural product-derived leads from many different marine, plant and microbial sources, and acting through important new mechanisms, which are at various stages of development. Neville Nicholson gave a medicinal chemistry perspective on current lead-finding practice in the pharmaceutical industry by summarizing a GlaxoSmithKline (Harlow, UK) program that identified an agonist of a putative pain receptor.[9] Although this was initially based on synthetic library screening, he went on to describe some natural product-inspired mechanisms to increase bioavailability that might be applicable for lead optimization, adopted from compounds such as FK506, clarithromycin and amphotericin B. The complexity of pain as a pharmaceutical target was also discussed and the use of herbal medicinal data for identification of receptors relevant to the curing of human neurological diseases was advocated.

Recent natural product-derived successes and promising new development candidates were covered in several presentations. Richard Jarvest (GlaxoSmithKline, Stevenage, UK) gave the first public presentation on the optimization of pleuromutilins as antibacterials for human use, resulting in the approval of Retapamulin for topical applications.[2] He also outlined the ongoing work to develop further candidates from the same scaffold for systemic use. Rapamycin was discovered as a result of its antifungal activity but first found use as an immunosuppressive agent and more recently has yielded semi-synthetic derivatives approved for the treatment of various forms of cancer.[3,4] Guy Carter (Wyeth, Pearl River, NY, USA) outlined a further program targeted at optimizing the neurotrophic effects of this class of compounds that has yielded another semi-synthetic rapamycin analog ('rapalog'), ILS-920, which binds to FKBP52, an immunophilin associated with the central nervous system and that is non-immunosuppressive and shows promising activity in *in vivo* models for the treatment of stroke.[10] Mike Dawson (Novacta, Welwyn Garden City, UK) described the company's research into the optimization of lantibiotics as lead compounds, as exemplified by the tetracyclic lantibiotic mersacidin, through mutagenesis of the peptide residues not involved in cycle formation.[11] The most advanced lantibiotic derivative had been selected as a drug candidate for the treatment of *Clostridium difficile* infections and was undergoing formal preclinical development.

Hypha Discovery Ltd., Russell Building, Brunel Science Park, Kingston Lane, Uxbridge, Middlesex, UK
Correspondence: Dr SK Wrigley, Hypha Discovery Ltd., Russell Building, Brunel Science Park, Kingston Lane, Uxbridge, Middlesex UB8 3PQ, UK.
E-mail: stephen.wrigley@hyphadiscovery.co.uk
Organising committee: Robert Thomas (University of Sussex, Chairman), Colin Bedford (University College London), Martin Hayes (AstraZeneca), Martine Verhoeyen (Unilever R&D), Neville Nicholson (Consultant) and Stephen Wrigley (Hypha Discovery Ltd).
Received 19 August 2009; accepted 31 August 2009; published online 2 October 2009

During the first of two lectures dedicated to screening approaches for the discovery of antibacterial agents, Sheo Singh described strategies developed by Merck Research Laboratories (Rahway, NJ, USA) for discovering new antibiotics with novel modes of action, focusing on the highly sensitive antisense-based approach that had led to the identification of a number of novel leads, most notably platensimycin and platencin.[12] Tony Buss of Merlion Pharmaceuticals (Singapore) pointed out that successful antibacterial agents in clinical use had physicochemical properties (for example, molecular weight/polarity ranges) that were distinctly different compared with the parameters recognized as important for drugs interacting with mammalian protein targets. He proposed that chemical fingerprinting approaches could be used to assess the outputs of microbial fermentation processes and to bias them toward the production of compounds more likely to be useful as antibiotics.

A major theme of the conference was the elucidation and manipulation of microbial product biosynthetic pathways. Jason Micklefield (Univ. Manchester, UK) described the elucidation of the key steps in the biosynthesis of the calcium-dependent antibiotic from *Streptomyces coelicolor*, a lipopeptide related to daptomycin, and the biosynthetic engineering of new lipopeptides with improved biological properties.[13] Jurgen Rohr (Univ. Kentucky, USA) described the biosynthesis of the potent anticancer agent mithramycin, a type II polyketide modified by an intricate array of post polyketide synthase tailoring modifications including oxidations, reductions and glycosylations, and manipulation of the pathway to generate analogs with superior biological activities. Greg Challis (Univ. Warwick, UK) outlined recent findings on the biosynthetic pathways of the *S. coelicolor* antibiotics, methylenomycin, undecylprodiginine and streptorubin.[14] Daniel Oves-Costales from the same university described the elucidation of the main steps in the biosynthesis of the anthrax stealth siderophore petrobactin.

Much less time was dedicated to natural products from other sources. Andrew Mearns Spragg (Aquapharm Biodiscovery, Oban, Scotland) summarized the record of marine sources in providing valuable drug leads and outlined his company's strategy for the exploitation of marine microbial metabolites. On the phytochemical front, Rob Nash (Summit Wales, Aberystwyth, UK) discussed the potential of imino sugars to provide leads for wide ranging therapeutic uses, and the isolation and synthesis of a new generation of compounds with improved glycosidase inhibitory selectivity, including casuarines and casuarine glucosides, which showed promising immunomodulatory properties. Gerhard Bringmann (Univ. Würzburg, Germany) described the structure elucidation and biosynthesis of acetogenic anthraquinones and alkaloids including joziknipholone A and ancistrocladinium A. He drew attention to the remarkable contrast in biosynthetic pathways leading to the anthraquinone chrysophanol by different modes of folding of a common octaketide precursor, namely F in eukaryotes and S and S′ in prokaryotes.[15]

Gerhard Bringmann's talk also highlighted another theme of the conference, advancing the development of technologies for natural product purification and identification. His use of coupled HPLC–MS–NMR–CD must represent a culmination in the application of hyphenated chromatographic-spectroscopic technologies. Other technology-focused presentations were given by Ian Garrard (Brunel Univ., UK) who described new high-capacity countercurrent chromatography technology for rapid natural product isolation and Jonathon Nielson of Advanced Chemistry Development (Bracknell, UK), who illustrated the combined use of automated structure elucidation software and natural products structure databases for marine natural product dereplication based on ^{13}C NMR data.

In the closing session of the conference Peter Leadlay (Univ. Cambridge, UK) highlighted the large numbers of cryptic or silent biosynthetic gene clusters that are being identified by genome-scale sequencing of *Streptomyces* and other polyketide-producing organisms. Studies of *Streptomyces violaceusniger* DSM4137 had resulted in the characterization of genes for multiple products including elaiophylin, meridamycin and nigericin. Cross talk between these clusters was evident as knock out of one cluster often affected the products of others. In contrast to bacterial biosynthetic pathways, fungal pathways are more challenging in terms of genetic manipulation. Tom Simpson (Univ. Bristol, UK) described results of the complementation of classical biosynthetic studies with molecular genetic approaches, heterologous gene expression, gene disruption and silencing for a number of fungal metabolites including xenovulene A and tenellin A. The two concluding lectures focused on agrochemical applications, with two very different approaches. John Pickett (Rothamsted Research, Rothamsted, UK) described the development of new strategies for the control of insect and weed pests through generation of genetically modified organisms in which the biosynthesis of small lipophilic molecules such as semiochemicals (E-β-farnesene) or plant activators (cis-jasmone) is manipulated to provide crop protection by intrinsically benign mechanisms. John Clough outlined the value of natural products to Syngenta (Jealott's Hill, UK), as leads for the development of new synthetic herbicides, insecticides and fungicides through a number of case studies including the highly commercially successful strobilurins.

'Functional Molecules from Natural Sources' was attended by representatives from 20 different countries and took place at the historically renowned Magdalen College in a wonderful setting that was highly conducive to discussion and networking. The lecture program was complemented by the submission of a highly diverse selection of posters including many from international postgraduate researchers and students. There was much appreciation for the excellent quality of the presentations, which stimulated a high degree of optimism for future natural product successes.

ACKNOWLEDGEMENTS

The author is grateful to Robert Thomas for reading and commenting on the paper.

1 Baltz, R. H., Miao, V. & Wrigley, S. K. Natural products to drugs: daptomycin and related lipopeptide antibiotics. *Nat. Prod. Rep.* **22,** 717–741 (2005).
2 Daum, R. S., Kar, S. & Kirkpatrick, P. Retapamulin. *Nat. Rev. Drug Disc.* **6,** 865–866 (2007).
3 Rini, B., Kar, S. & Kirkpatrick, P. Temsirolimus. *Nat. Rev. Drug Disc.* **6,** 599–600 (2007).
4 Atkins, M. B., Yasothan, U. & Kirkpatrick, P. Everolimus. *Nat. Rev. Drug Disc.* **8,** 535–536 (2009).
5 Conlin, A., Fornier, M., Hudis, C., Kar, S. & Kirkpatrick, P. Ixabepilone. *Nat. Rev. Drug Disc.* **6,** 953–954 (2007).
6 Wrigley, S., Hayes, M., Thomas, R. & Chrystal, C. (eds). *'Phytochemical Diversity: A Source of New Industrial Products'* (Royal Society of Chemistry: Cambridge, UK, 1997).
7 Wrigley, S. K., Hayes, M. A., Thomas, R., Chrystal, E. J. C. & Nicholson, N. (eds). *'Biodiversity: New Leads for the Pharmaceutical and Agrochemical Industries'* (Royal Society of Chemistry: Cambridge, UK, 2000).
8 Newman, D. J. & Cragg, G. M. Natural products as sources of drugs over the last 25 years. *J. Nat. Prod.* **70,** 461–477 (2007).
9 Wroblowski, B. *et al.* The discovery of a selective, small molecule agonist for the Mas-related gene X1 receptor. *J. Med. Chem.* **52,** 818–825 (2009).
10 Ruan, B. *et al.* Binding of rapamycin analogs to calcium channels and FKBP52 contributes to their neuroprotective activities. *Proc. Natl. Acad. Sci. USA* **105,** 33–38 (2008).
11 Appleyard, A. N. *et al.* Dissecting structural and functional diversity of the lantibiotic mersacidin. *Chem. Biol.* **16,** 490–498 (2009).
12 Wang, J. *et al.* Discovery of platencin, a dual FabF and FabH inhibitor with *in vivo* antibiotic properties. *Proc. Natl Acad. Sci. USA* **104,** 7612–7616 (2007).
13 Micklefield, J. Biosynthesis and biosynthetic engineering of calcium-dependent lipopeptide antibiotics. *Pure Appl. Chem.* **81,** 1065–1074 (2009).
14 Mo, S. J. *et al.* Elucidation of the *Streptomyces coelicolor* pathway to 2-undecylpyrrole, a key intermediate in undecylprodiginine and streptorubin B biosynthesis. *Chem. Biol.* **15,** 137–148 (2008).
15 Bringmann, G. *et al.* Different polyketide folding modes converge to an identical molecular architecture. *Nat. Chem. Biol.* **2,** 429–433 (2006).

The Journal of Antibiotics (2009) 62, 651

www.nature.com/ja

CORRIGENDUM

Pentacecilides, new inhibitors of lipid droplet formation in mouse macrophages, produced by *Penicillium cecidicola* FKI-3765-1: I. Taxonomy, fermentation, isolation and biological properties

Hiroyuki Yamazaki, Kakeru Kobayashi, Daisuke Matsuda, Kenichi Nonaka, Rokuro Masuma, Satoshi Ōmura and Hiroshi Tomoda

The Journal of Antibiotics (2009) **62,** 651; doi:10.1038/ja.2009.104

Correction to: *The Journal of Antibiotics* (2009) **62**, 195–200; doi:10.1038/ja.2009.18

The authors of the above noted an error in publication of this paper in Figure 1. The correct figure is shown below.

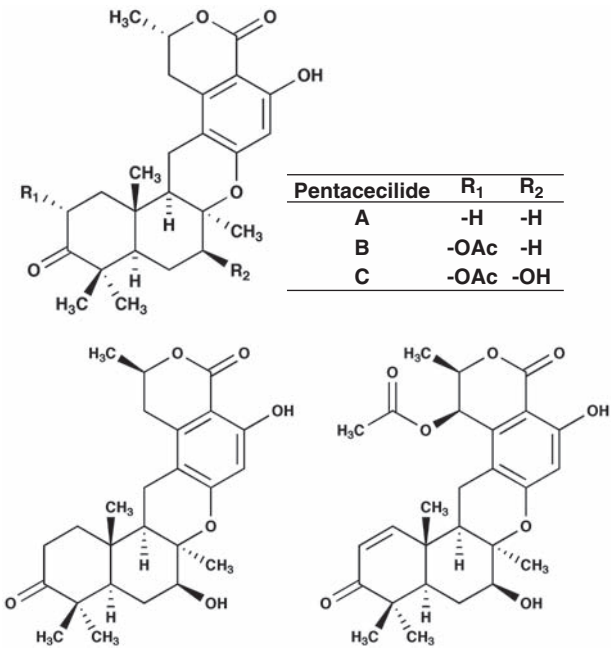

Figure 1 Structures of pentacecilides A to C and thailandolides A and B.

The Journal of Antibiotics (2009) 62, 653–654

www.nature.com/ja

CORRIGENDUM

Pentacecilides, new inhibitors of lipid droplet formation in mouse macrophages, produced by *Penicillium cecidicola* FKI-3765-1: II. Structure elucidation

Hiroyuki Yamazaki, Satoshi Ōmura and Hiroshi Tomoda

The Journal of Antibiotics (2009) **62,** 653–654; doi:10.1038/ja.2009.105

Correction to: *The Journal of Antibiotics* (2009) **62,** 207–211; doi:10.1038/ja.2009.19

The authors of the above article noted an error in publication of this paper in Figures 1 and 4 and in the legend of Figure 3. The correct figures and Figure 3 legend are shown below.

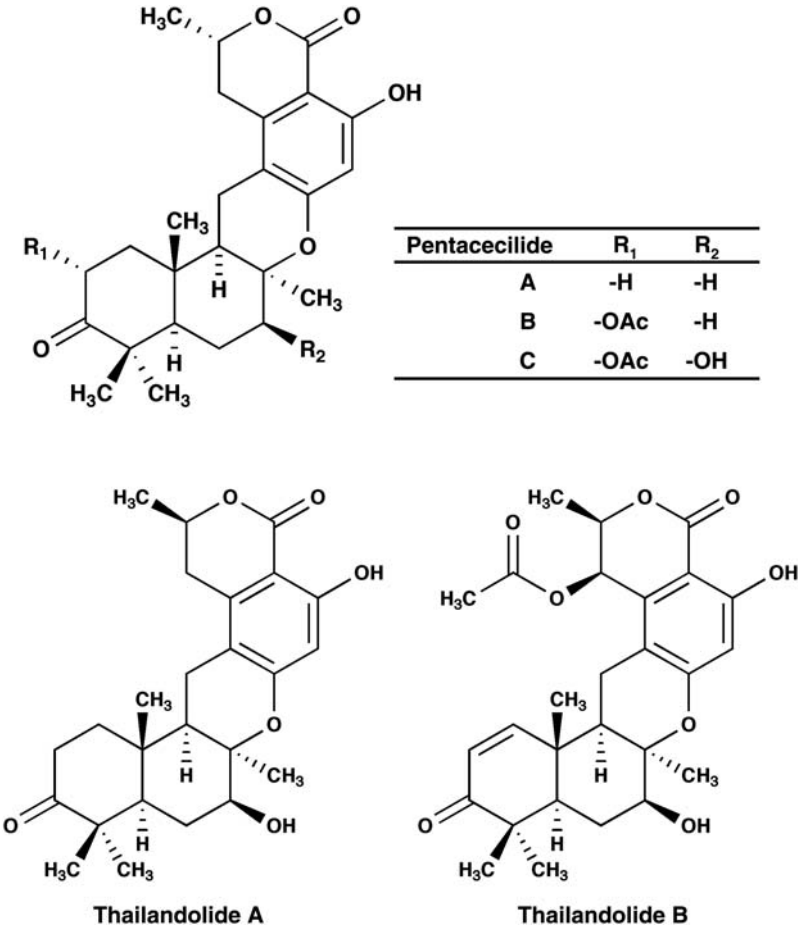

Pentacecilide	R_1	R_2
A	-H	-H
B	-OAc	-H
C	-OAc	-OH

Figure 1 Structures of pentacecilides A to C and thailandolides A and B.

Figure 3 ^{1}H–^{1}H COSY and ^{13}C–^{1}H HMBC experiments of pentacecilides C (**a**), B (**b**) and A (**c**).

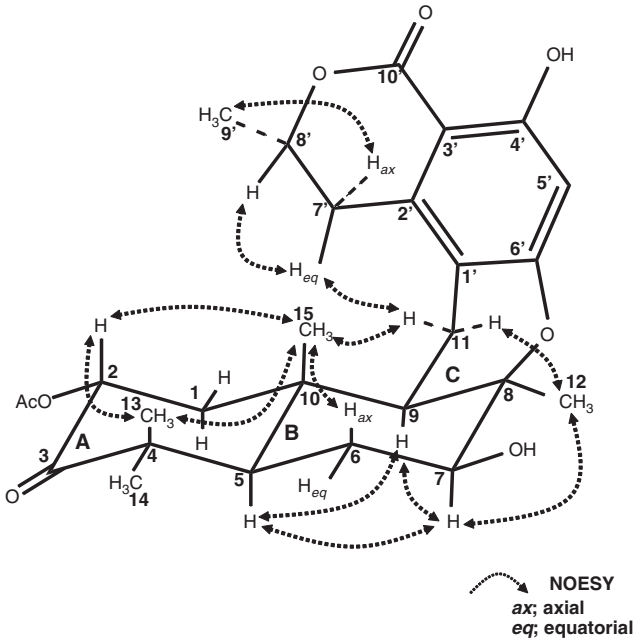

Figure 4 NOESY experiments of pentacecilide C.